IMMUNE MODULATION OF MAMMOGRAPHIC DENSITY AND BREAST CANCER RISK

MADDISON ROSE MCKINNON ARCHER

DISCIPLINE OF SURGERY

SCHOOL OF MEDICINE

FACULTY OF HEALTH SCIENCES

THE UNIVERSITY OF ADELAIDE

December 2019

A thesis submitted to the University of Adelaide in fulfilment of the requirements for admission to the degree Doctor of Philosophy

SUPERVISORS:

ASSOCIATE PROFESSOR WENDY INGMAN

DR PALLAVE DASARI

PROFESSOR ANDREAS EVDOKIOU

CONTENTS

ABSTRACT I

DECLARATION III

ACKNOWLEDGEMENTS IV

ABBREVIATIONS VI

CHAPTER ONE: LITERATURE REVIEW 1

1.1 INTRODUCTION 1

1.2 MAMMOGRAPHIC DENSITY AND BREAST CANCER RISK 2

1.3 CONTRIBUTION OF GENETIC AND ENVIRONMENTAL FACTORS TO MAMMOGRAPHIC DENSITY 8

1.4 HISTOPATHOLOGY OF THE HUMAN BREAST AND MAMMOGRAPHIC DENSITY 10

1.4.1 Mammary Epithelium in Mammographic Density 12

1.4.2 Mammary Stroma in Mammographic Density 12

1.5 IMMUNE CELLS IN MAMMOGRAPHIC DENSITY 17

1.5.1 Macrophages 18

1.6 INFLAMMATION AS A DRIVER OF MAMMOGRAPHIC DENSITY AND BREAST CANCER RISK 20

1.6.1 Monocyte Chemotactic Protein 1 (CCL2) 21

1.6.2 Peroxidase Enzymes 23

1.6.3 Tumour Necrosis Factor Alpha (TNFA) 23

1.7 CONCLUSION 25

1.8 HYPOTHESIS & AIMS 26

CHAPTER TWO: MATERIALS AND METHODS 27

2.1 HUMAN NON-NEOPLASTIC BREAST TISSUE.....27

2.1.1 Study Population 27

2.1.2 Tissue Embedding, Sectioning and Staining. 27

2.1.3 Histological Classification of Mammographic Density 28

2.2 CELL CULTURE 31

2.2.1 Isolation and culture of Human Mammary Fibroblasts 31

2.2.2 Culture of THP-1 Monocytes 32

2.2.3 Cryopreservation and Thawing 32

2.2.4 Cytokine and Peroxidase Treatment in Human Mammary Fibroblast Culture 32

2.2.5 Indirect Co-Culture of Human Mammary Fibroblasts and Differentiated THP-1 Cells 33

2.3 PROTEIN ANALYSIS.....34

2.3.1 Enzyme-Linked Immunosorbent Assay 34

2.3.2 Sirius Red Analysis of Insoluble Collagen 34

2.4 FLOW CYTOMETRY OF THP-1 MACROPHAGES.....35

2.5 ANIMALS.....37

2.5.1 Mice 37

2.5.2 Blood Collection 38

2.5.3 Tumour Detection by Palpation 38

2.5.4 Histology and Immunohistochemistry 38

2.5.5 Image Capture and Quantifications 41

2.6 NUCLEOTIDE ANALYSIS……42

2.6.1 Genotyping Mice 42

2.6.2 Total RNA Extraction..... 45

2.6.3 Reverse Transcription and cDNA Synthesis 46

2.6.4 Quantitative Real Time PCR 46

2.6.5 Next Generation Sequencing of Mmtv-Ccl2 Mammary Glands……47

2.7 STATISTICAL ANALYSIS……50

CHAPTER THREE: IMMUNE REGULATION OF MAMMARY FIBROBLASTS AND THE IMPACT OF MAMMOGRAPHIC DENSITY……..52

3.1 INTRODUCTION……52

3.2 RESULTS……54

3.2.1 CAF and ECM mRNA expression and collagen production of mammary fibroblasts from women with high and low MD 54

3.2.2 The effect of MPO on CAF and ECM mRNA expression and collagen production by mammary fibroblasts 57

3.2.3 The effect of EPO on ECM and CAF mRNA expression, and collagen production by mammary fibroblasts 61

3.2.4 The effect of TGFB on CAF and ECM mRNA expression and collagen production by mammary fibroblasts 65

3.2.5 The effect of TNFA on CAF and ECM mRNA expression and collagen production by mammary fibroblasts 69

3.3 DISCUSSION……73

3.3.1 Mammary fibroblasts isolated from high MD tissue are not inherently different from those isolated from low MD tissue 73

3.3.2 Modulation of extracellular matrix regulation and collagen production in mammary fibroblasts by peroxidase enzymes 74

3.3.3 TGFB1 signalling modulates extracellular matrix regulation and collagen production in mammary fibroblasts 75

3.3.4 TNFA Signalling and fibroblast function 76

3.3.5 Limitations 78

3.4 CONCLUSION.....80

CHAPTER FOUR: MACROPHAGE-FIBROBLAST INTERACTIONS THAT CONTRIBUTE TO A PRO-TUMOUR MICROENVIRONMENT.....81

4.1 INTRODUCTION.....81

4.2 RESULTS.....83

4.2.1 The effect of CCL2 on CAF and ECM mRNA expression and collagen production by mammary fibroblasts 83

4.2.2 The effect of mammary fibroblasts and CCL2 on THP-1 derived macrophage phenotype in co-culture 88

4.2.3 The effect of mammary fibroblasts and CCL2 on THP-1 derived macrophage gene expression. 90

4.2.4 The effect of THP-1 derived macrophages and CCL2 on mammary fibroblast gene expression in co-culture ..... .94

4.2.5 The effect of THP-1 derived macrophages and CCL2 on mammary fibroblast collagen production in co-culture…...……100

4.3 DISCUSSION.....103

4.3.1 The effect of CCL2 on ECM regulation in mammary fibroblasts……..……103

4.3.2 Mammary fibroblasts drive differentiation of THP-1 derived macrophages 104
4.3.3 M2 polarised macrophages promote tissue remodelling in mammary fibroblasts 106
4.3.4 Limitations 107
4.4 CONCLUSION 108
CHAPTER FIVE: THE EFFECT OF CCL2 ON MAMMARY TUMORIGENESIS AND GLOBAL GENE EXPRESSION IN MICE 109
5.1 INTRODUCTION 109
5.2 RESULTS 111
5.2.1 The effect of CCL2 on early tumourigenesis in 9 week old PyMT mice 111
5.2.2 The effect of CCL2 on tumour latency 112
5.2.3 The effect of CCL2 on mammary tumour burden 115
5.2.4 The effect of CCL2 on primary tumour progression 118
5.2.5 The effect of CCL2 on macrophage infiltration 125
5.2.6 The effect of CCL2 on global gene expression in the mammary gland 130
5.3 DISCUSSION 134
5.3.1 The role of CCL2 in mammographic density 134
5.3.2 The role of CCL2 in tumour development and progression 135
5.3.3 Constitutive CCL2 expression downregulates fatty acid synthesis and metabolism 137
5.3.4 Limitations 137
5.4 CONCLUSION 138

CHAPTER SIX: GENERAL DISCUSSIONS AND CONCLUSIONS 139

6.1 BREAST CANCER PREVENTION……..139

6.2 CELLULAR AND INFLAMMATORY INTERACTIONS DRIVING MAMMOGRAPHIC DENSITY AND BREAST CANCER RISK……..140

6.3 USE OF ANTI-INFLAMMATORIES TO PREVENT BREAST CANCER……..145

6.4 FUTURE RESEARCH TO UNDERSTAND THE BIOLOGICAL DRIVERS OF BREAST CANCER RISK……..146

6.5 CONCLUSIONS……..150

REFERENCES……151

ABSTRACT

Mammographic density (MD) is a strong risk factor for breast cancer that can increase breast cancer risk by 4-6 fold independently of age and BMI. High MD is characterised by breast tissue containing high proportions of stroma, containing fibroblasts, collagen and immune cells, indicative of an inflammatory pro-tumour environment. Currently, the biological mechanisms that drive MD and the associated breast cancer risk are not yet understood. Immune signalling factors such as monocyte chemotactic protein 1 (CCL2), peroxidase enzymes, transforming growth factor beta (TGFB) and tumour necrosis factor alpha (TNFA) have been implicated in breast cancer risk, and are also known to influence functions of stromal fibroblasts. The work in this thesis aims to investigate how these immune signalling factors and the immune microenvironment may act as drivers of MD through their interactions with mammary fibroblasts *in vitro*, and this effect mammary tumorigenesis in a transgenic tumour mouse model.

Firstly, primary mammary fibroblasts from women with high and low MD were treated *in vitro* with immune factors myeloperoxidase (MPO), eosinophil peroxidase (EPO), TGFB, TNFA and CCL2 for 72 hours. The abundance of mRNA encoding cancer associated fibroblast (CAF) markers and genes involved in extracellular matrix (ECM) regulation were investigated. Production of soluble collagen 1 and insoluble collagen fibres were also measured. No significant differences were observed in gene expression and collagen production between fibroblasts from women with low or high mammographic density. MPO and EPO significantly increased production of collagen 1 in mammary fibroblasts. TGFB and TNFA induced variable changes in CAF and ECM gene expression. TGFB and CCL2 increased deposition of insoluble collagen fibres.

Further investigation of the crosstalk between mammary fibroblasts and macrophages utilised an indirect co-culture of primary mammary fibroblasts with THP-1 derived

macrophages in the presence or absence of CCL2 for 72 hours. THP-1 derived macrophages underwent differentiation to an M2 phenotype, and had high expression of genes involved in tissue remodelling including *MMP2*, *TIMP1* and *VEGF*. Co-culture with THP-1 macrophages induced high expression of ECM remodelling genes by mammary fibroblasts such as *MMP1*, *MMP3*, *MMP9* and *TIMP1*, as well as inflammatory genes *COX2*, *IL6* and *IL8*. Production of insoluble collagen fibres was increased in mammary fibroblasts in co-culture with THP-1 macrophages and CCL2.

Thirdly, the effect of CCL2 on mammary tumourigenesis and global gene expression was investigated. Mmtv-CCL2 mice overexpressing CCL2 in the mammary gland were crossbred with Mmtv-PyMT tumour model mice. Tumour development was monitored until 9 and 12 weeks of age. CCL2 overexpressing mice were found to have increased macrophage infiltration to primary tumours and increased number of areas of early tumorigenesis in the mammary gland at 9 weeks age. No differences were observed in tumour latency, tumour burden, tumour grade, or pulmonary metastasis between CCL2 overexpressing mice and controls. Global gene expression was analysed by RNAseq in mammary glands from 12 week old Mmtv-CCL2 mice and FVB controls. Mmtv-CCL2 mice exhibited increased expression of genes involved in cancer, DNA damage and extracellular matrix deposition. Expression of genes involved in fatty acid metabolism and adaptive immunity were reduced in Mmtv-CCL2 mice.

These results suggest that fibroblasts from women with high mammographic density are not inherently different to those from women with low mammographic density. The role of fibroblasts in MD and breast cancer risk may be a result of immune signals from surrounding cells in the breast microenvironment, which may be through interactions with macrophages and inflammation driven by CCL2.

DECLARATION

I, Maddison Archer, certify that this work contains no material which has been accepted for the award of any other degree or diploma in my name, in any university or other tertiary institution and, to the best of my knowledge and belief, contains no material previously published or written by another person, except where due reference has been made in the text. In addition, I certify that no part of this work will, in the future, be used in a submission in my name for any other degree or diploma in any university or other tertiary institution without the prior approval of the University of Adelaide and where applicable, any partner institution responsible for the joint award of this degree.

I give permission for the digital version of my thesis to be made available on the web, via the University's digital research repository, the Library Search and also through web search engines, unless permission has been granted by the University to restrict access for a period of time

I acknowledge the support I received for my research through the provision of an Australian Government Research Training Program Scholarship.

Name: Maddison Archer

Signed:

_____

Date: 17th December 2019

ACKNOWLEDGEMENTS

Firstly, I would like to thank the patients and surgeons at The Queen Elizabeth Hospital for generously donating their tissue samples for use in this research. I would like to show my appreciation to the University of Adelaide, School of Medicine for providing me with the financial support of the Faculty of Health Sciences Divisional Scholarship.

I would like to express my deepest gratitude to my principle supervisor Associate Professor Wendy Ingman. I consider myself very fortunate to have been given the opportunity to study under her guidance. I am eternally grateful for her knowledge and encouragement throughout all aspects of my research, as well as the patience and kindness she has shown me along the way. I am grateful to my co-supervisor Dr Pallave Dasari for her mentorship and assistance in study design, writing and other technical skills. I would like to acknowledge my other co-supervisor Professor Andreas Evdokiou for his contribution and advice during my candidature. My sincere gratitude goes to all members of the Breast Biology and Cancer Unit both past and present, in particular Leigh Hodson for sharing her expertise in histology, her encouragement and cherished friendship. I sincerely thank Mark Van Der Hoek and Suzanne Edwards for their assistance with RNAseq and statistical analysis.

I would like to thank my partner Dr Sebastian Stead for his love, encouragement and support. I am greatly appreciative to him for sharing his expertise in immunology and flow cytometry to contribute to my research. I feel extremely lucky be with someone who always believes in me, and pushes me to achieve all I want to in life.

I wish to thank my friend Ashlee Caldwell for our daily motivational discussions, and her support to help get through the challenging periods of my candidature.

Last but not least, I would like to thank my family for their never ending love, support and encouragement. They are the most generous people I know and I would never have been able to pursue my PhD studies without them.

ABBREVIATIONS

ActB: Beta actin

AMPK: Adenosine monophosphate-activated protein kinase

BIRADS: Breast Imaging Reporting and Data System

BMI: Body mass index

BSA: Bovine serum albumin

CAF: Cancer-associated fibroblast

CCL2: C-C chemokine ligand 2

CCR2: C-C chemokine receptor type 2

CD: Cluster of differentiation

COL: Collagen

COX2: Cyclooxygenase 2

CRP: C-reactive protein

CTGF: Connective Tissue Growth Factor

DAB: 3,3 diaminobenzadine

DMBA: 1,3-Dimethylbutylamine

DNA: Deoxyribonucleic acid

ECM: Extracellular Matrix

ELISA: Enzyme-linked immunosorbent assay

EPO: Eosinophil peroxidase

FBN: Fibronectin

FCS: Fetal calf serum

FGF: Fibroblast growth factor

HER2: Human epidermal growth factor receptor 2

HRT: Hormone replacement therapy

HPRT1: Hypoxanthine-guanine phosphoribosyltransferase

IFNG: Interferon gamma

IL: Interleukin

iNOS: Nitric oxide synthase

LOX: Lysyl oxidase

LPS: Lipopolysaccharide

MD: Mammographic Density

MMPs: Matrix metalloproteinases

MMTV- Mouse mammary tumour virus

MPO: Myeloperoxidase

NK: Natural killer cells

NSAID: Non-steroidal anti-inflammatory drugs

mRNA: Messenger Ribonucleic acid

PBS: Phosphate buffered saline

PDGF: Platelet derived growth factor

PI3K-Akt: Phosphoinositide 3-kinases, protein kinase B

PMA: Phorbol 12-myristate 13-acetate

PPAR: Peroxisome proliferator-activated receptor

PyMT: Polyoma middle T antigen

qRT-PCR: Quantitative Real-time Polymerase Chain Reaction

Ras: Retrovirus-associated DNA sequences

SEM: Standard error of the mean

SMA: Smooth muscle actin

TAM: Tumour-associated macrophage

TGFB: Transforming growth factor beta

TIMPs: Tissue Inhibitors of matrix metalloproteinases

TNC: Tenascin C

TNFA: Tumour necrosis factor alpha

VEGF: Vascular endothelial growth factor

VIM: Vimentin

WNT: Wingless-related integration site

CHAPTER ONE

LITERATURE REVIEW

1.1 INTRODUCTION

The breast is indisputably one of the most susceptible tissues in a woman's body to cancer. A quarter of all cancers in women originate in the breast and 1 in 7 Australian women will be diagnosed with this disease before the age of 85 [1]. Strategies aimed at reducing the incidence of breast cancer begin with understanding the etiology of increased risk. Although family history is an important risk factor breast cancer, familial breast cancer is relatively rare. Mutations in genes encoding the tumour suppressor genes BRCA1 and BRCA2 account for approximately two percent of all breast cancers [2] and around ten percent of cases are linked to family history of the disease [3]. The majority of breast cancers are attributed to nonhereditary risk factors [4] and therefore there is potential to reduce the burden of breast cancer through strategies that modify these. More research is required to understand the underlying biology of nonhereditary breast cancer risk factors and why the breast is so susceptible to cancer.

There are many nonhereditary risk factors for breast cancer including age, obesity, menstrual and reproductive history, and mammographic density. Mammographic density (MD) is one the strongest independent risk factors for breast cancer, accounting for 30% of breast cancer occurrences [5, 6]. Women with breasts classified as 'extremely dense' on the Breast Imaging Reporting and Data system (BIRADS) have a 4- to 6- fold increased breast cancer risk compared to women with breasts classified as 'mostly fatty', when matched for age and body mass index (BMI) [6]. The underlying biological mechanisms that lead to high MD and the associated increased breast cancer risk are poorly understood. However, there is some evidence that interactions between epithelium,

stroma, the extracellular matrix, and immune signalling together with ovarian hormones may contribute to both elevated MD and breast cancer risk.

This chapter reviews the current knowledge and understanding of the underlying biological mechanisms that lead to high MD and the associated increased risk of breast cancer, with particular consideration to potential immune factors that may contribute to this process.

1.2 Mammographic Density and Breast Cancer Risk

The term 'mammographic density', or MD, refers to the radiographic appearance of the breast on a mammogram (Figure 1.1) [7, 8]. MD cannot be determined by self-exam and is not associated with the appearance or feel of the breast [9]. High MD is indicated by a high proportion of white and bright regions on a mammogram, while low MD is indicated by a high proportion of dark regions [7]. The most common method for classifying MD in the clinic is the Breast Imaging Reporting and Data system (BIRADS) developed by the American College of Radiologists. This method is based on a qualitative assessment by the radiologist and classifies breasts on a scale of A to D; A is 'mostly fatty' with dark transparent appearance on a mammogram; B is 'scattered density'; C is 'homogeneously dense'; and D is 'extremely dense' with mostly white and opaque appearance on a mammogram [10]. Approximately 8% of women aged between 40 and 74 have breasts classified as 'extremely dense', and 35% have 'heterogeneously dense' breasts [11], and these two categories of density are often grouped together and referred to as 'high MD'. Other quantitative and semi-quantitative methods for MD classification are also used, including software programs such as Volpara and Quantra, and the Cumulus method, which is a semi-automated software program that determines a threshold to estimate the percentage MD on the mammogram [12, 13].

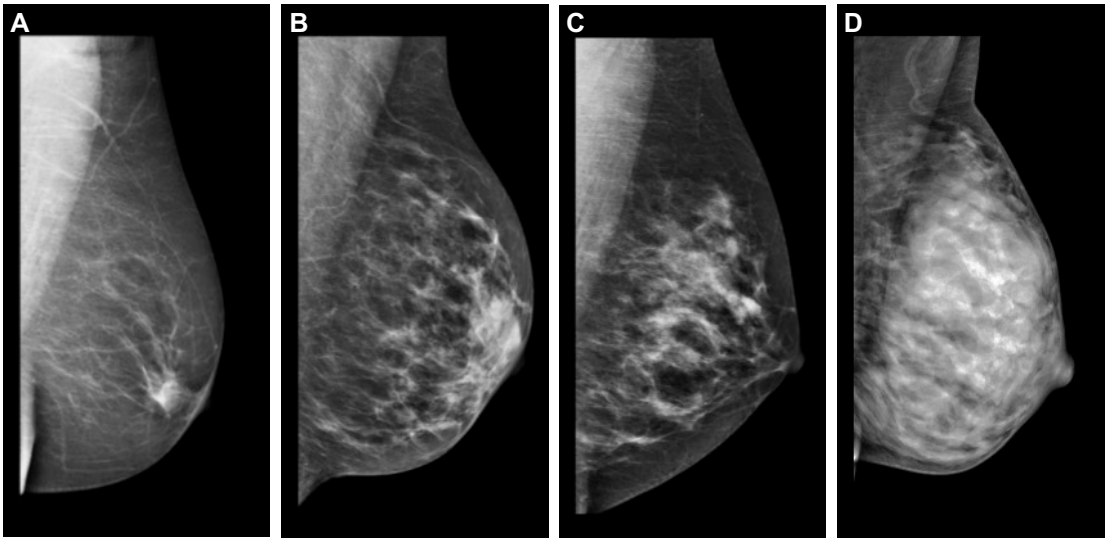

Figure 1.1: Example images of BIRADs classification of mammographic density
Mammogram images of mammographic density according to BIRADS classifications; mostly fatty (A), scattered density (B), heterogeneously dense (C), and extremely dense (D), reproduced from Hugo et al **[8].**

In 1976, Wolfe proposed that MD is positively associated with breast cancer risk [14]. Although contentious at first, many case-control studies compounded with information on reproductive, heredity and anthropomorphic factors such as age and BMI, have supported this notion and provided evidence beyond doubt that MD is one of the strongest independent risk factors for breast cancer [15-17]. A large meta-analysis demonstrates women with breasts classified as 'extremely dense' have a 4- to 6- fold increased breast cancer risk compared to women with breasts classified as 'mostly fatty', when matched for age and BMI [5]. Whilst this study provides the most robust evidence, it compares the two extremes of MD and is not reflective of the increased breast cancer risk associated with high MD above average MD. More recent studies have sought to address this, and show that premenopausal women with breasts classified as 'heterogeneously dense' and 'extremely dense' have a respective 50% and 80% increased risk of breast cancer above women with breasts classified as 'scattered density' [6]. For postmenopausal women, the increased risk above those with breasts classified as scattered density' is 40% and 60% for women with breasts classified as 'heterogeneously dense' and 'extremely dense' respectively.

Breast cancer is not a single disease. There are a number of different breast cancer subtypes that each have a different disease etiology and can have a different prognosis. If a risk factor elevates risk of a specific breast cancer subtype, this can provide some clues as to the underlying mechanisms that drive increased risk. Several studies have attempted to determine if there is an association between MD and increased risk of a specific breast cancer subtype, however the results of these studies have not yielded consistent results. While some studies reported that MD was not specifically associated with increased risk of estrogen receptor positive breast cancer, others reported an inverse relationship with density and ER positivity and a positive relationship with progesterone receptor positive breast cancers [18-21]. However, the population analysed in these

studies were biased towards users of hormone replacement therapy, which is known to increase MD [19]. Overall, the evidence suggests that high MD is associated with an increased risk of all breast cancer subtypes, and the association is not greater in hormone receptor positive breast cancers or in cancers expressing HER2 [18].

Although it seems there is no correlation between MD and a specific subtype of breast cancer, there is some indication that MD may be associated with tumour characteristics that generally indicate a poor prognosis. In a study by Yaghjyan et al, over 1000 case control pairs were examined, and reported that MD measured by the Cumulus method was associated with more invasive, larger and higher grade tumours [19]. This was consistent with another case control study by Bertrand et al that reported an association between MD and large tumour size [22]. However, several studies have demonstrated MD is not associated with reduced survival in breast cancer patients [23-25]. One study of nearly 20,000 women reported an association between MD and breast cancer mortality, after adjusting for age, BMI, menopausal status, and reproductive history [26]. However, this result might be confounded by the masking effect of high MD in detection of breast cancer. High MD appears white on the mammogram, and as potential tumours also appear white, high MD reduces the sensitivity of mammography to detect breast cancer [27]. Therefore the association of MD with poor prognosis may be a result high density breast tissue masking the appearance of tumours in mammography, leading to later detection. High MD has also been associated with a greater rate of breast cancer recurrence, and risk of recurrence is decreased when MD is reduced by greater than 10%, compared to women whose MD who remained constant [23, 28-30].

In summary, high MD is associated with increased risk of all breast cancer subtypes. Although delayed detection of breast cancer due to the masking effect of MD contributes to a poorer prognosis, women with high MD are also at greater risk of developing breast

cancer. However, it is important to consider that the epidemiological studies that demonstrate the association between high MD and breast cancer risk do not demonstrate a causal relationship. Whilst it is possible that high MD causes increased risk of breast cancer (Figure 1.2), it is also possible that elevated risk of breast cancer causes high MD (reverse causation). Furthermore, the association may be due to a common cause, whereby an as yet unidentified factor independently increases both MD and breast cancer risk (spurious association).

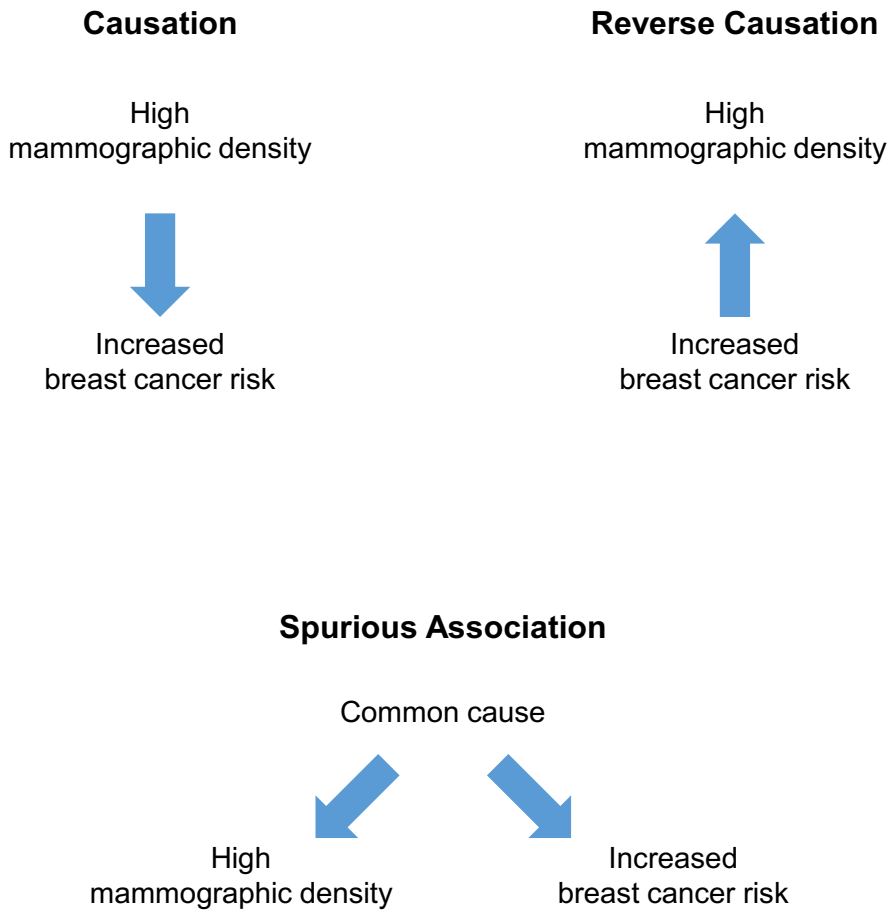

Figure 1.2: Possible mechanistic relationships between high mammographic density and increased breast cancer risk
The association between high mammographic density and increased breast cancer risk demonstrated in epidemiological studies may be the result of causation, reverse causation, or it may be a spurious association.

1.3 CONTRIBUTION OF GENETIC AND ENVIRONMENTAL FACTORS TO MAMMOGRAPHIC DENSITY

Many factors contribute to a woman's MD, and there are likely to be complex interactions at the biological level that ultimately determine how dense the tissue is. Studies on large cohorts of women that investigate relationships between MD and genetic and environmental factors can provide clues to the underlying biology of MD that can be further investigated in mechanistic studies. Epidemiological studies have shown that mammographic density is associated with a number of factors, including genetics, age, BMI, and reproductive history.

MD is partially inheritable. In a study of race and ethnicity, MD was observed to be highest amongst Asian women, and lowest in African American women, and MD tends to be higher in Chinese populations [31]. Both MD and cancer risk are correlated in sisters and in mother and daughter pairs [32]. Furthermore, studies of mammograms from monozygotic and dizygotic twin pairs reported higher correlation with monozygotic twins than dizygotic twins and the genetic contribution to MD is calculated to be approximately 60% [33]. The individual genes that provide this genetic component have not been identified, and there are likely to be many that interact with environmental factors and each other to contribute to the overall MD of the breast.

Age and BMI also affect MD. BMI is strongly positively associated with breast area and non-dense area [15] and there is a negative association between BMI and percent MD [15, 34-36]. There is also a negative association between MD and age; as age increases MD declines [37-39]. These inverse associations between MD, BMI and age may seem paradoxical, as both increasing age and BMI are associated with increased breast cancer risk [1]. However, it is important to consider that epidemiological studies of MD statistically

adjust their results for the confounding factors of age and BMI to demonstrate that MD is risk factor for breast cancer independent of age and BMI.

Factors associated with a woman's reproductive history and exposure to ovarian hormones may affect MD. An inverse correlation between parity and MD exists whereby there is a 4% decrease in breast cancer risk for every live birth in premenopausal women [40, 41]. However, MD has been reported to be higher in women where the first live birth occurred at the age of 30 or higher [41]. The association between MD and breastfeeding is unclear. One study by Lope et al reported a positive relationship between lactation and MD, and greater density in women who breastfed for longer duration (longer than 9 months) [42]. Another study in Chinese women found that longer duration of lactation was associated with a lower density in postmenopausal women, but no association in premenopausal women [31].

There is evidence that MD is altered by exposure to drugs that affect ovarian hormone signalling. In postmenopausal women, it is well-established that hormone replacement therapy (HRT) increases MD, and also is associated with an increase in breast cancer risk [43-47]. Further, women who have never used HRT exhibit a greater decline in MD with age than users of estrogen only and combine hormone replacement therapies [48]. Hormonal therapies for treatment of breast cancer also influence MD. Treatment with tamoxifen, a drug that interferes with estrogen signalling, is associated with a decrease in MD [49-53]. Studies on the effect of aromatase inhibitors on MD have been less clear. One study reported that treatment with aromatase inhibitors reduced mammographic density and this reduction is associated with tumour free survival after at least two years of treatment [54, 55]. However, some studies have found no reduction in MD in response to aromatase inhibitors [56].

It is not surprising that drugs that affect ovarian hormone signalling have a profound effect on MD. Ovarian hormones provide the stimulus for breast development and as such the composition and function of the breast is fundamentally dependent on them. However, Huo et al demonstrated that there is no difference in estrogen or progesterone receptor staining in paired tissue samples from high and low MD areas within the breast [57]. Further, there is no association between high MD and endogenous circulating hormones [35, 58, 59]. This suggests that although hormones are fundamental to MD, whether or not a woman has high MD is not due to the abundance or activity of endogenous hormones.

1.4 Histopathology of the Human Breast and Mammographic Density

The human breast, or mammary glands, are a unique bilateral tissue that undergoes major development during puberty, pregnancy, and during lactation [60]. Mammary glands are a classifying feature of all mammals, and the primary function is to produce milk to their offspring during infancy [61]. The mammary gland is composed of a network of ducts and lobules, connected to the nipple, which expand to become milk secreting elements during lactation [62]. These structures are composed of mammary epithelial cells, which are also the cells from which most breast cancers manifest [63]. The epithelial structures are surrounded by stroma, composed of mammary fibroblasts, collagen, immune cells and the extracellular matrix (ECM) [61]. The role of the mammary stroma is to provide structural and signalling support and promote appropriate development and function of the epithelium [64]. The crosstalk between cells of the stroma and other cells of the mammary gland can mediate breast cancer risk [65]. Interactions between epithelium, stroma, the extracellular matrix, and immune signalling together with ovarian hormones may contribute to both elevated MD and the associated increased risk of breast cancer (Figure 1.3).

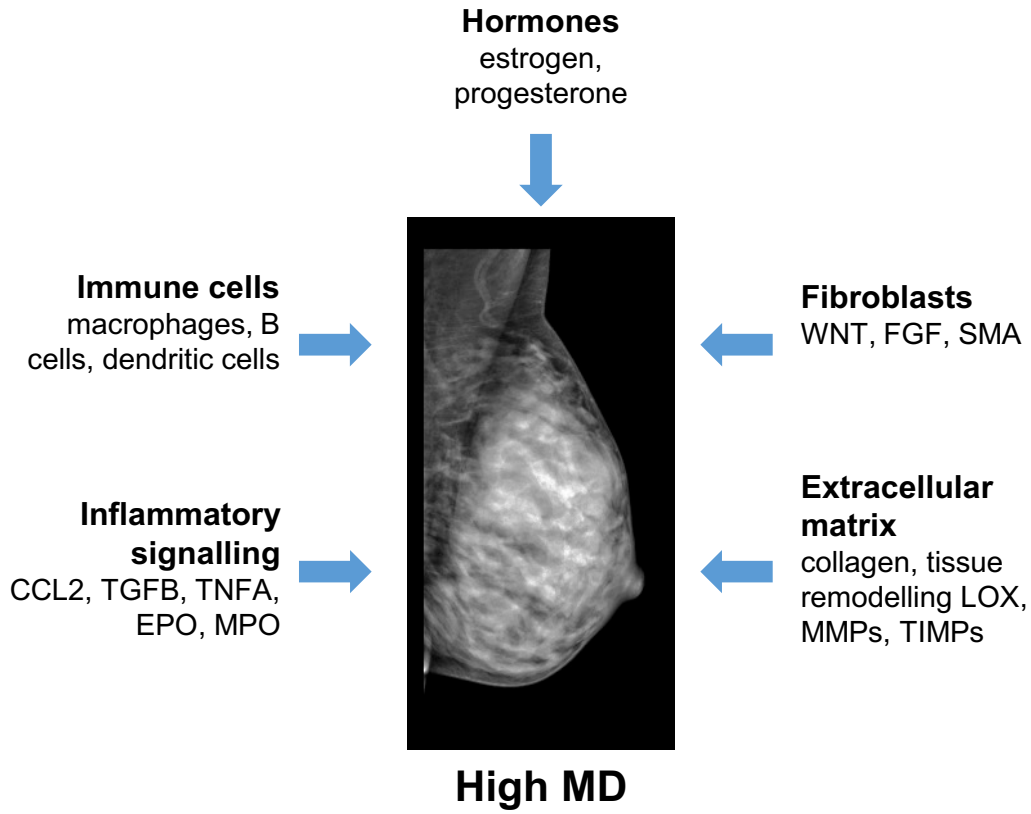

Figure 1.3: Biological mechanisms that are likely to contribute to mammographic density
Interactions between epithelium, stroma, the extracellular matrix, and immune signalling together with ovarian hormones may contribute to both elevated MD and breast cancer risk.

1.4.1 Mammary Epithelium in Mammographic Density

To understand how the mammary epithelium might contribute to MD, a number of studies have compared histology of breast biopsies or breast tissue collected from autopsies of known MD determined by the mammogram. These studies demonstrate that there is a greater abundance of epithelial cells, and epithelial cell hyperplasia in radiographically dense breast tissue [66-69]. However, many of these studies compared tissues with benign lesions, instead of normal breast tissue. Therefore, more recent studies have used tissues from women undergoing prophylactic mastectomies or reduction mammoplasties to analyse the tissue composition of MD. Two studies used X-ray guided biopsies to extract paired samples of high and low MD from within one breast. This is a powerful tool, as it eliminated interpatient variability providing greater statistical power. One study found no difference in glandular area between high and low density tissues from the same breast [70]. However, a later study with a greater sample size determined that areas of high MD are composed of a greater proportion of epithelium compared to low density regions [57]. It has been thought that MD may be attributed to a greater rate of cellular proliferation, however, there is no difference in proliferation between high and low density tissues, as determined by staining with Ki67 [57, 71, 72].

1.4.2 Mammary Stroma in Mammographic Density

The mammary stromal compartment is comprised of fibroblasts, immune cells, and ECM proteins such as collagen fibres [64]. The role of the stroma in the normal mammary gland is to provide physical support for the ductal network, and the cells of the stroma interact with the epithelium to regulate epithelial cell development and function [73]. However, these interactions can also play a role in breast cancer risk and tumour progression.

Some of the studies that investigated the epithelial composition of MD also analysed the proportions of stroma. This was analysed in multiple ways, some studies determined the proportion of stroma in breast tissues by measuring the area of non-epithelial cells and

collagen [69]. More recent studies using image guided biopsy of high and low density tissues from within one breast quantified stroma by calculating the percentage of stromal fibroblasts. Studies using both methods of measurement have reported that tissue from high density areas have a greater proportion of stroma, and greater percentage of stromal fibroblasts compared to low density tissues [69-71, 74]. In a study by Huo et al, it was reported that high MD tissues have 30% more stroma, and 40% less adipose tissue than low MD tissues. To further delineate the components of MD, further studies have investigated individual components of the stroma in high and low density tissues [57].

1.4.2.1 Mammary Fibroblasts

Fibroblasts are the most prominent cell type within the mammary stroma. They are non-inflammatory, non-vascular, non-epithelial cells. The primary role for mammary fibroblasts is production and regulation of turnover of collagen and other components of the extracellular matrix [75]. Fibroblasts also regulate the growth and differentiation of the surrounding epithelial cells through expression of paracrine factors [76].

Fibroblasts have been well studied for their roles in cancer, where the tumour stroma is composed of cancer associated fibroblasts (CAFs). CAFs produce growth factors and cytokines that directly promote breast cancer cell proliferation, and indirectly by signalling to other cells in the microenvironment [77]. CAFs can modulate the immune microenvironment by recruiting immune cells such as M2 macrophages and T cells to dampen anti-tumour immunity by expression of chemotactic cytokines [78]. They also secrete several cytokines to sustain a chronic inflammatory environment to drive pro-tumorigenic signals such as CCL2, interleukin 6 (IL6), inteleukin 8 (IL8), wingless related integration (WNT) and cyclooxygenase 2 (COX2) [75, 78, 79]. CAFs produce high levels of collagen and ECM remodelling proteins such as tenascin-C, fibronectin and matrix metalloproteinases (MMPs) [80, 81]. This creates a microenvironment that promotes

tumour invasion and metastasis and is associated with reduce survival in breast cancer patients [77, 82]. Though there is no standard marker of CAFs, they are generally identified by high gene expression of smooth muscle actin (SMA) and fibroblast growth factors (FGF) [83]. CAFs, or CAF-like fibroblasts, arise when fibroblasts are stimulated by activating signals from surrounding cells such as TGFB and TNFA [84, 85].

As described in the previous section, areas of the breast with high MD are comprised of high proportions of stroma. As fibroblasts are the most abundant cell type in the stroma, some studies determined the amount of stroma present by the percentage of stromal fibroblasts present in the tissue. High density breast tissue has a higher percentage of fibroblasts than low density tissues. Due to their high abundance in high MD breast tissue, and their known roles in cancer, their role in MD and breast cancer risk should be examined.

1.4.2.2 Collagen

The extracellular matrix and collagen are key components of the mammary stroma and are produced primarily by mammary fibroblasts [86]. ECM proteins and collagen provide structural integrity to the breast, and can have roles in breast cancer [87]. Previous studies have investigated the relationship between collagen and MD using different methods. Two studies compared screening mammograms to haematoxylin and eosin stained biopsies and determined collagen content by visual inspection by a pathologist [66, 74]. More recently, studies have used image guided paired samples of high and low density breast tissue and Masson's trichrome stain. This method is a more reliable measurement as it specifically stains collagen fibres, allowing for quantitative assessment of the percentage area occupied by collagen. These studies reported that high MD tissues have a greater percentage of collagen compared to low MD tissues [57, 69]. The study by Huo et al, further analysed the collagen content in high and low MD tissues by Second Harmonic

Generation imaging and discovered that the collagen fibres in high MD tissues are more tightly packed and have higher organisation than low MD tissues [57]. Continuous activation of fibroblasts can result in excessive deposition of collagen and other ECM components to develop fibrosis [88]. This can occur under stimulation from immune cytokines such as transforming growth factor beta (TGFB) and tumour necrosis factor alpha (TNFA) [89].

High abundance of collagen has been implicated in breast cancer risk. Previous studies used a transgenic mouse with increased stromal collagen in the mammary glands. These mice exhibited three times the amount of tumour formation compared to control mice, and the tumours were more invasive and had greater metastasis [90]. This study proposed that the high abundance of collagen may directly promote tumorigenesis by influencing mammary fibroblasts to secrete growth factors and cytokines to promote tumorigenesis in neighbouring epithelial cells, or directly in epithelial cells through perturbation of focal adhesion by ECM stiffness [90, 91]. ECM stiffness is facilitated by lysyl oxidase (LOX), which mediates covalent cross-linking between collagen molecules to assemble collagen fibres. Expression of LOX is elevated in cancer, and has been demonstrated to promote tumour growth and invasion in mouse models of breast cancer [92].

In the mammary gland, collagen is regulated by other proteins in the stroma produced by surrounding fibroblasts and immune cells [64]. Matrix metalloproteinases (MMPs) break down components of the ECM including collagen and the basement membrane, and this action is inhibited by Tissue Inhibitors of Metalloproteinases (TIMPs) [93, 94]. One study has investigated these enzymes in MD, however the associations were inconsistent and appeared to be dependent on ethnicity [95]. In breast cancer, MMPs are secreted by the tumour, surrounding fibroblasts, and infiltrating immune cells to remodel the ECM, promoting tumorigenesis, invasion, angiogenesis and metastasis [96, 97].

1.4.2.3 Transforming Growth Factor Beta 1 (TGFB1)

Transforming growth factor beta 1 (TGFB1) is a highly pleiotropic cytokine with a diverse number of cellular functions. It is involved in proliferation, differentiation, apoptosis, extracellular deposition, as well as modulating inflammation and immune responses [98, 99]. TGFB1 is secreted by almost all cell types in the body including epithelial cells, fibroblasts, macrophages and other immune cells and its receptors are expressed on most cell types [98, 100].

TGFB1 plays many roles in breast cancer, however, these functions can be both tumour suppressive and tumour promoting. The tumour suppressive functions are shown in murine studies of early tumorigenesis when constitutive expression of TGFB1 in the mammary gland results in decreased mammary tumour susceptibility when challenged with the chemical carcinogen DMBA [101]. When TGFB1 signalling is inhibited in the mammary gland, mice exhibit shorter tumour latency and increased tumour incidence [102]. In early cancer development, TGFB1 can disrupt the cell cycle in breast cancer cells to induce apoptosis to inhibit growth and suppress tumour development [103-106]. However, TGFB1 can also act as a tumour promotor during later stages of tumour development. TGFB1 functions to promote transformation of cells and is associated with tumour invasion [106-108]. Many studies have linked TGFB1 to metastasis. Mice with overexpression of TGFB1 in the mammary glands had greater tumour invasion and metastasis [109]. Further, expression of TGFB1 in breast cancers is associated with metastasis [110]. TGFB1 is a key modulator of angiogenesis, by regulating cell proliferation and migration, as well as regulation of ECM turnover and suppression of anti-tumour immunity [111, 112].

TGFB1 is a key regulator of fibroblast activity and regulation of ECM deposition and turnover, and is therefore implicated in many fibrotic diseases. Animal models have

demonstrated the link between TGFB1 and fibrosis, for example overexpression of TGFB1 in rat lungs induces pulmonary fibrosis [113]. In a mouse model, constitutive expression of TGFB1 in the liver results in extensive hepatic fibrosis [114]. Inhibition of TGFB signalling in animal models of fibrosis has been shown to reduce renal, cardiac and hepatic fibrosis [115-117]. TGFB1 can contribute to fibrosis by stimulation of fibroblast activation through upregulation of connective tissue growth factor (CTGF) [118]. It also promotes expression of collagen genes and downregulates ECM proteinases such as MMP1 to preserve the ECM structure [119].

There have been few studies that have investigated the role of TGFB in MD. ChipSeq analysis revealed several genes involved in TGFB signalling exhibited decreased expression in breast tissue of women with high MD compared to those with low MD [120]. Further, another study reported single nucleotide polymorphisms in TGFB1 gene which impaired TGFB signalling were associated with increased percentage MD in nulliparous women [121]. The multifunctional and contradictory roles of TGFB1 in fibrotic activity in the stroma, and in both promoting and suppressing breast cancer development highlights that more investigation is required to determine the role of TGFB1 in MD and breast cancer risk.

1.5 Immune Cells in Mammographic Density

Immune cells are a key component of the mammary gland and are vital in facilitating mammary gland development and in immune surveillance to protect against potentially tumorigenic cells [122]. However, immune cells in the mammary gland can also contribute to breast cancer risk and progression of breast cancer.

Two studies have examined the immune cell profile using paired, image guided samples of high and low density breast tissue to histologically stain for several immune markers.

This study reported that the epithelium of high MD breast tissue had a higher percentage of vimentin+/CD45+ immune cells suggestive of local inflammation in these areas [57]. Further analysis revealed that high MD tissues had a greater percentage of CD4+ T cells, CD20cy+ B cells and CD11c+ dendritic cells, and no difference in populations of CD8+ cytotoxic T cells, CD56+ natural killer cells (NK), compared to low MD tissues [123].

Infiltration of immune cells can influence the growth and progression of breast cancer, and can be an indicator of prognosis. Infiltration of CD8+ cytotoxic T cells and CD56+ NK cells has been observed to be favourable the patient outcomes with breast cancer, as both these cells play a role in anti-tumour immunity [124, 125]. Dendritic cells, T cells and B cells are important in the normal mammary gland to maintain tumour surveillance [122]. Dendritic cells present tumour antigens to activate T cells to mediate killing of tumour cells [126]. However, depending on the immune cell profile, infiltration of immune cells in the tumour microenvironment can have both have anti-tumour effects or tumour promoting effects. Infiltration of breast cancers with T cells and B cells has been associated with increased invasiveness and poor prognosis [127, 128]. It is suggested that the CD4+ T cells in high MD tissues are of the Th2 subtype, as these tissues express high levels of IL-6 and IL-4 that drive differentiation to Th2 T cells [123]. These cells are associated with tumour promoting signals and are often secreted by tumours themselves to help tumour cells grow and evade immune surveillance [129].

1.5.1 Macrophages

Macrophages are highly plastic cells and key immune cell in the mammary gland. They have multiple functions in regulating mammary gland development during the ovarian cycle, pregnancy, lactation, and remodelling the mammary gland back to its pre-pregnant state [130]. They also play a role in breast cancer, and can have both pro-tumorigenic and anti-tumorigenic activities. In high MD tissues, there is a greater percentage of CD68+

macrophages in the epithelium, however the phenotype and function of these cells in high MD are currently unknown [123].

The function of macrophages in the mammary gland depend on their phenotype. Macrophages differentiate into different phenotypes when exposed to different cytokine signals in the microenvironment. Polarisation to classically activated macrophages, or M1 macrophages, occurs in response to infection or injury, and can be induced by exposure to microbial by-products such as lipopolysaccharide (LPS) or by cytokines interferon gamma (IFNG) and TNFA [131, 132]. They have anti-microbial and anti-tumorigenic functions by secreting an array of pro-inflammatory cytokines including reactive oxygen species to induce tissue damage and impair wound healing [133-135]. M1 macrophages can be identified by expression of CD80 and nitric oxide synthase (iNOS) surface markers [131, 136].

Alternatively activated, or M2 macrophages, are predominantly polarised by signals from cytokines IL-4 and IL-13 and can be identified by surface marker expression of CD163 or CD206 [137, 138]. M2 macrophages are anti-inflammatory and produce abundant IL-10 and TGFB [132]. These cells are pro-tumorigenic, as they have immune suppression functions that help tumour cells evade the immune system [139]. They are also involved in tissue remodelling through production of ECM components, and enzymes such as MMPs to degrade collagen and other ECM components [135, 140, 141]. This helps to facilitate angiogenesis and metastasis of tumour cells along with production of pro-angiogenic factors such as vascular endothelial growth factor (VEGF) and platelet derived growth factor (PDGF) [132, 142]. Polarisation to the M2 phenotype can occur during chronic inflammation [127].

Due to their involvement with tumour progression, a subset of M2 macrophages have been identified in the tumour microenvironment as tumour associated macrophages (TAMs) [131, 143, 144]. Like M2 macrophages, TAMs have high expression of IL-10, TGFB and VEGF [131, 132]. Infiltration of TAMs in the tumour microenvironment is associated with a more aggressive disease, poor prognosis, and decreased survival in breast cancer patients [136, 144]. Recent research is investigating the potential of repolarising M2-like TAMs towards an M1 phenotype to promote anti-tumorigenic immunity [136]. Currently, macrophage polarisation in a stroma rich environment such as high MD breast tissue has not been investigated.

1.6 Inflammation as a Driver of Mammographic Density and Breast Cancer Risk

Chronic inflammation is one of the hallmarks of cancer, and can promote mammary tumour initiation, growth, invasion, and metastasis. Elevated markers of inflammation such as C-reactive protein (CRP), IL-6 and TNFA are associated with an increased risk of breast cancer, increased risk of recurrence, and reduced tumour free survival [145]. The use of non-steroidal anti-inflammatory drugs (NSAIDs) can be employed as a preventative agent that reduces the risk of many different types of cancer [146, 147]. Daily use of NSAIDs, particularly aspirin, can reduce risk of breast cancer by up to 39% [147].

Studies have implicated inflammation as a driver of MD. In a study that compared mammograms to healthy breast tissue taken from breast surgeries, it was reported that COX2 expression was greater in the stroma of high MD breasts compared to low MD breasts [120]. This was confirmed in a study of image guided paired sampling of high and low MD tissues from within one breast that revealed a greater abundance of COX2 in the epithelium and stroma of high MD, compared to low MD tissues [148]. Further, paired high and low MD tissue analysis has demonstrated that high MD tissues have higher expression

of IL6 and IL4, and increased infiltration of vimentin-positive immune cells than low MD tissue [123]. Genome wide studies have detected genetic variations in the IL-6 gene are associated with high MD [149] indicative of an inflammatory microenvironment in high MD breast tissue. Therefore, there is potential for NSAID use to decrease mammographic density. In a mouse model with high abundance of collagen in the mammary glands, reminiscent of MD, treatment with a COX2 inhibitor reduced tumour size and metastasis [150]. In women, it is unclear whether NSAID reduces MD, however, one study found that NSAID use decreased the risk of MD increasing over a 9-28-month time frame [151, 152].

Currently, the cause of inflammation in MD is unknown, however there are a number of inflammatory mediators that are potential drivers of MD and the associated increased breast cancer risk.

1.6.1 Monocyte Chemotactic Protein 1 (CCL2)

Monocyte chemotactic protein 1, or CCL2, is a pro-inflammatory cytokine. It is produced by many cell types including epithelial cells, tumour cells, fibroblasts, and adipocytes, as well as immune cells such as monocytes and macrophages [153, 154]. The CCL2 receptor, CCR2, is predominantly expressed on monocytes and macrophages, but also other leukocytes, fibroblasts, and endothelial cells [155, 156]. The primary function of CCL2 is as a chemoattractant for leukocytes, particularly monocytes and macrophages, and recruits these cells areas of tissue injury and inflammation [156].

Many studies have investigated the role of CCL2 in breast cancer, and suggest that CCL2 increases breast cancer risk and tumour progression. In an *Mmtv-Ccl2* transgenic mouse model, constitutive expression of CCL2 in the mammary glands reduced tumour latency and tumour free survival when challenged with the chemical carcinogen 1, 3-Dimethylbutylamine (DMBA) [157]. Intravenous administration of CCL2 to mice with

xenograft human breast tumours increased metastasis to the lungs and bone, and an increase in macrophage infiltration to these sites [158]. This has been further confirmed in CCL2 knockout mice in which metastasis of tumour cells was reduced [159]. In humans, expression of CCL2 is highly elevated during tumour development, and is associated with infiltration of macrophages [160-162]. CCL2 expression by breast tumours is associated with high tumour grade, angiogenesis, metastasis, and poor prognosis [163, 164]. However, there is some evidence that CCL2 can also have some suppressive effects on tumour development through recruitment of T cells that mediate anti-tumour immunity, although these effects of CCL2 have not been studied extensively [165, 166].

CCL2 has been implicated in many fibrotic diseases. CCL2 is highly expressed in the lungs of patients with lung fibrosis [167]. Animal studies have demonstrated that CCL2 deficient mice do not develop pulmonary fibrosis in response to bleomycin, a drug that induces fibrosis [168]. Bleomycin-induced fibrosis can also be reduced in mice when treated with anti-CCL2 therapies [169]. CCL2 promotes excessive production of ECM and collagen in hepatic fibrosis and renal fibrosis [170]. CCL2 can drive fibrosis by activating fibroblasts directly to exacerbate ECM and collagen production [171]. In *Mmtv-Ccl2* mice, constitutive expression of CCL2 in the mammary glands results in greater stromal thickness and collagen deposition surrounding the epithelium [157].

The roles of CCL2 in breast cancer risk and fibrosis suggest that CCL2 could promote increased MD. In women, paired high and low MD tissue samples revealed that CCL2 expression is elevated in the epithelium of high MD breast tissue [157]. This study, along with the literature suggest that CCL2 could be an inflammatory driver of MD and the associated breast cancer risk.

1.6.2 Peroxidase Enzymes

Myeloperoxidase (MPO), produced by monocytes, and eosinophil peroxidase (EPO), produced by eosinophils, are peroxidase enzymes released by cells during inflammation and primarily known for their role in oxidative defence against invading bacterial pathogens [172]. However, MPO and EPO can also promote fibrosis associated with inflammatory diseases. For example, MPO has been identified to have pro-fibrotic effects in the liver during non-alcoholic steatohepatitis, and is found in high levels in the sputum of patients with cystic fibrosis [173, 174]. EPO has been implicated in renal fibrosis, and is increased in the serum of cystic fibrosis patients [175, 176]. In a previous study by DeNichilo et al, the role of peroxidase enzymes in fibrotic diseases was investigated by examining the direct effects of MPO and EPO on fibroblasts from different tissue types. This study found that both MPO and EPO can stimulate mammary fibroblasts to produce collagen I and IV *in vitro* [177]. In breast cancer, it has previously been reported that deposits of EPO can be found within and around the tumours and play a role in HER2 positive breast cancers to promote tumour growth [178-180]. Several studies have reported that concentration of circulating MPO in serum is elevated in breast cancer patients [127].

1.6.3 Tumour Necrosis Factor Alpha (TNFA)

Tumour necrosis factor alpha (TNFA) is a pleiotropic cytokine involved in inflammation [181]. It is produced primarily by macrophages, but also several other cells including CD4+ T lymphocytes, mast cells, endothelial cells, adipocytes, fibroblasts and tumour cells, including breast cancer cells [182].

Studies have investigated the role of TNFA in breast cancer, however, the literature suggests that it plays opposing roles. Circulating concentration of TNFA is positively correlated with breast cancer invasiveness and poor prognosis [183, 184]. *In vitro* studies have implicated TNFA in tumour growth, invasion, and enhanced metastasis to the lungs.

In ER positive, HER2 positive, and in triple negative breast cancer cell lines, TNFA has induced proliferation, migration, and invasion [185, 186]. Further, TNFA induces production of MMP9 by cancer cells that enhances tissue remodelling to promote angiogenesis and metastasis [186, 187]. Conversely, TNFA can also inhibit tumour growth and kill different types of tumour cells in leukaemia, lymphoma, liver cancer and breast cancer. In one study TNFA induced cytotoxic cell death in ER positive breast cancer cell lines [188]. Its use as a targeted anti-cancer treatment is being investigated in combination with chemotherapeutics and radiation to treat breast cancer, however, some studies have reported that TNFA can promote resistance to chemotherapy in some breast cancer cells [189, 190]. Clearly, the role of TNFA in breast cancer is complex, and its role in inflammation driven breast cancer risk still requires investigation.

There have been few studies investigating the role of TNFA in MD. One study measured the relationship between circulating inflammatory markers in relation to MD obtained from screening mammograms, this study found no association between serum TNFA concentration and MD [191]. However, another study measured breast tissue gene expression of TNFA in post-menopausal women and found that high MD was associated with higher expression of TNFA [192]. The role of TNFA in MD is currently unknown, however it could regulate mammary fibroblast activity and fibrosis. Studies of TNFA have revealed that it can have both pro and anti-fibrotic effects in models of fibrotic diseases [193]. TNFA promotes proliferation of fibroblasts, increases production of tissue remodelling enzymes including MMPs [194]. In diseases characterised by fibrosis, such as Crohn's disease, TNFA has been shown to increase collagen accumulation [195]. Conversely, other studies have reported that TNFA can inhibit production of collagen I in cultured fibroblasts [196]. The role of TNFA in MD and mammary fibroblast activity appear to be complex and requires investigation.

1.7 CONCLUSION

Mammographic density is strong independent risk factor for breast cancer. Women with high MD have a 4- to 6-fold increased risk of breast cancer compared to women with low MD when matched for age and BMI. MD is influenced by age, hereditary factors, BMI, parity, menopausal status, and hormonal therapies. Histological studies have revealed that high MD is characterised by high proportions of stroma containing fibroblasts and an immune cell profile indicative of an inflammatory, tumour promoting environment. However, the underlying biological mechanisms that mediate MD are yet to be elucidated. Chronic inflammation has been established to contribute to breast cancer risk and development. There are number of immune and inflammatory factors that contribute to breast cancer risk, as well influence the stromal environment. Peroxidase enzymes, TGFB, TNFA and CCL2 have been demonstrated to influence the stromal environment through effects on fibroblast activity and immune cells, as well as contributing to breast cancer risk and development. Particularly, CCL2 has directly been implicated as a driver of MD and breast cancer risk in both mouse models and paired high and low MD human breast tissue. However, biological pathways and mechanisms by which these immune factors may contribute to MD and breast cancer risk is currently unknown. Understanding the drivers of MD and the associated increased breast cancer risk may provide targets for preventative therapies in the future for women with high MD.

1.8 HYPOTHESIS & AIMS

The experiments described in this thesis aim to address the following hypotheses:

- Mammary fibroblast gene expression and collagen production are altered by inflammatory and immune regulatory factors.
- Crosstalk between mammary fibroblasts, macrophages and CCL2 influences fibroblast activity and macrophage phenotype.
- CCL2 affects biological pathways that contribute to mammographic density, and promotes tumour development and progression.

The experiments described in this thesis will address the following aims:

1. To investigate the effects of mammographic density and immune regulatory factors on the phenotype and fibrotic activity of primary human mammary fibroblasts *in vitro*.
2. To investigate the crosstalk between mammary fibroblasts, macrophages, and CCL2 using human *in vitro* models.
3. To investigate the role of CCL2 in mammary tumour development and progression, and the effects of CCL2 on biological pathways in the mammary gland using *in vivo* mouse models.

CHAPTER TWO

MATERIALS AND METHODS

2.1 HUMAN NON-NEOPLASTIC BREAST TISSUE

2.1.1 Study Population

This study was approved by the Human Ethics Committee at the University of Adelaide and The Queen Elizabeth Hospital (TQEH Ethics Approval #2011120). Between 2011 and 2017, participants undergoing reduction mammoplasty, mastectomy for breast cancer removal, or prophylactic mastectomy donated healthy breast tissue as confirmed by TQEH pathology department, a blood sample at the time of surgery, and completed a comprehensive medical and personal history questionnaire following surgery. All participants were between the age of 18 and 70, and were capable of giving informed consent. In the event that a participant was pregnant or currently undergoing chemotherapy, the participant was excluded from the study. The protocol followed for tissue collected is detailed in Figure 2.1. The total tissue collected is divided in two, one undergoes enzymatic digestion for isolation of cells such as fibroblasts as detailed in section 2.2.1. The other half of the tissue is cut into fragments (approximately 1-2cm^3) and fixed and embedded in wax for histological analysis as detailed in sections 2.1.2 and 2.1.3.

2.1.2 Tissue Embedding, Sectioning and Staining.

Small fragments of breast tissue were dissected from each participant and fixed in 4% paraformaldehyde (Sigma Aldrich; Cat#P6148) for 7 days at 4°C, tissue was then washed twice in PBS and transferred to 70% ethanol until processing. Tissue was processed using the Leica TP1020 Tissue Processor (Leica Microsystems) with the following dehydration and embedding protocol; 75 minutes 70% ethanol, 75 minutes 85% ethanol, 75 minutes 90% ethanol, 75 minutes 96% ethanol, 2 x 75 minutes 100% ethanol, 2 x 75 minutes

Xylene, 2 x 75 minutes paraffin wax under vacuum conditions. Tissue was moulded into paraffin wax blocks and stored at room temperature. Tissue sections were cut at 5 µm thickness using the Leica Rotary Microtome (Leica Microsystems) onto SuperFrost Plus Slides (Menzel-Gläser, Germany). Tissue sections were bonded onto slides by heating on a 37°C heating block for 30 minutes and stored at room temperature for histology.

2.1.2.1 Haematoxylin and Eosin Staining of Human Breast tissue

Paraffin embedded breast tissue sections were dewaxed using Xylene (Merck Millipore, Germany; Cat#108298) for 3 x 5 minutes, and rehydrated in gradual dilutions of ethanol for 3 minutes each (2 x 100%, 1 x 90%, 1 x 70% and 1 x 50%) followed by 2 minutes in MilliQ water. Tissue sections were stained in haematoxylin (Sigma Aldrich; Cat#HHS16) for 30 seconds, then stained in eosin (Sigma Aldrich; Cat#318906) for 10 seconds. Sections were then dehydrated through gradual increase of ethanol concentration (2 minutes 90%, 2 x 1 minute 100%), and cleared by 2 x 5 minutes in Xylene. Slides were then mounted with coverslips using Entellan mounting media (Proscitech, Australia; Cat#IM022).

2.1.3 Histological Classification of Mammographic Density

Haematoxylin and eosin stained breast tissue sections were observed by a panel of 4 scientists to categorise each section into a semi-quantitative scale based on the percentage of fibroglandular tissue comprised of stroma and epithelium in relation to adipose tissue. One tissue section was assessed for each tissue block collected. Each patient had 10 or more tissue blocks collected from the donated sample. Tissue was collect from different areas of the sample to ensure tissue blocks would be representative of the whole sample. Greater percent of stroma and epithelium corresponded to higher density scores. The classification scale ranged from 1-5, 1 is 0 – 10%, 2 is 10-25%, 3 is 25-50%, 4 is 50-75% and 5 is >75% (Figure 2.2).

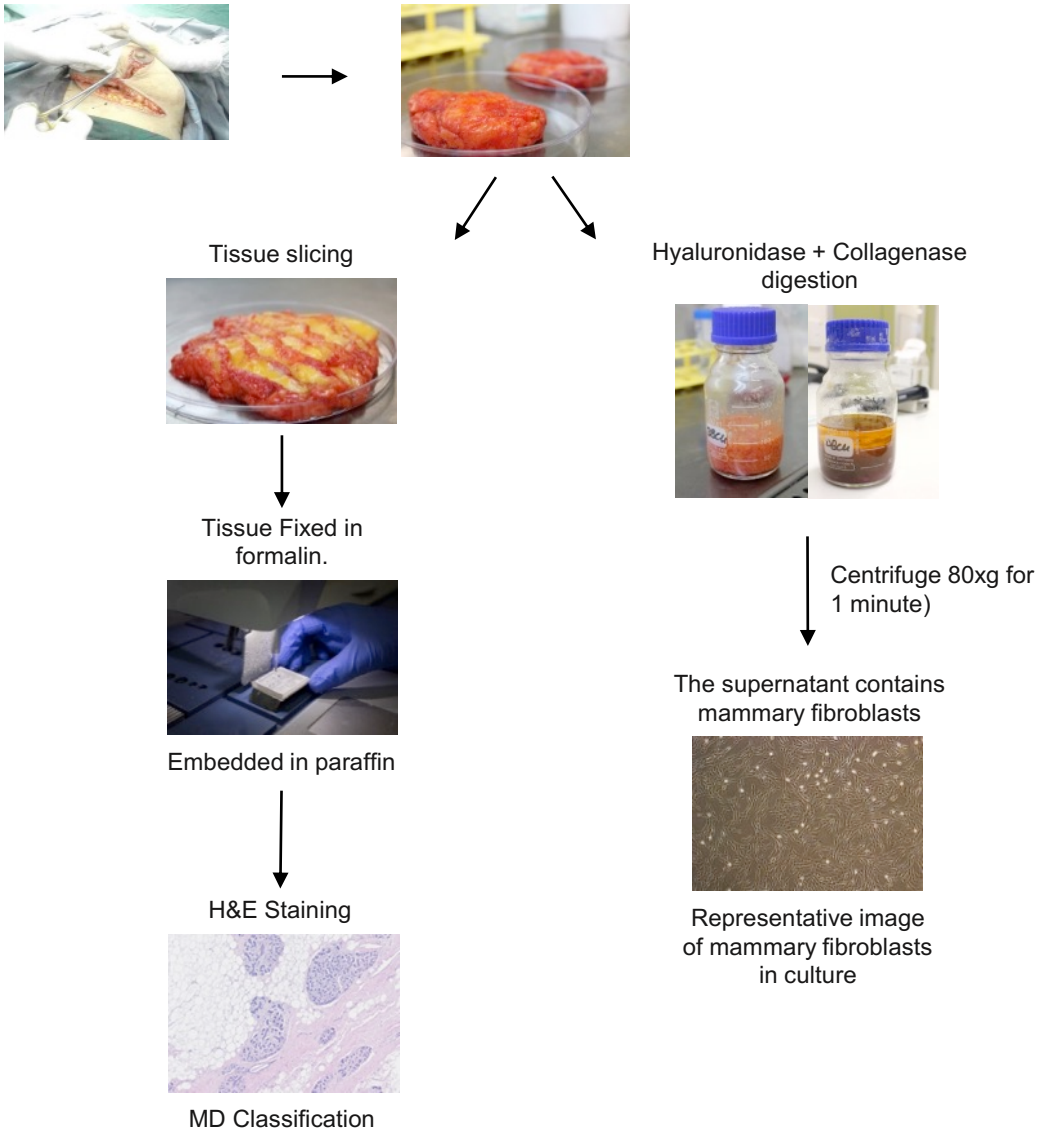

Figure 2.1: Protocol for breast tissue processing.
Human breast tissues were collected from surgery patients. One portion of this tissue was enzymatically digested for 16 hours. Mammary fibroblasts were obtained through several steps of washing the stromal cell component. Another portion of breast tissue was formalin fixed paraffin embedded and stained with haematoxylin and eosin for histological scoring of density.

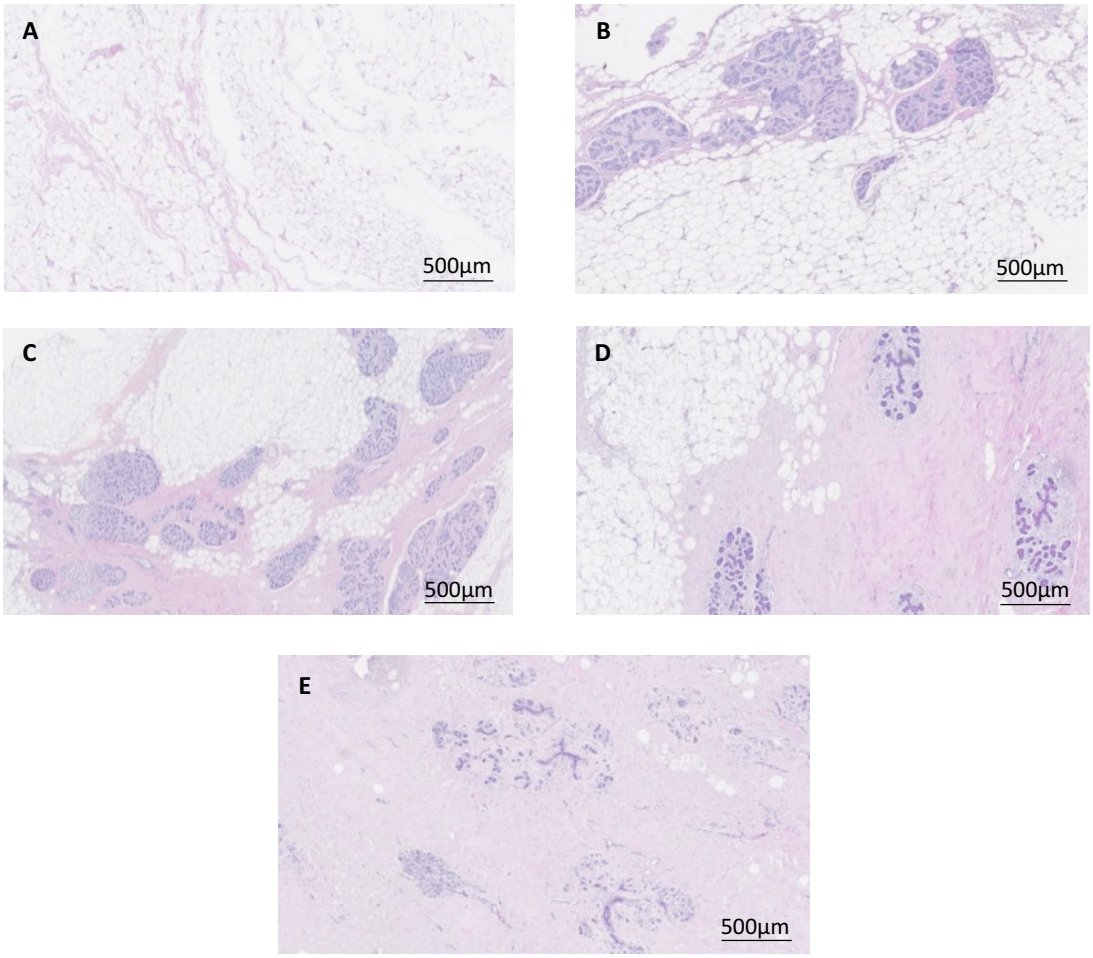

Figure 2.2: Histological classification of mammographic density.
Haematoxylin and eosin stained breast tissue was assessed by a panel of scientists to grade mammographic density according to the percentage area occupied by fibroglandular tissue. A density score of 1 is 0-10% (A), score of 2 is 11-25% (B), score of 3 is 26-50% (C), score of 4 is 51-75% (D) and score of 5 is greater than 75% fibroglandular tissue (E). These density scores were then used to select patient fibroblasts to be used in cell culture experiments.

2.2 CELL CULTURE

2.2.1 Isolation and culture of Human Mammary Fibroblasts

A portion of participant breast tissue was designated for fibroblast isolation. This tissue is manually digested using a tissue knife then enzymatically digested using 100U/mL hyaluronidase (Sigma Aldrich, St Louis, USA; Cat#H3506) and 480U/mL collagenase (Sigma Aldrich; Cat#C0130) in Advanced DMEM/F12 medium (Life Technologies, Australia; Cat#12634010) supplemented with 10% foetal calf serum (FCS) (Thermo Fischer Scientific, USA; Cat#10099141), 10mM HEPES (Life Technologies; Cat#15630080), 2.5mg/mL Fungizone (Life Technologies; Cat#15290018) , 1 x L-Glutamine (Life Technologies; Cat#25030081) and 1 x Penicillin/Streptomycin (Life Technologies; Cat#15240062). The tissue digestion flask was sealed using parafilm and was incubated overnight for 16-18 hours in a 37°C shaking water bath. The digest was then centrifuged at 80 x g for 1 minute and the top liquefied fat layer carefully removed and discarded. The supernatant containing stromal cells was carefully harvested to not disturb the pellet of undigested tissue, then transferred to a clean Falcon tube and pellet re-suspended and brought to 50mL with supplemented Advanced DMEM/F12. The product was then centrifuged at 400 x g for 5 minutes, supernatant was discarded and the pellet re-suspended in 40mL of supplemented Advanced DMEM/F12 medium. This was repeated until the supernatant became clear. The stromal cell pellet was treated with red blood cell lysis buffer (BD Bioscience, USA; Cat#555899) for 15 minutes, equilibrated with PBS, and filtered through 40µm cell strainers (Sigma Aldrich; Cat#CLS431750) to remove debris. The cell suspension was washed 3 times in PBS by centrifugation at 400 x g for 5 minutes and the supernatant discarded. The pellet was re-suspended in 8mL of supplement Advanced DMEM/F12 with 10% heat inactivated foetal calf serum and cultured in a T25 tissue culture flask and maintained at 37°C in 5% CO_2. Mammary fibroblasts were confirmed by morphological appearance in culture and production of collagen 1.

2.2.2 Culture of THP-1 Monocytes

The human monocyte cell line THP-1 cells were cultured in RPMI-1640 (Life Technologies; Cat#32404014) supplemented with 10% FCS, 1x penicillin/streptomycin, 1x L-glutamine and 10mM HEPES at 37°C in 5% CO_2. Suspended cells were split by dividing suspension fluid into multiple flasks and fresh media was added every 3 days to maintain a cell density of 0.5-1.0 x 10^6 cells/mL in T75 flasks.

2.2.3 Cryopreservation and Thawing

Human mammary fibroblasts isolated from patient human breast tissue were expanded to 90% confluence in 4 x T75 tissue culture flasks. These cells were then pooled and re-suspended in 50% foetal bovine serum in DMEM/F12 media containing 6% dimethyl sulfoxide (Sigma Aldrich; Cat#D5879) and aliquoted into 1mL cryovials and stored in the Basil Hetzel Institute liquid nitrogen storage facility at The Queen Elizabeth Hospital for later studies. For the use of cryopreserved cells in later studies, cryovials were collected and thawed in a 37°C water bath. The cell suspension was transferred to a Falcon tube. DMEM/F12 media supplemented with 10% foetal bovine serum, 1% HEPES, Fungizone, L-glutamine and penicillin/streptomycin was added drop-wise with constant agitation to a volume of 20mL. The cell suspension was centrifuged at 300 x g for 5 minutes and re-suspended in 8mL of media in a T25 tissue culture flask.

2.2.4 Cytokine and Peroxidase Treatment in Human Mammary Fibroblast Culture

Mammary fibroblasts were selected for cell culture according to their histological mammographic density score. For these studies, fibroblasts were used from women with low density scores 1, and high density scores 4 and 5 (Figure 2.2). Mammary fibroblasts from human participants were cultured with supplemented Advanced DMEM/F12 containing 10% heat inactivated FCS in a T25 tissue culture flask to 90% confluence. The

cells were then split into 5 x T75 tissue culture flasks to 90% confluence. Cell were then distributed into 2 x 6 well plates at a density of 2 x 10^5 cells per well and 1 x 96 well plate at a density of 1.2 x 10^5 cells per well and grown to 90% confluence in supplemented Advanced DMEM/F12 with 10% FC. Cells were then serum starved overnight in serum free supplemented Advanced DMEM/F12. Cells were treated for 72 hours with either TGFB1 (10ng/mL) (R&D Systems, USA; Cat#240-B-010), eosinophil peroxidase (2.5µg/mL) (Lee Biosolutions, USA; Cat#342-60), myeloperoxidase (5µg/mL) (R&D Systems; Cat#3174-MP-250), TNFA (10ng/mL) (Life Technologies; Cat#PHC3016) or CCL2 (500µg/mL) (R&D Systems; Cat#RDS27MC050) in the presence or absence of 100µmol/L ascorbic acid (Wako Chemical Industries, Japan; Cat#50990141) in serum free, supplemented standard DMEM medium (Life Technologies; Cat#12430054).

2.2.5 Indirect Co-Culture of Human Mammary Fibroblasts and Differentiated THP-1 Cells

Mammary fibroblasts were seeded into the base of a 6 well plate at 5 x 10^4 cells/mL in supplemented DMEM media, and grown to 90% confluence before serum starvation overnight. Separately, 2mL of THP-1 monocyte cell suspension was added to the internal compartment of 24mm trans-well with 0.4µm pore polycarbonate membrane (Corning, USA; Cat#3412) at 0.5 x 10^6 cells/mL and were activated by 5ng/mL of phorbol-12-myristate-13-acetate (Abcam, UK; Cat#ab120297) in supplemented RPMI media for 72 hours to differentiate THP-1 cells to adherent M0 macrophages. Trans-well inserts were then placed into the wells containing mammary fibroblasts along with macrophage only controls, and were incubated in supplemented, serum free DMEM with or without CCL2 (500µg/mL) for 72 hours.

2.3 PROTEIN ANALYSIS

2.3.1 Enzyme-Linked Immunosorbent Assay

Soluble collagen type I in cell conditioned media was measured using a direct coat enzyme-linked immunosorbent assay (ELISA). Standard curves were developed using purified collagen I derived from human placental collagen (BD Biosciences, Australia; Cat#354265). Cell supernatants and standardised samples were added to a 96-well Maxisorp plate (Nunc, Denmark; Cat#423501) at a volume of 100µL per well and stored at 4°C overnight. The plate was washed with PBS-Tween 0.05% and blocked using a solution of 2.5% bovine serum albumin (BSA) in PBS for 1hr at room temperature. The primary antibody used was rabbit anti-human collagen I polyclonal antibody (Rockland Immunochemicals, USA; Cat#600-401-103-0.5) and was added to the plate at 0.25µg/mL in a 5% skim dairy milk solution for 3 hours at room temperature with agitation. After washing, the secondary antibody europium-tagged anti-rabbit antibody (Perkin Elmer Life Sciences, Finland; Cat#AD105) was added at 0.5µg/mL in 1% BSA/PBS for 1 hour at room temperature. After the plate was washed, an enhancement solution (Perkin Elmer Life Sciences, Cat#1244-105) was added for 15 minutes before measuring fluorescence using the FLUOstar Optima plate reader (BMG Labtech Australia, VIC, Australia) at excitation 355nm and emission 620nm. The collagen concentration for each sample was determined using the standard curve and expressed in µg/mL.

2.3.2 Sirius Red Analysis of Insoluble Collagen

Sirius red dye was used to determine changes in insoluble collagen deposition. Media was aspirated from fibroblast culture plates and washed in PBS. Cells were fixed for 10 minutes using 100% ethanol. The plate was washed under running tap water and picric acid-sirius red solution (Sigma Aldrich; Cat#365548, Cat#P6744) was added for 1 hour. After the stain was removed, the plate was washed with 0.01M hydrochloric acid and allowed to air dry.

To elute the dye, 0.1M sodium hydroxide was added to the plate. Absorbance was then measured on the FLUOstar Optima plate reader (BMG Labtech Australia) at 550nm.

2.4 FLOW CYTOMETRY OF THP-1 MACROPHAGES

Differentiated THP-1 cells were detached from the internal channel of trans-wells with trypsin for 2 minutes at 37°C. Cells were harvested and placed in 5ml FACS polypropylene tubes, and washed twice in FACS wash buffer (PBS, 1% FCS, 20 mM sodium azide), 500 x g for 5 minutes. Cells were re-suspended in FACS wash to $1x10^6$/ml and blocked in a 1% human serum for 20 min at RT. Cells ($1x10^5$) were aliquoted into FACS tubes containing antibodies: PE/Cy5 conjugated anti-CD80 (clone 2D10) (Biolegend, USA; Cat#305210), FITC conjugated anti-CD68 (clone YI/82A) (Biolegend; Cat#333806), APC-H7 conjugated anti-HLA-DR (clone G46-6) (BD Bioscience; Cat#561358) and Alexa Fluor® 647 conjugated anti-CD163 (clone GHI/61) (BD Bioscience; Cat#562669). Staining was performed at 4˚C for 10 min followed by two washes in wash buffer. Cells were re-suspended in 100µl of buffer and analysed by flow cytometry using FACS Canto II (BD Biosciences, USA). Isotype controls were used to develop the gating strategy shown in Figure 2.3.

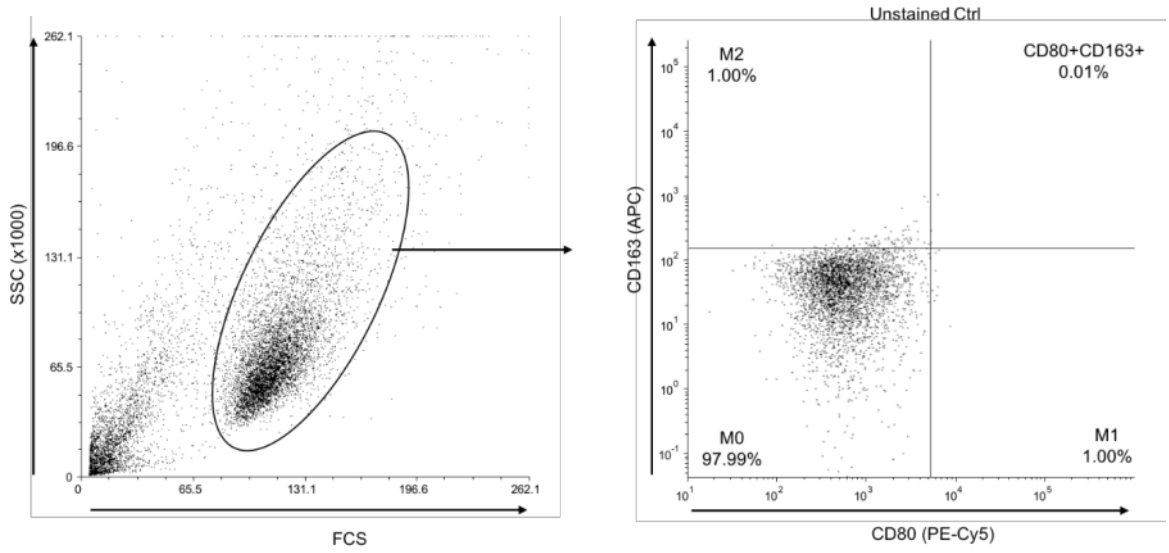

Figure 2.3:Gating strategy for flow cytometry of THP-1 derived macrophages.
Viable Cells were gated (oval gate) and levels of CD163 and CD80 were assessed to differentiation between M1 and M2 phenotypes respectively. Isotype controls serve as a baseline for quadrant gating. CD80, CD163 double negative cells were defined as M0 phenotype. A discrete population of CD80, CD163 double positive cells could be seen, potentially representing a transitionary macrophage population.

2.5 ANIMALS

2.5.1 Mice

Experiments involving use of animals were approved by the University of Adelaide Animal Ethics Committee and were conducted in accordance with the Australian Code of Practice for the Care and Use of Animals for Scientific Purposes (8th Ed. 2013). All mice were housed in specific pathogen free conditions with 12hr light cycling (12hr light, 12hr dark) and temperature controlled at the Laboratory Animal Services Medical School Facility. All breeding was performed under ethics approval M-2015-088, tumour studies were performed under ethics number M-2017-043.

2.5.1.1 MMTV-Ccl2 Mice

The Mmtv-Ccl2 transgenic mouse was originally generated through sub-cloning and pronuclear microinjection techniques [157]. The mouse mammary tumour virus (MMTV) promoter drives constitutive expression of chemokine ligand 2 (CCL2) on an FVB background. A breeding colony of homozygous MMTV-Ccl2 mice is maintained and experiments using these mice use FVB mice as wildtype controls.

2.5.1.2 MMTV-PyMT Mice

A breeding colony of heterozygous Mmtv-PyMT mice on an FVB background were maintained in the University of Adelaide Laboratory Animal Services Medical school Facility (Ethics number: M-2015-088). These mice contain the polyomavirus middle T antigen (PyMT) oncogene which is driven by the mouse mammary tumour virus (MMTV) promoter. This results in mice with mammary gland tumours with 100% penetrance in FVB mice.

2.5.1.3 Generation of PyMT/CCL2 Cohort

Male Mmtv-PyMT mice on an FVB background were mated with homozygous Mmtv-Ccl2 female (FVB background) mice or FVB control mice. The females from their litters were genotyped after weaning at 21 days, for the PyMT oncogene, PyMT positive mice were used for subsequent experiments.

2.5.2 Blood Collection

Prior to dissection, blood was collected from the mice by cardiac puncture. Firstly, mice were put under deep anaesthesia with 0.4-0.5mL or 2% Avertin, confirmed by lack of reflex to toe pinch. Up to 1mL of blood was collected using a 20g needle directly from the heart. Blood was incubated at room temperature for 30 minutes and centrifuged for 10 minutes at 500 x g. The serum was then collected and stored at -80°C.

2.5.3 Tumour Detection by Palpation

To detect tumours, female PyMT and PyMT/CCL2 mice were monitored weekly from 6 weeks of age. Mice were restrained by the scruff of the neck by holding firmly between the thumb and forefinger. While holding the mouse upright, each of the 10 mammary glands were gently palpated for tumours. The first three mammary pairs were palpated against the rib cage using the forefinger, while the fourth and fifth pairs were palpated by pinching between the thumb and forefinger. Upon detection, mammary tumours were measured using callipers to approximate tumour volume. Mice were sacrificed at 9 and 12 weeks or when tumour volume exceeded 2000mm^3.

2.5.4 Histology and Immunohistochemistry

2.5.4.1 Tissue Collection, Embedding and Sectioning of Mouse Tissues

At the time of autopsy, fourth pair mammary glands, all tumours (half of the primary tumour) and one lung lobe was collected and fixed overnight in neutral buffered formalin (Sigma

Aldrich). Tissue was washed twice in PBS over the following two days before being transferred into 70% ethanol and stored until tissue processing. Tissue was processed using the Excelsior AS Tissue Processor (Thermofischer Scientific) with the following dehydration and embedding protocol; 60 minutes 70% ethanol, 60 minutes 85% ethanol, 60 minutes 90% ethanol, 60 minutes 96% ethanol, 2 x 60 minutes 100% ethanol, 2 x 60 minutes Xylene and held in paraffin wax at 62°C under vacuum conditions until embedding. Tissue was moulded into paraffin wax blocks and stored at room temperature. Tissue sections were cut at 5µm thickness using the Leica Rotary Microtome (Leica Microsystems) onto SuperFrost Plus Slides. Tissue sections were then bonded onto slides on a 37°C heating block for 30 minutes and stored at room temperature for histology.

2.5.4.2 Mammary Gland Whole Mount Preparation

Upon dissection, the fourth pair mammary glands were collected from PyMT and PyMT/CCL2 mice at 9 weeks of age and spread on a glass slide. Whole mounted mammary glands were fixed for a minimum of 4 hours in Carnoy's fixative (60% ethanol, 30% chloroform and 10% glacial acetic acid). Once fixed, the slides were washed in 70% ethanol for 15 minutes then rinsed in MilliQ water for 5 minutes. The slides were stained with carmine alum (2% carmine (Sigma Aldrich; Cat#C1022), 5% aluminium potassium sulphate (Sigma Aldrich; Cat#237086)) overnight. Stained whole mounted mammary glands were washed in 70% ethanol for 15 minutes, then twice in 100% ethanol for 15 minutes each. Slides were then places in xylene to be cleared for 1 week before mounting with a coverslip with Entellan mounting media (Proscitech, Australia; Cat#IM022).

2.5.4.3 Haematoxylin and Eosin Staining

Paraffin embedded mammary gland tissue sections were dewaxed using Xylene (Merck Millipore, Germany; Cat#108298) for 3 x 5 minutes, and rehydrated in gradual dilutions of ethanol for 3 minutes each (2 x 100%, 1 x 90%, 1 x 70% and 1 x 50%) followed by 2

minutes in MilliQ water. Tissue sections were stained in haematoxylin (Sigma Aldrich; Cat#HHS16) for 30 seconds, then stained in eosin (Sigma Aldrich; Cat#318906) for 10 seconds. Sections were then dehydrated through gradual increase of ethanol concentration (2 minutes 90%, 2 x 1 minute 100%), and cleared by 2 x 5 minutes in Xylene. Slides were then mounted with coverslips using Entellan mounting media (Proscitech, Australia; Cat#IM022).

2.5.4.4 Immunohistochemistry to detect F4/80

Mouse tissue sections were dewaxed in xylene for 2 x 5 minutes and rehydrated by graduated dilutions of ethanol (100% ethanol for 3 x 5 minutes, 90%, 70% and 50% ethanol for 3 minutes each) then milliQ water for 1 minute. Sections were then incubated in a freshly made quench solution to block endogenous peroxidase activity comprised of 10mL of hydrogen peroxide, 90mL of water and 100mL of methanol. Following 3 x 3 minute washes in water, the sections were blocked using 15% normal rabbit serum in PBS for 30 minutes at 37°C. The primary antibody (rat anti-mouse F4/80 (Ebioscience; 14480182)) was added at a 1 in 50 dilution with 1.5% normal rabbit serum, and incubated overnight at 4°C in a humidified chamber. Sections were washed twice in PBS for 5 minutes and then incubated with the secondary antibody (biotinylated rabbit anti-rat IgG antibody (Vector Laboratories, USA; Cat#BA4000)) at a dilution of 1 in 500 for 40 minutes at room temperature. Slides were washed for 3 x 5 minutes in PBS and Incubated with the Vectastain ABC Elite Kit (Vector Laboratories; Cat#PK4000) for 30 minutes, and positive staining was then detected using 3,3'-diaminobenzidine (DAB) (Dako, USA; Cat#K3468) according to manufacturer's instructions for 10 minutes at room temperature. Tissue sections were then counterstained with haematoxylin for 30 seconds and rinsed in running tap water. Sections were dehydrated through graduated increases in ethanol concentrations (2 x 2 minutes in 90% ethanol, 2 x 1 minute in 100%) and then cleared for

2 x 5 minutes in xylene. Slides were mounted using DPX mounting media (Merck). Slides stained with secondary antibody only were included as negative controls.

2.5.5 Image Capture and Quantifications

2.5.5.1 Haematoxylin and Eosin Stained Mouse Tissues

Mouse mammary glands, primary tumours and lungs were collected from PyMT/FVB and PyMT/CCL2 mice at 9 and 12 weeks of age and tissue sections were stained with haematoxylin and eosin. Sections were analysed by veterinary pathologist Dr. Lucy Woolford (University of Adelaide) blinded to mouse genotype for tumour grade, cytological atypia, tumour necrosis and pulmonary metastasis. Mouse mammary gland sections were also assessed for various tumour grade regions across the whole mammary gland at 9 weeks.

2.5.5.2 Whole mounted Mammary Glands

Whole mounted mammary glands were imaged using an Olympus SZ61 stereo microscope and an SC50 camera (Olympus). Images were de-identified and analysed using Image J. The total number of hyperplastic areas were manual counted both distal to the lymph node as well as the entirety of the mammary gland. The total hyperplastic area and percentage hyperplasia were both calculated by measuring the total area of the mammary gland and measuring the areas occupied by hyperplastic tissue.

2.5.5.3 F4/80 Quantification in Mouse Tumours

F4/80 stained primary tumours and fourth pair mammary glands collected from PyMT and PyMT/CCL2 mice at 9 and 12 weeks stained with F4/80 were captured as digital images using a Nanozoomer digital scanner (Hamamatsu photonics, Japan) with a zoom equivalent to a 40x objective lens. To quantify F4/80 staining in primary tumours, areas containing positively stained macrophages were measured across the entire section and

the number of positively stained cells were manually counted. Data was expressed as an average positive cells/mm^2 for each section. To quantify F4/80 staining in fourth pair mammary glands at 9 weeks, 3 areas of hyperplasia were identified distal to the lymph node. The number of F4/80 positive cells around the border of these areas were manually counted. Data was expressed as the average positively stained cells/mm. All quantifications was done blinded to mouse genotype.

2.6 NUCLEOTIDE ANALYSIS

2.6.1 Genotyping Mice

Genotypes of mice were determined using polymerase chain reaction (PCR) using DNA extracted from mouse tail tips. DNA from PyMT and PyMT/CCL2 mice were analysed for presence of the Pymt oncogene.

2.6.1.1 DNA Extraction

Tail tips were digested in 350µL of digestion buffer containing 17mM tris, 17mM EDTA, 170mM sodium chloride, 0.85% SDS (PH 7.8) with 0.1mg proteinase K (all from Sigma Aldrich) at 55°C overnight. 5µL of the tail digest was diluted in 95µL of MilliQ water and incubated for 15 minutes at 95°C to inactivate the proteinase K. Extracted genomic DNA was stored at 4°C until PCR analysis was performed.

2.6.1.2 PCR Primers and Conditions

Presence of the Mmtv-PyMT gene was performed using PCR. The primers to detect the PyMT allele are; forward 5'-GAGCGAGGAACTGAGGAGAG-3' and reverse 3'-CTTAGGCGGCGACTGGTAGC-5' with product size 195 base pairs (Geneworks, Australia). The PCR reaction mixture (25µL) contained 2.5uL of 10x DNA polymerase reaction buffer (Fisher Biotec, Australia; Cat#230924), 2.5µL of 25mM $MgCl_2$ (Fisher Biotec; Cat#210924), 0.5µL of 10mM dNTPs (Roche, Germany; Cat#1277049), and

1.25µL of each forward and reverse primer, 0.125µL of Taq polymerase (Fisher Biotec; Cat#2309090), 16µL of MilliQ water and 2µL of sample DNA. The PCR conditions were 5 minutes at 94°C for 5 minutes, followed by 35 cycles of 30 seconds at 94°C, 30 seconds at 55°C, 1 minute at 72°C and one cycle of 7 minutes at 72°C.

2.6.1.3 Detection of PCR Products

PCR products of DNA encoding PyMT genotyping were detected using gel electrophoresis. The PCR products were separated on a 2% agarose gel (Sigma Aldrich; Cat#A9539) by dissolving agarose in tris-acetate-EDTA (TAE) buffer containing 0.01% GelRed™ (Biotium, USA; Cat#41002) as intercalating agents to detect DNA. The PCR products were loaded to the gel with 1x loading buffer and run for 40 minutes at 80 volts. Gel images were captured using Gel Doc™ EZ Imager (BioRad) under UV light. Representative image of gel used for genotyping to identify presence of the PyMT transgene is shown in Figure 2.4.

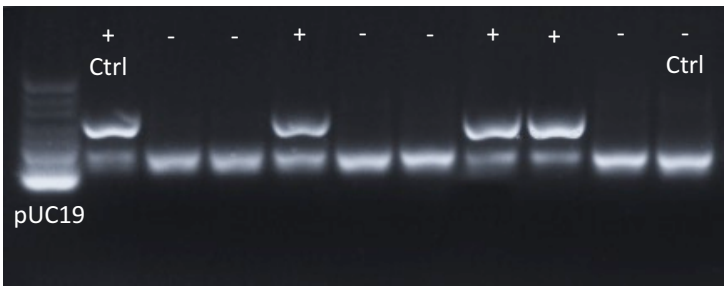

Figure 2.4: Genotyping to detect presence of PyMT transgene.
Pymt+ males (FVB background) were mated with Mmtv-Ccl2, and FVB control females. Their female offspring were weaned at 21 days and genotyped for the presence of the Pymt transgene. Each lane represents DNA from each mouse amplified by Pymt primers.

2.6.2 Total RNA Extraction

2.6.2.1 RNA Extraction from Cell Culture

After 72-hour culture in the conditions detailed in 1.2.4 and 1.2.5, cells were trypsinised and lysis buffer was added to the pellet, RNA was then isolated using RNeasy Mini Plus Kit (QIAGEN, Australia; Cat#74104) as per manufacturer's instructions. RNA was measured using 1µL of sample on the Spectrophotometer ND 1000 Nanodrop using the program ND-1000 V3.7.1 and stored at -80°C until use.

2.6.2.2 RNA Extraction from Frozen Tissues

Third pair mammary glands were collected from Mmtv-Ccl2 and FVB mice at 12 weeks age during metestrus and diestrus, and snap frozen in liquid nitrogen. Tissues were then stored at -80°C under RNAse free conditions until use for RNA applications. To extract RNA, these tissues were transferred to a new tube containing 0.6g of 1.4mm ceramic beads (QIAGEN, Australia; Cat#13113-325) and 1mL of Trizol reagent was added (Invitrogen; Cat#15596026). Tissue was homogenised with the Powerlyser 24 Bench Top Bead Based Homogenizer (MoBio, USA) at 30Hz for 3 x 2 minutes, and repeated if the tissue was still not homogenous. Samples were incubated at room temperature for 5 minutes, then 200µL of chloroform (Sigma Aldrich; Cat#288306-1L) was added and the tubes were shaken vigorously, incubated on ice for 15 minutes, then centrifuged for 15 minutes at 11000 x g at 4°C. Approximately 500µL was collected of the aqueous phase containing RNA, and transferred into a new tube. An equal volume of isopropanol (Sigma Aldrich; Cat#563935) was added to the tubes and samples were incubated at -20°C overnight. The following day, samples were centrifuged for 30 minutes at 11000 x g at 4°C. The RNA pellet was then washed twice with ice cold 70% ethanol and centrifuged for 10 minutes at 11000 x g at 4°C. The pellet was air dried on ice for 30 minutes and dissolved in 50µL of RNase free water. RNA samples were then treated with DNase to remover genomic DNA contamination using the TURBO DNase Kit (Invitrogen; Cat#AM1907).

According to the manufacturer's instructions, 5µL of 10x TURBO DNase Buffer and 1µL of TURBO DNase was added to each sample, then incubated at 37°C for 30 minutes. To deactivate the DNase enzyme, 5µL of the DNase inactivation reagent was added to each sample and continuously mixed for 5 minutes at room temperature. Samples were then centrifuged at 10000 x g for 1.5 minutes at 4°C and transferred the RNA into a fresh tube. DNase treated RNA was then quantified using 2µL of sample on the spectrophotometer ND 1000 Nanodrop using the program ND-1000 V3.7.1 and stored at -80°C until later application.

2.6.3 Reverse Transcription and cDNA Synthesis

The iScript cDNA synthesis kit was used to reverse transcribe all RNA samples into cDNA (Bio-rad technologies; Cat#1708890). Each cDNA reaction contained 500ng of RNA from cell lines and 1µg from mouse tissues, 1µL of iScript reverse transcriptase, 4µL of 5 x iScript reaction mix and nuclease free water to a total volume of 20µL. Samples were then incubated for on a thermocycler for 5 minutes at 25°C, 30 minutes at 42°C and 5 minutes at 85°C. cDNA was then diluted 1:10 in nuclease free water to a volume of 200µL and stored at -20°C until later application.

2.6.4 Quantitative Real Time PCR

2.6.4.1 SYBR Green-Based Detection

Quantitative real time PCR (qRT-PCR) was performed to determine mRNA expression of genes of interest. Reaction mixtures were prepared in a volume of 10µL, each containing 5µL of SYBR green master mix (Bio-Rad), 0.4µL of each forward and reverse primer, 2.2µL of nuclease free water and 2µL of sample cDNA. Reactions were run on a thermocycler using CFX96 Real Time Detection System running CFX Manager 3.0 software (Bio-Rad). The cycle conditions were 3 minutes at 95°C, 40 amplification samples of 15 seconds at 95°C, 15 seconds at 60°C and 30 seconds at 72°C. Each PCR plate contained no template

controls of each gene and all samples were run in triplicate. Quantitative RT-PCR data was analysed by the comparative Ct method, relative to a housekeeping gene (*HPRT1* in human samples and *ActB* in mice). Results were normalised to housekeeping gene expression and normalised such that the average of control samples was 1 ($\Delta\Delta$CT).

2.6.4.2 PCR Primers

All primers were obtained from Geneworks. The sequence of each primer pair used for gene expression studies in mammary fibroblasts is shown in Table 2.1, and primers used for gene expression studies in THP-1 derived macrophages are shown in Table 2.2.

2.6.5 Next Generation Sequencing of Mmtv-Ccl2 Mammary Glands

Total RNA was converted to strand specific Illumina compatible sequencing libraries using a NEXTflex Rapid Directional mRNA-Seq library kit (BIOO Scientific, USA; Cat#NOVA-5138-07) as per the manufacturer's instructions (v14.10). Briefly, 400ng of total RNA was polyA selected and the mRNA fragmented prior to reverse transcription and second strand cDNA synthesis using dUTP. The resultant cDNA is poly adenylated before the ligation of Illumina-compatible barcoded sequencing adapters. The cDNA libraries were treated with UDG to degrade the second strand and PCR amplified for 14 cycles prior to assessment by Bioanalyzer (Agilent, California, USA) for quality and Qubit fluorescence assay for amount. Sequencing pools were generated by mixing equimolar amounts of compatible sample libraries based on the Qubit measurements. Sequencing of the library pool was done with an Illumina Nextseq 500 using single read 75bp v2 sequencing chemistry. Functional gene enrichment analysis was performed on differentially expressed genes, and altered gene pathways were identified using the Database for Annotation, Visualisation and Integrated Discovery (DAVID, Version 6.8) [197, 198].

Table 2.1: PCR primers used to quantify mRNA gene expression in human primary mammary fibroblasts.

Gene	Abbreviation	Primer Sequence 5'-3'
Hypoxanthine-guanine phosphoribosyltransferase	*HPRT1*	(F)TGCAGACTTTGCTTTCCTTGGTCAGG (R) CCAACACTTCGTGGGGTCCTTTTCA
Matrix Metalloproteinase 1	*MMP1*	(F)GACGTTCCCAAAATCCTGTCCAG (R)GGTAGAAGGGATTTGTGCGCATGT
Matrix Metalloproteinase 3	*MMP3*	(F)AGAGGCATCCACACCCTAGGTTTC (R)CCTGGCTCCATGGAATTTCTCTTC
Matrix Metalloproteinase 9	*MMP9*	(F)AGACCTGGGCAGATTCCAAAC (R) CGGCAAGTCTTCCGAGTAGT
Tissue Inhibitor of Metalloproteinase 1	*TIMP1*	(F)CTTCTGCAATTCCGACCTCGT (R) ACGCTGGTATAAGGTGGTCTG
Connective Tissue Growth Factor	*CTGF*	(F)GTGTGACGAGCCCAAGGACCAA (R)GGACCAGGCAGTTGGCTCTAATCA
Lysyl Oxidase	*LOX*	(F)TGCTGCGGAGGAGAAGTGTCTG (R)TGTGCCCTGGTTCTTCACGC
Fibronectin	*FBN*	(F)CTCCTGGAAGTTTTGTCTGTACCTGC (R)GGGCTGTTCTTGCAGACTCCATTA
Collagen 1A1	*COL1A1*	(F)AGGGCTCCAACGAGATCGAGATCCG (R)TACAGGAAGCAGACAGGGCCAACGTCG
Collagen 4A5	*COL4A5*	(F)TATGTCATCACTGCCAGGACCAAAGG (R)CAATTGGCCCTGGTATACCAGTGG
Alpha Smooth Muscle Actin	*SMA*	(F)ACTGCCTTGGTGTGTGACAA (R) CACCATCACCCCCTGATGTC
Cyclooxygenase 2	*COX2*	(F)CCTGTGCCTGATGATTGC (R) CTGATGCGTGAAGTGCTG
Fibroblast Growth Factor 5	*FGF5*	(F)CGGATGGCAAAGTCAATGGATCC (R)CGCTCCCTGAACTTGCAGTCAT
Transforming Growth Factor Beta 3	*TGFB3*	(F)GGCCCTTGCCCATACCTCCG (R)AGCAAGGCGAGGCAGATGCT
Wingless Related Integration 5A	*WNT5A*	(F)AAGGAGTTCGTGGACGCCCG (R)GCAGGCCACATCAGCCAGGT
Vimentin	*VIM*	(F)ATTGCAGGAGGAGATGCRRCAGAGAG (R)CCACTTTGCGTTCAAGGTCAAG
Tenascin C	*TNC*	(F)CCTGAGGGAGCAATGTACTGCAGG (R)TGAAGTTGCCCCGACCGCTA
Interleukin 8	*IL8*	(F)AAACCACCGGAAGGAACCATCTC (R)CACTCCTTGGCAAAACTGCACC
Interleukin 6	*IL6*	(F)GAGTAGTGAGGAACAAGCCAGAGCTG (R)CTGGCATTTGTGGTTGGGTCAG

Table 2.2: PCR primers used to quantify mRNA expression in THP-1 derived human macrophages.

Gene	Abbreviation	Primer Sequence 5'-3'
Hypoxanthine-guanine phosphoribosyltransferase	*HPRT1*	(F)TGCAGACTTTGCTTTCCTTGGTCAGG (R)CCAACACTTCGTGGGGTCCTTTTCA
Transforming Growth Factor Beta 1	*TGFB1*	(F)CTAATGGTGGAAACCCACAACG (R) TATCGCCAGGAATTGTTGCTG
Interleukin 10	*IL10*	(F)GACTTTAAGGGTTACCTGGGTTG (R) TCACATGCGCCTTGATGTCTG
Interferon Gamma	*IFNG*	(F)TCGGTAACTGACTTGAATGTCCA (R) TCGCTTCCCTGTTTTAGCTGC
Tumour Necrosis Factor Alpha	*TNFA*	(F)AGCCTCTTCTCCTTCCTGATCGTG (R) GGCTGATTAGAGAGAGGTCCCTGG
C-C Chemokine Receptor 2	*CCR2*	(F)GACAAGCCACAAGCTGAACA (R)GAGCCCACAATGGGAGAGTA
Matrix Metalloproteinase 2	*MMP2*	(F)GCTCAGATCCGTGGTGAGATCTTC (R) GGTGCTGGCTGAGTAGATCCA
Matrix Metalloproteinase 9	*MMP9*	(F)AGACCTGGGCAGATTCCAAAC (R) CGGCAAGTCTTCCGAGTAGT
Tissue Inhibitor of Metalloproteinase 1	*TIMP1*	(F)CTTCTGCAATTCCGACCTCGT (R) ACGCTGGTATAAGGTGGTCTG
Platelet Derived Growth Factor	*PDGF*	(F)CAGCGACTCCTGGACATAGACT (R) CGATGCTTCTCTTCCTCCGAATG
Vascular Endothelial Growth Factor	*VEGF*	(F)AGGGCAGAATCATCACGAAGT (R) AGGGTCTCGATTGGATGGCA

2.7 STATISTICAL ANALYSIS

Statistical analysis was performed using SPSS software, version 20.0 for Windows (SPSS, Illinois, USA) with consultation with a statistician (Ms Suzanne Edwards, Adelaide Health Technology Assessment, University of Adelaide). Data was considered statistically significant when $p<0.05$. An asterisk (*) identified result that is statistically significant from the control. If more than two groups are being compared, different letters (a, b, c, d) were used to signify statistical significance between groups. Groups labelled with shared letters are not statistically different.

All cell culture data, including RT-PCR and collagen production experiments, are presented as mean±SEM (standard error of mean). Statistical analysis of RT-PCR data was performed using ΔCT values. This data was analysed using a Linear Mixed-effects Model to account for variables such as patient density and treatment groups. Tukey's post-hoc comparisons were performed to determine statistically significant differences in mRNA expression or collagen production between patients with high or low mammographic density, and then between cells treated with immune regulatory proteins and untreated controls.

Kaplan Meier survival analysis was performed to determine differences in tumour latency between PyMT and PyMT/CCL2 in studies described in Chapter 5 with LogRank test to compare survival curves of each group. Data on of tumorigenic areas at 9 weeks of age, tumour burden, primary tumour weigh and quantification of F4/80 stained mammary glands and tumours at 9 and 12 weeks of age were presented as mean±SEM. Analyses were performed using Linear Regression Models with Post-hoc Wald Chi-square comparisons to determine significance. Data from mice at 9 and 12 week of age were analysed separately. Count data including number of tumorigenic areas at 9 weeks and number of tumours at 12 weeks were analysed using a Negative Binomial Regression Model with

Wald Chi-square post hoc comparison. Analysis of primary mammary tumours such as tumour grade, cytological atypia, tumour necrosis and lung metastasis at 12 weeks of age were presented as percentage proportions stratified by mouse groups PyMT and PyMT/CCL2. Comparison of proportions were analysed using cross tabulations with Fischer's exact test.

CHAPTER THREE

IMMUNE REGULATION OF MAMMARY FIBROBLASTS AND THE IMPACT OF MAMMOGRAPHIC DENSITY

3.1 INTRODUCTION

Histological studies have reported that the key features of high MD breast tissue are a higher abundance of stroma and greater deposition of collagen compared to low MD tissue [57, 69]. Therefore, high MD breast tissue can be considered to resemble tissue with fibrosis, which is characterised by excessive deposition of collagen and extracellular matrix (ECM) [199]. The most abundant cell type in the mammary stroma are fibroblasts, which are the key cell type responsible for fibrotic activities such as regulation of the synthesis and turnover of collagen and extracellular matrix (ECM) components [75, 200]. High abundance of collagen associated with fibrosis increases breast cancer risk in a transgenic mouse model [90] and this suggests fibroblast-mediated fibrosis could be a key driver of MD.

Fibroblasts can contribute to breast cancer risk and tumour development by acting as cancer associated fibroblasts (CAF's) [201]. CAFs can be identified by high level of expression of genes such as smooth muscle actin (*SMA*), vimentin (*VIM*), tenascin C (*TNC*), and fibroblasts growth factor 5 (*FGF5*) [201, 202]. CAFs can promote the transformation of normal epithelial cells to adopt more tumorigenic properties including increased invasion, motility and migration [203]. In breast cancer, CAFs promote tumour cell proliferation and survival [204]. CAFs drive metastasis through remodelling of the ECM through expression of collagen genes, lysyl oxidase (*LOX*), and matrix metalloproteinases (*MMPs*), as well as suppression of anti-tumour immunity through expression of interleukin 6 and 8 (*IL6, IL8*) [77, 205, 206].

The activity of mammary fibroblasts can be influenced by signals from surrounding immune cells in the mammary stroma. Studies have reported that high MD tissue is associated with a more pro-inflammatory environment compared to low MD tissues and this is a driver of breast cancer risk [123]. Immune and inflammatory factors including peroxidase enzymes, transforming growth factor beta 1 (TGFB1) and tumour necrosis factor alpha (TNFA) have been shown to modulate some fibrotic and CAF functions of fibroblasts and play a role in other fibrotic diseases [177, 195, 207]. These factors have also been demonstrated to have roles in breast cancer [103, 172, 178, 184]. How fibroblasts respond to these signals in high and low MD have not been previously investigated. We hypothesise that inflammatory immune factors that promote fibrotic and CAF related activities of mammary fibroblasts may be drivers of MD and breast cancer risk.

Currently, it is unknown whether fibroblasts are a driving factor for MD, if fibroblasts from women with high MD are inherently different in their behaviour to those from women with low MD, or if they respond differently to immune stimuli such as peroxidase enzymes, TGFB1 or TNFA. The aim of this study was to investigate whether fibroblasts derived from high MD breast tissue may be creating a favourable environment for tumour development through expression of genes indicative of a CAF like phenotype such as *SMA*, *COX2*, *FGF5*, *TGFB3*, *WNT5*, *VIM*, *TNC*, *IL6* and *IL8*. This study also aims to investigate the fibrotic activity of fibroblasts derived from high and low MD breast tissue by analysing expression of genes involved in ECM regulation including *MMP1*, *MMP3*, *CTGF*, *LOX*, *FBN*, *COL1A1* and *COL4A5* as well as production of soluble collagen 1 and insoluble collagen.

3.2 RESULTS

3.2.1 CAF and ECM mRNA expression and collagen production of mammary fibroblasts from women with high and low MD

To investigate whether mammary fibroblasts are inherently different if they are derived from patient breast tissue with high or low MD, primary mammary fibroblasts were isolated from women with high or low MD as identified by histological density categories 1 (low) or 4 and 5 (high) (n=8 per group) and cultured for 72 hours in serum free media. mRNA expression of CAF related genes and genes involved in ECM regulation were measured using quantitative real-time PCR relative to expression of housekeeping gene *HPRT1* from the same patient. Results are expressed in arbitrary units, were the data were normalised so that the average expression of each gene in untreated controls was equal to 1.

No significant differences in expression of CAF genes were observed between fibroblasts from women with high or low mammographic density. mRNA expression of *IL8* had a large amount of variability between patient samples ranging from 0.10 to 5.42 arbitrary units in fibroblasts from high MD tissues (Figure 3.1.A). No significant differences were observed in mRNA expression of genes involved in ECM regulation between high and low MD mammary fibroblasts, and there was a large amount of variation in expression of *MMP1* (0.08 to 8.83 arbitrary units) between high MD patient samples (Figure 3.1.B).

Collagen production was measured by ELISA to detect production of soluble collagen I, and Sirius red dye to measure insoluble collagen fibres. No significant differences were seen in collagen production between fibroblasts from women with high or low MD (Figure 3.1.C, D).

These studies suggest that fibroblasts from high MD breast tissue are not inherently different from those derived from low MD. However, fibroblasts are responsive to signals

in the surrounding environment that can affect fibroblast function and may differentially stimulate their activity dependent on whether they were derived from tissue of high or low MD. Therefore, we investigated the effects of immune regulatory proteins MPO, EPO, TGFB and TNFA on mammary fibroblast activity and whether the response is dependent on whether fibroblasts were derived from high and low MD breast tissue.

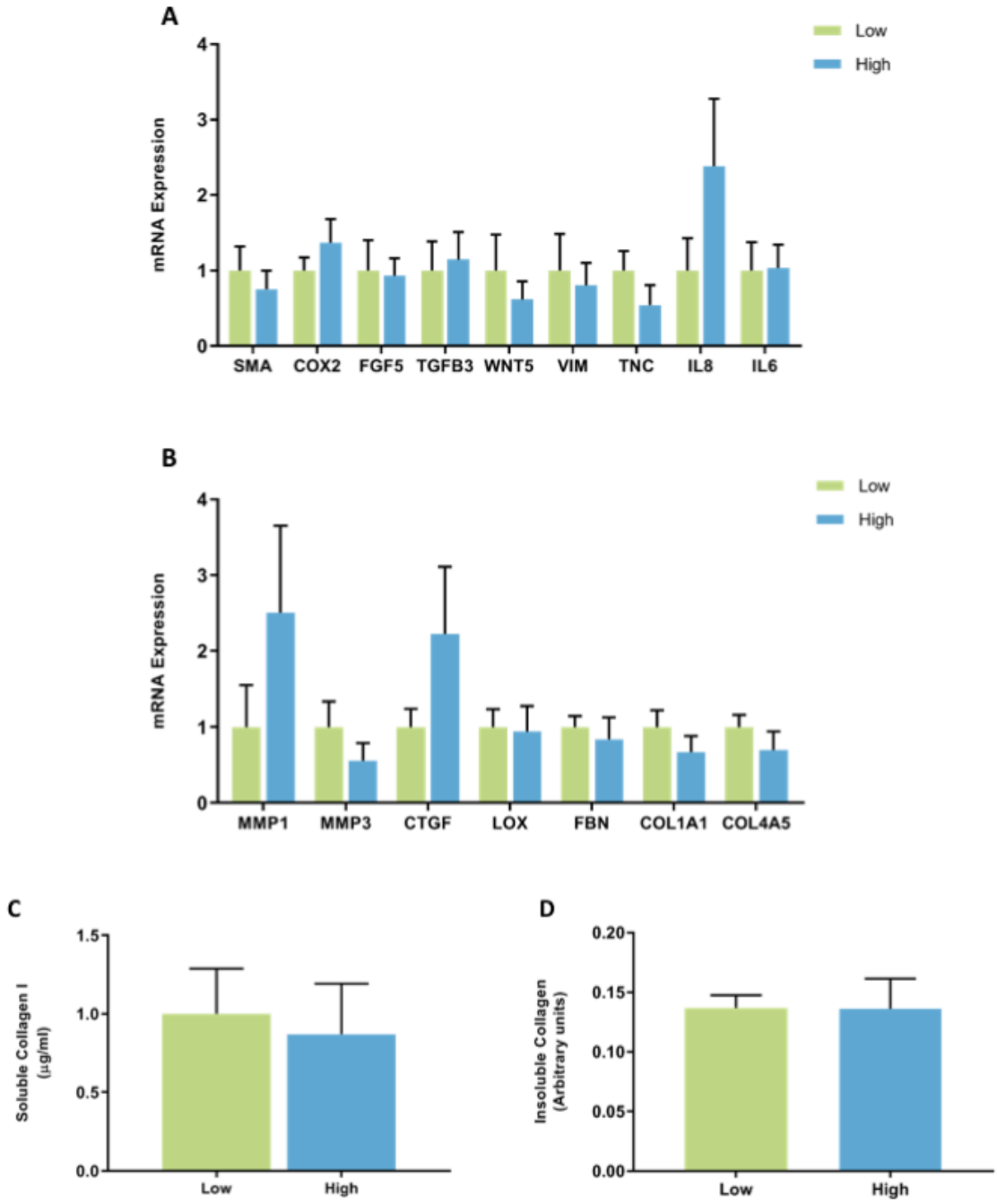

Figure 3.1: mRNA expression and collagen production in mammary fibroblasts isolated from women with high and low mammographic density.
Messenger RNA expression of cancer associated genes (A) and genes involved in extracellular matrix regulation and collagen production (B) measured by RT-PCR in human mammary fibroblasts from women with high and low mammographic density (n=8 per group). mRNA expression normalised to HPRT1 expression, and presented as relative expression where the average for untreated control is 1. Collagen production was measured using collagen 1 ELISA (C) and insoluble collagen measured by sirius red staining (D). Data presented as mean + SEM with statistical analysis performed using a Linear Mixed-Effects model Tukey's post-hoc comparison.

3.2.2 The effect of MPO on CAF and ECM mRNA expression and collagen production by mammary fibroblasts

To investigate the effects on MPO and mammographic density on mammary fibroblasts, primary mammary fibroblasts were cultured for 72 hours with 5μg/mL of MPO in serum free media (n=16). mRNA expression of CAF related genes and ECM regulation were measured using quantitative real time PCR relative to expression of housekeeping gene *HPRT1* from the same patient. Results are expressed in arbitrary units, were the data were normalised so that the average expression of each gene in untreated controls was equal to 1.

No significant differences in mRNA expression of CAF related genes were observed in mammary fibroblasts treated with MPO (Figure 3.2.A). No significant differences in mRNA expression of genes encoding genes involved in ECM regulation were observed when cells were treated with MPO (Figure 3.2.B).

Collagen production was measured by ELISA to detect production of soluble collagen I, and Sirius red dye to measure insoluble collagen fibres. Results were normalised so that collagen production for untreated controls was 1. Collagen I production was significantly increased in fibroblasts treated with MPO (1.61±0.26μg/mL) (Figure 3.2.C) compared to controls (1 ± 0.22μg/mL), and this increase was not dependant on if the fibroblasts were from a woman with high or low MD (Figure 3.4.C). No significant differences were observed in production of collagen fibres in fibroblasts treated with MPO (Figure 3.2.D).

3.2.2.1 The effect of MPO on gene expression and collagen production by mammary fibroblasts from high and low MD breast tissue.

When fibroblast samples were separated according to whether they came from a patient with high or low MD (n=8 per group), no differences in mRNA expression of CAF related

genes were observed between fibroblasts from high and low MD tissues when treated with MPO (Figure 3.3.A). MPO did not have differential effects on mRNA expression of ECM regulatory genes from high MD fibroblasts compared to low MD fibroblasts (3.3.B). No differences in soluble collagen I or insoluble collagen production were observed between fibroblasts from high and low MD tissues when treated with MPO (Figure 3.3.C,D).

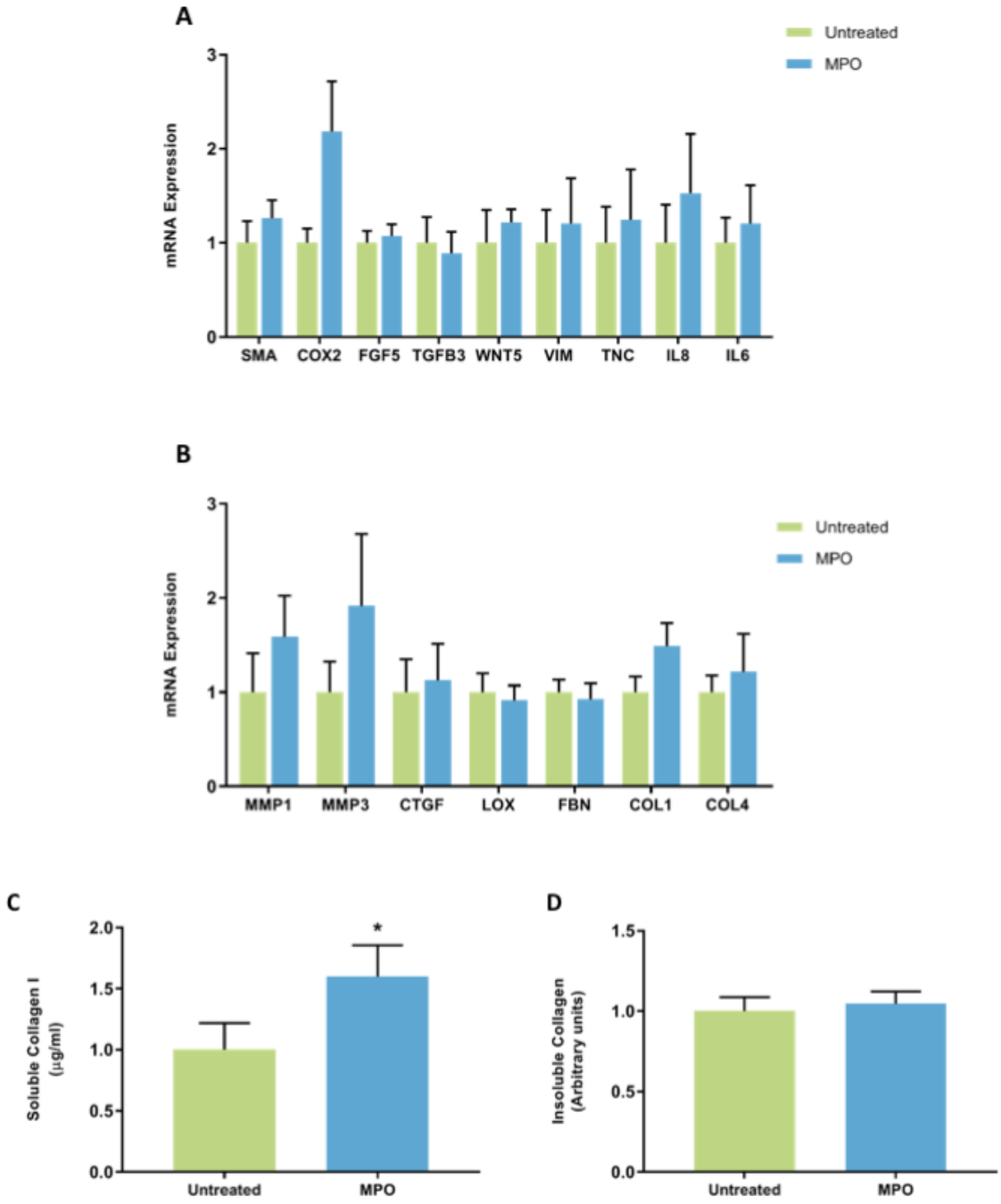

Figure 3.2: The effect of MPO on mRNA expression and collagen production in mammary fibroblasts. Messenger RNA expression of cancer associated genes (A) and genes involved in extracellular matrix regulation and collagen production (B) measured by RT-PCR in human mammary fibroblasts following treatment with 5µg/mL of MPO for 72hrs (n=16). mRNA expression normalised to HPRT1 expression, and presented as relative expression where the average for untreated control is 1. Collagen production was measured using collagen 1 ELISA (C) and insoluble collagen measured by sirius red staining (D). Data presented as mean + SEM with statistical analysis performed using a Linear Mixed-Effects model Tukey's post-hoc comparison. Statistical significance indicated by * when $p<0.05$.

.

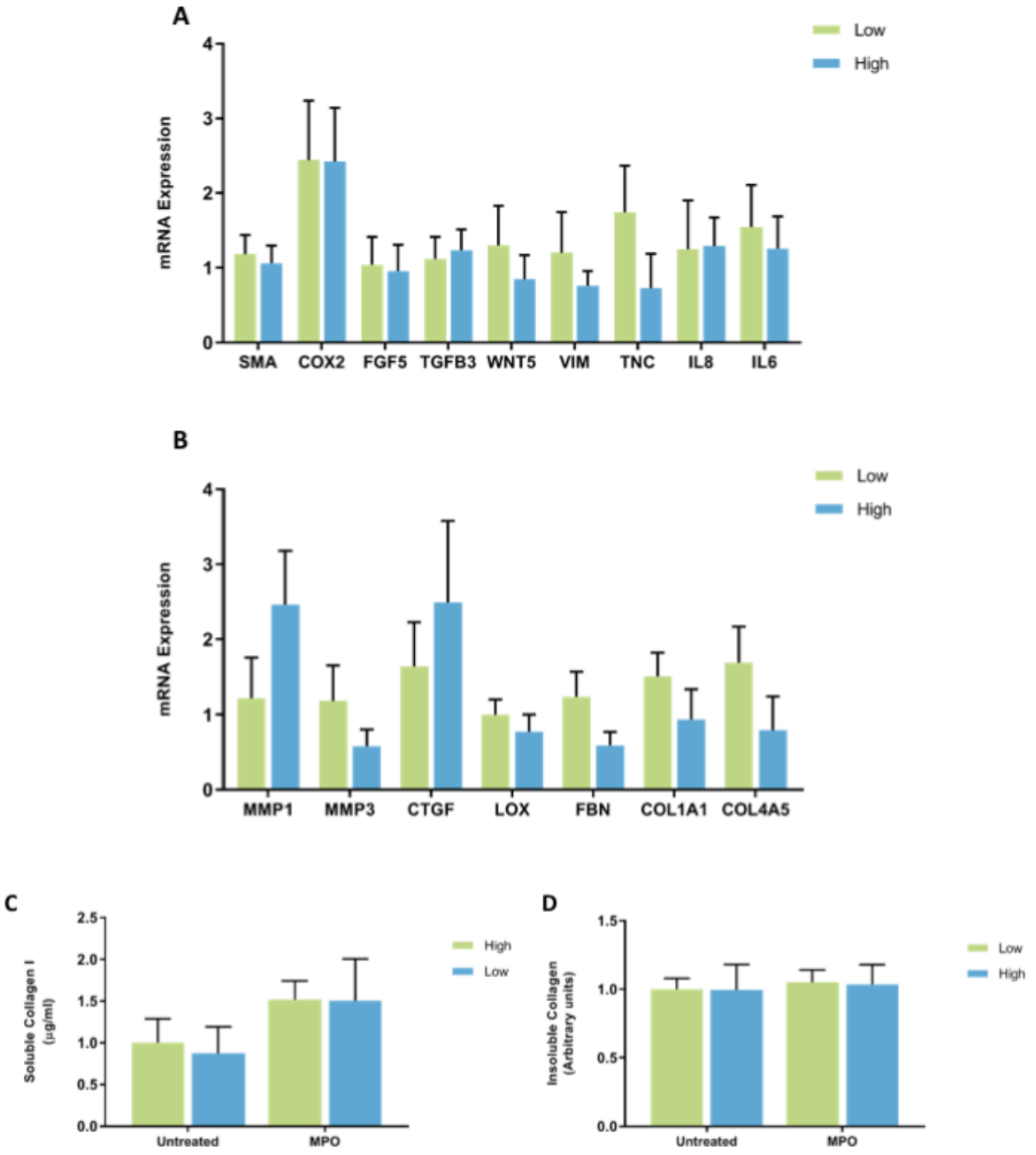

Figure 3.3: The effect of MPO on mRNA expression and collagen production in mammary fibroblasts isolated from women with high and low mammographic density.
Messenger RNA expression of cancer associated genes (A) and genes involved in extracellular matrix regulation and collagen production (B) measured by RT-PCR in human mammary fibroblasts from women with high and low mammographic density (n=8 per group) following treatment with 5µg/mL of MPO for 72 hours. mRNA expression normalised to HPRT1 expression, and presented as relative expression where the average for untreated control is 1. Collagen production was measured using collagen 1 ELISA (C) and insoluble collagen measured by sirius red staining (D). Data presented as mean + SEM with statistical analysis performed using a Linear Mixed-Effects model Tukey's post-hoc comparison.

3.2.3 The effect of EPO on ECM and CAF mRNA expression, and collagen production by mammary fibroblasts

To investigate the effects on EPO and mammographic density on mammary fibroblasts, primary mammary fibroblasts were cultured for 72 hours with 2.5µg/mL of EPO in serum free media (n=16). mRNA expression of CAF genes and genes involved in ECM regulation were measured using quantitative real time PCR relative to expression of housekeeping gene *HPRT1* from the same patient. Results are expressed in arbitrary units, were the data were normalised so that the average expression of each gene in untreated controls was equal to 1.

The expression of mRNA encoding *COX2* was significantly attenuated by treatment with EPO (11.76±4.37 arbitrary units), with expression increased by over 10-fold compared to untreated controls (1±0.15) ($p<0.05$). Expression of *IL8* was also significantly increased by nearly 50-fold in fibroblasts treated with EPO (48.55±28.50 arbitrary units), compared to untreated controls (1±0.41 arbitrary units) ($p<0.05$). No other changes in expression of cancer associated genes were observed in fibroblasts treated with EPO (Figure 3.4.A).

Expression of mRNA encoding *MMP1* was significantly increased in fibroblast treated with EPO (10.10±3.17 arbitrary units) compared to untreated controls (1±0.41 arbitrary units) ($p<0.01$). There was a significant decrease in expression of *LOX* in EPO treated fibroblasts (0.39±0.06 arbitrary units) compared to untreated controls (1±0.19 arbitrary units) ($p<0.01$) (Figure 3.4.B). No other changes in expression of genes involved in ECM regulation were observed in fibroblasts treated with EPO (Figure 3.4.B).

Collagen production was measured by ELISA to detect production of soluble collagen I, and Sirius red dye to measure insoluble collagen fibres. Results were normalised so that collagen production in untreated controls was equal to 1. Collagen I production was

significantly increased in fibroblasts treated with EPO (2.04±0.43 μg/mL) compared to untreated controls (1±0.22μg/mL) ($p<0.01$) (Figure 3.4.C). No significant differences were observed in production of collagen fibres in fibroblasts treated with EPO (Figure 3.4.D).

3.2.3.1 The effect of EPO on gene expression and collagen production by mammary fibroblasts from high and low MD breast tissue.

When the results were separated according to the MD score of each patient sample, it was observed that there were no differences in expression of cancer associated genes between fibroblasts from high and low MD patient samples when treated with EPO (Figure 3.5.A). No differences in mRNA expression of ECM regulatory genes was observed between fibroblasts from high and low MD patient samples when treated with EPO (Figure 3.5.B). No differences in soluble collagen I or insoluble collagen production were observed between fibroblasts from high and low MD tissues when treated with EPO (Figure 3.5.C,D).

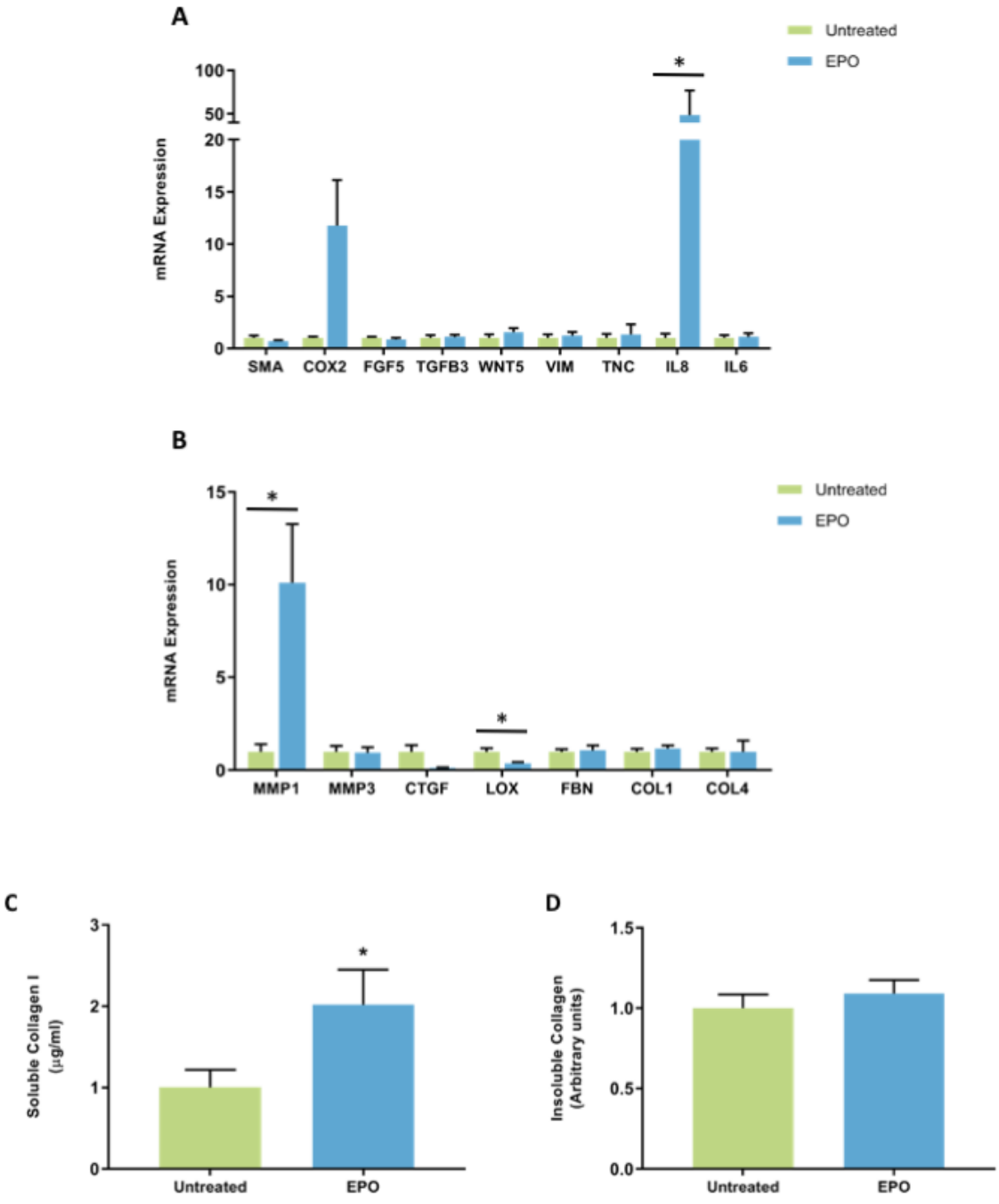

Figure 3.4: The effect of EPO on mRNA expression and collagen production in mammary fibroblasts. Messenger RNA expression of cancer associated genes (A) and genes involved in extracellular matrix regulation and collagen production (B) measured by RT-PCR in human mammary fibroblasts following treatment with 2.5µg/mL of EPO for 72hrs (n=16). mRNA expression normalised to HPRT1 expression, and presented as relative expression where the average for untreated control is 1. Collagen production was measured using collagen 1 ELISA (C) and insoluble collagen measured by sirius red staining (D). Data presented as mean + SEM with statistical analysis performed using a Linear Mixed-Effects model Tukey's post-hoc comparison. Statistical significance indicated by * when $p<0.05$.

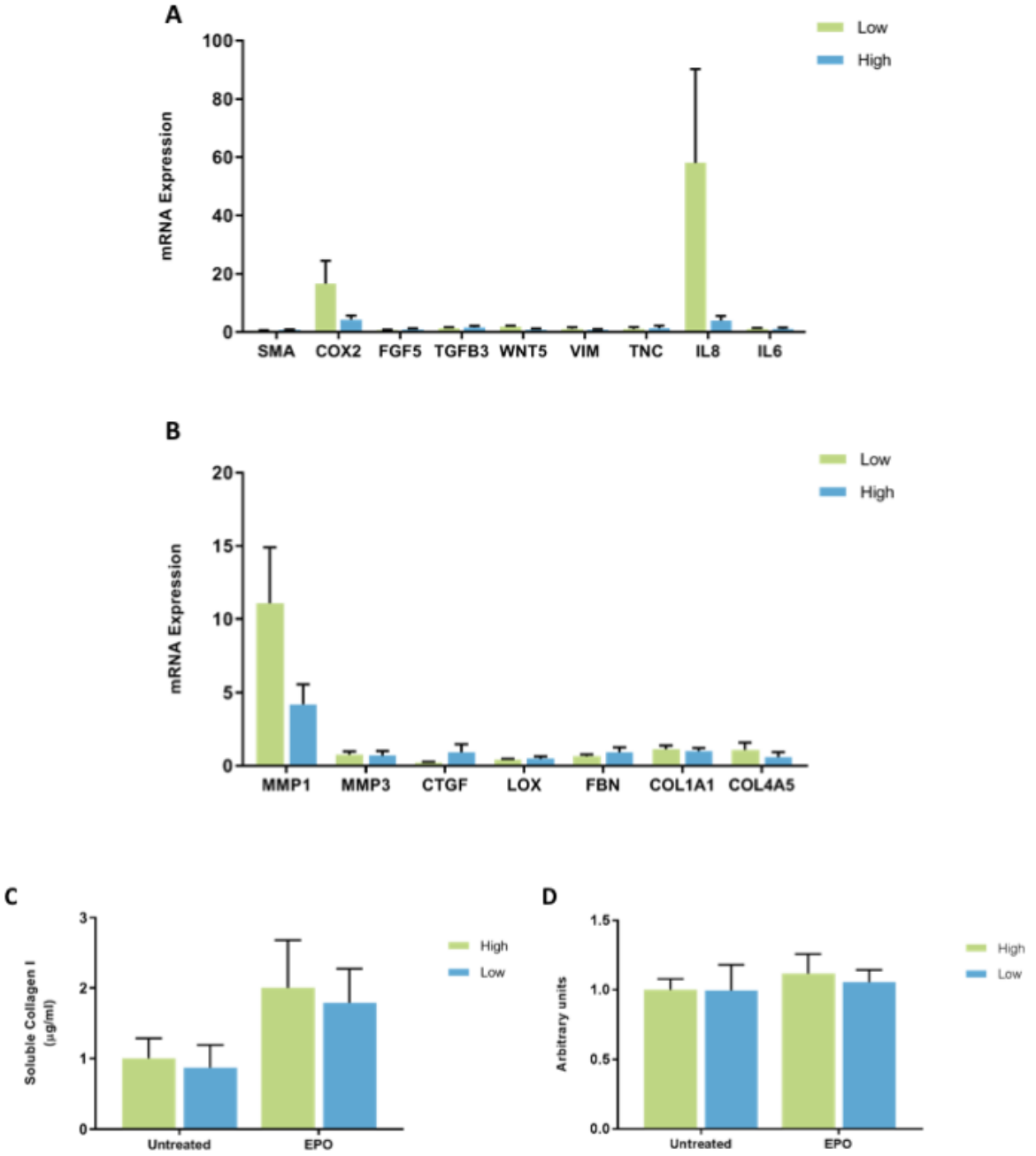

Figure 3.5: The effect of EPO on mRNA expression and collagen production in mammary fibroblasts isolated from women with high and low mammographic density.
Messenger RNA expression of cancer associated genes (A) and genes involved in extracellular matrix regulation and collagen production (B) measured by RT-PCR in human mammary fibroblasts from women with high and low mammographic density (n=8 per group) following treatment with 2.5µg/mL of EPO for 72 hours. mRNA expression normalised to HPRT1 expression, and presented as relative expression where the average for untreated control is 1. Collagen production was measured using collagen 1 ELISA (C) and insoluble collagen measured by sirius red staining (D). Data presented as mean + SEM with statistical analysis performed using a Linear Mixed-Effects model Tukey's post-hoc comparison.

3.2.4 The effect of TGFB on CAF and ECM mRNA expression and collagen production by mammary fibroblasts

To investigate the effects on TGFB and mammographic density on mammary fibroblasts, primary mammary fibroblasts were isolated from human breast tissue and cultured for 72 hours with 10ng/mL of TGFB in serum free media (n=16). mRNA expression of cancer associated genes and genes involved in extracellular matrix regulation were measured using quantitative real time PCR relative to expression of housekeeping gene *HPRT1* from the same patient. Results are expressed in arbitrary units, were the data were normalised so that the average expression of each gene in untreated controls was equal to 1.

Expression of mRNA encoding *TNC* was significantly increased in mammary fibroblasts treated with TGFB (2.64±1.51 arbitrary units) compared to untreated controls (1±0.38 arbitrary units). No other differences were observed in expression of CAF genes in fibroblasts treated with TGFB (Figure 3.6.A).

Expression of *MMP3*, was increased by 6-fold in fibroblasts treated with TGFB (6.34±0.73 arbitrary units) compared to untreated controls (1±0.32 arbitrary units) ($p<0.01$). Expression of mRNA encoding *CTGF* was significantly increased in TGFB treated fibroblasts (6.48±1.52 arbitrary units) compared to untreated controls (1±0.34 arbitrary units) ($p<0.05$). A small but significant increase in mRNA expression of *LOX* and in TGFB treated fibroblasts (1.58±0.21 arbitrary units) was observed compared to untreated controls (1±0.19 arbitrary units) ($p<0.01$). A trending reduction in expression of *COL4A5*, and a trending 2-fold increase in *MMP1* expression was observed fibroblasts treated with TGFB compared to untreated controls ($p= 0.059$, $p=0.074$ respectively). No other changes in expression of genes involved in extracellular matrix regulation were observed (Figure 3.6.B).

Collagen production was measured by ELISA to detect production of soluble collagen I, and Sirius red dye to measure insoluble collagen fibres. Results were normalised so that average collagen production in untreated controls was equal to 1. Collagen I production was significantly decreased in fibroblasts treated with TGFB (0.57±0.1 arbitrary units) compared to untreated controls (1±0.22 arbitrary units) ($p<0.01$) (Figure 3.6.C). There was a small but significant increase in insoluble collagen production in fibroblasts treated with TGFB (1.22±0.07 arbitrary units) compared to untreated controls (1±0.09 arbitrary units) ($p<0.01$) (Figure 3.6.D).

3.2.4.1 The effect of TGFB on gene expression and collagen production by mammary fibroblasts from high and low MD breast tissue.

When accounting for patient's MD score, there were no significant differences in expression of CAF genes in fibroblasts from patients with high and low MD when treated with TGFB (Figure 3.7.A). No significant differences were observed in mRNA expression of ECM regulatory genes by fibroblasts from high and low MD patient samples when treated with TGFB (Figure 3.7.B). No differences in soluble collagen I or insoluble collagen production were observed between fibroblasts from high and low MD tissues when treated with TGFB (Figure 3.7.C,D).

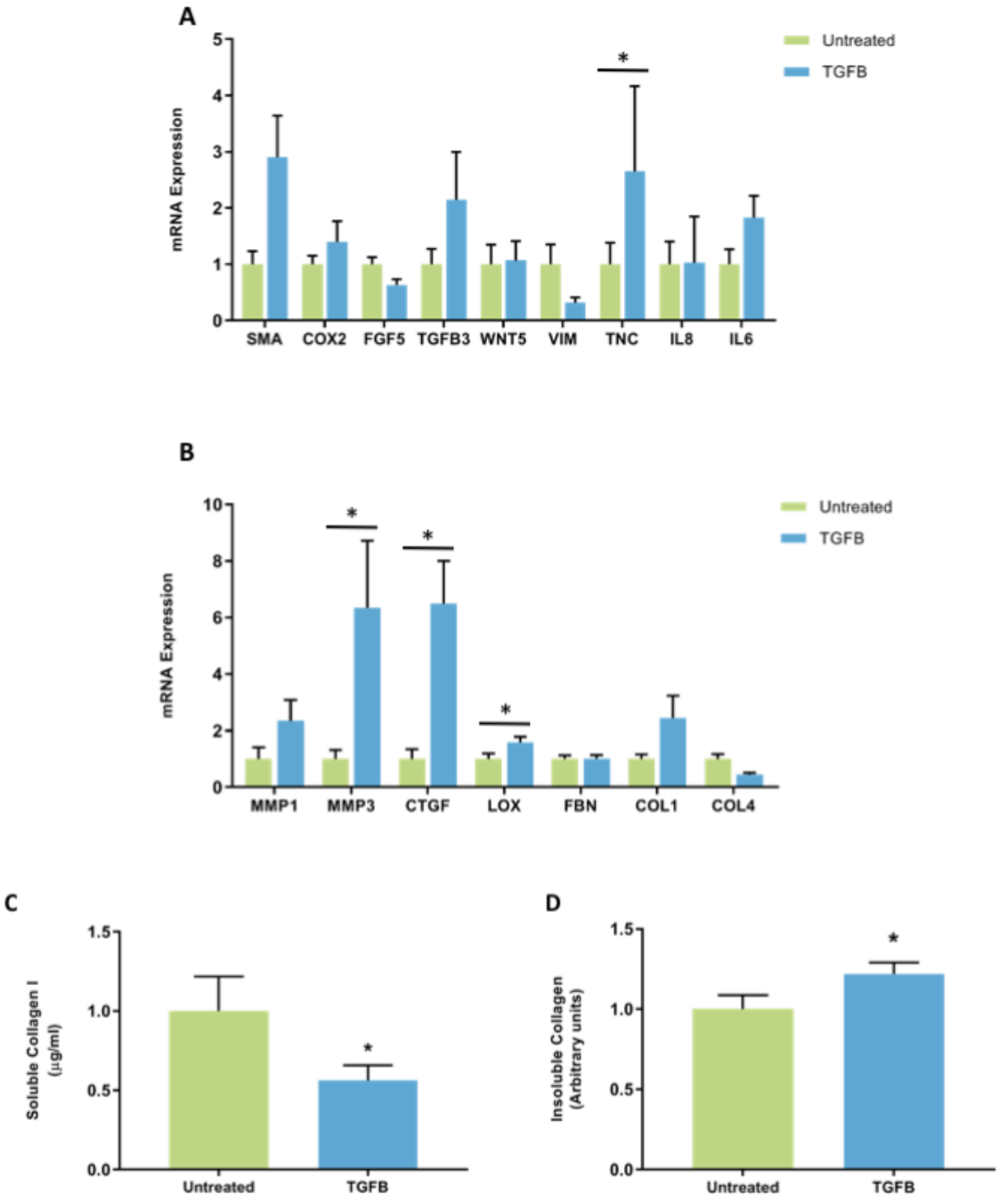

Figure 3.6: The effect of TGFB on mRNA expression and collagen production in mammary fibroblasts. Messenger RNA expression of cancer associated genes (A) and genes involved in extracellular matrix regulation and collagen production (B) measured by RT-PCR in human mammary fibroblasts following treatment with 10ng/mL of TGFB for 72hrs (n=16). mRNA expression normalised to HPRT1 expression, and presented as relative expression where the average for untreated control is 1. Collagen production was measured using collagen 1 ELISA (C) and insoluble collagen measured by sirius red staining (D). Data presented as mean + SEM with statistical analysis performed using a Linear Mixed-Effects model Tukey's post-hoc comparison. Statistical significance indicated by * when $p<0.05$.

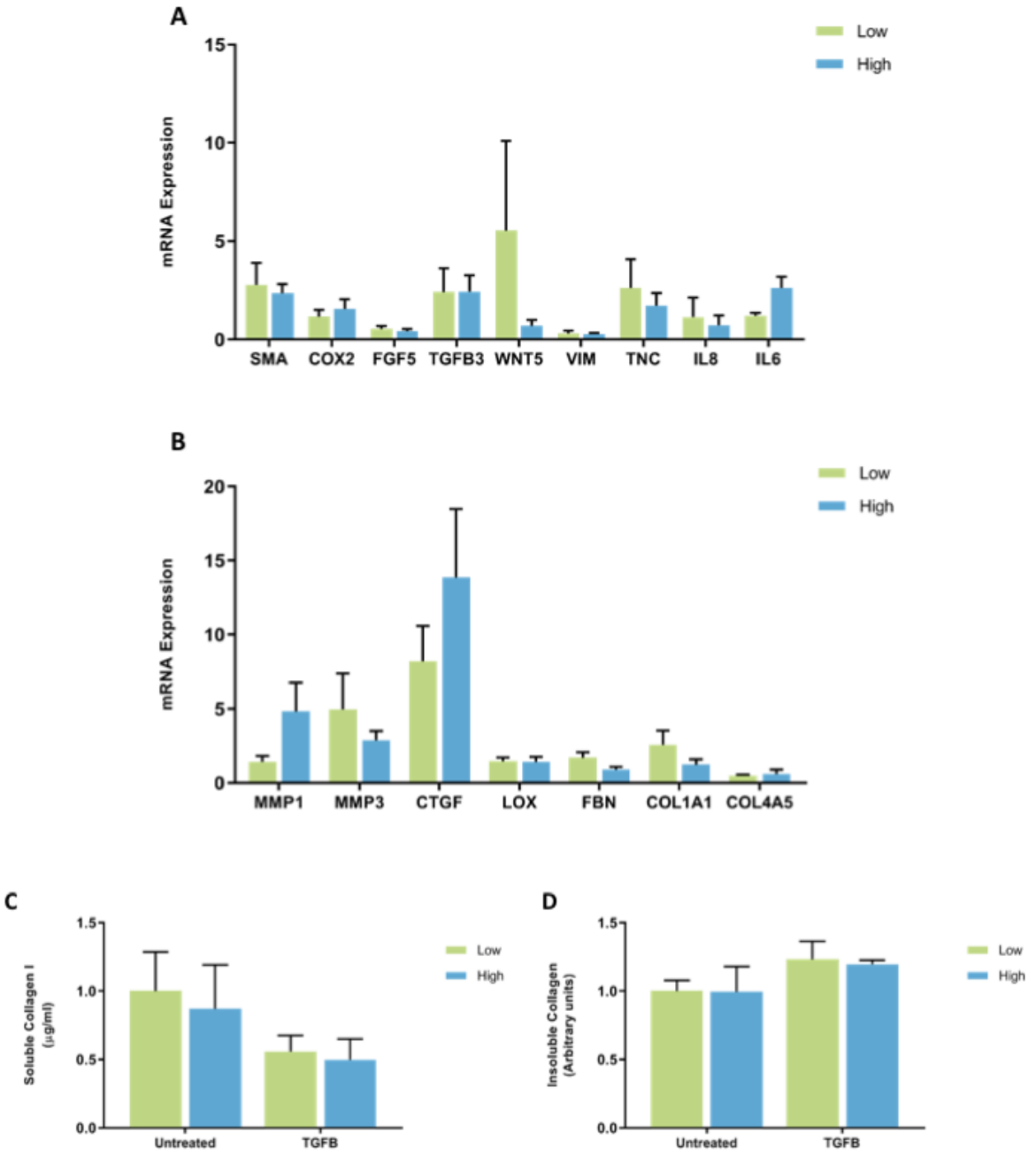

Figure 3.7: The effect of TGFB on mRNA expression and collagen production in mammary fibroblasts isolated from women with high and low mammographic density.
Messenger RNA expression of cancer associated genes (A) and genes involved in extracellular matrix regulation and collagen production (B) measured by RT-PCR in human mammary fibroblasts from women with high and low mammographic density (n=8 per group) following treatment with 10ng/mL of TGFB for 72 hours. mRNA expression normalised to HPRT1 expression, and presented as relative expression where the average for untreated control is 1. Collagen production was measured using collagen 1 ELISA (C) and insoluble collagen measured by sirius red staining (D). Data presented as mean + SEM with statistical analysis performed using a Linear Mixed-Effects model Tukey's post-hoc comparison.

3.2.5 The effect of TNFA on CAF and ECM mRNA expression and collagen production by mammary fibroblasts

To investigate the effects on tumour necrosis factor alpha (TNFA) and mammographic density on mammary fibroblasts, primary mammary fibroblasts were cultured for 72 hours with 10ng/mL of TNFA in serum free media (n=16). mRNA expression of CAF genes and genes involved in ECM regulation were measured using quantitative real time PCR relative to expression of housekeeping gene *HPRT1* from the same patient. Results are expressed in arbitrary units, were the data were normalised so that the average expression of each gene in untreated controls was equal to 1.

A significant decrease in mRNA expression of *SMA* was observed in TNFA treated fibroblasts (0.22±0.05 arbitrary units) compared to untreated controls (1±0.23 arbitrary units) ($p<0.05$). Expression of mRNA encoding *COX2* was significantly increased in TNFA treated fibroblasts (27.98±10.15 arbitrary units) compared to untreated controls (1±0.15 arbitrary units) ($p<0.01$). Expression of mRNA encoding *IL8* and *IL6* were highly increased in TNFA treated fibroblasts (1701.3±237.8 and 40.29±9.83 arbitrary units respectively) compared to untreated controls (1±0.40 and 1±0.27 arbitrary units respectively) ($p<0.001$ for both genes). A 4-fold trending increase in expression of *WNT5* was observed in TNFA treated fibroblasts, though this was not significant ($p=0.051$). No other differences in CAF gene expression were observed (Figure 3.8.A).

There were also strong effects of TNFA on expression of genes involved in regulation of the extracellular matrix. The most potent effects were on expression of *MMP1* and *MMP3*, which were significantly increased in TNFA treated fibroblasts (72.43±23.72 and 21.18±10.57 arbitrary units respectively) compared to untreated controls (1±0.41 and 1±0.32 arbitrary units respectively) ($p<0.001$ for both genes). A significant decrease in expression of *LOX* and *FBN* was observed in TNFA treated fibroblasts (0.53±0.11 and

0.25±0.04 arbitrary units respectively), compared to untreated controls (1±0.19 and 1±0.13 respectively) ($p<0.01$). Both collagen genes *COL1A1* and *COL4A5* were decreased in TNFA treated fibroblasts (0.22±0.03 and 0.07±0.01 arbitrary units respectively) compared to untreated controls (1±0.16 and 1±0.17 arbitrary units respectively) ($p<0.01$) (Figure 3.8.B).

Collagen production was measured by ELISA to detect production of soluble collagen I, and Sirius red dye to measure insoluble collagen fibres. Results were normalised so that average collagen production in untreated controls was equal to 1. Collagen I production was significantly decreased in fibroblasts treated with TNFA (0.54±0.06 arbitrary units) compared to untreated controls (1±0.22 arbitrary units) (Figure 3.8.C). A small but significant increase in Sirius red staining was observed in TNFA treated fibroblasts (1.13±0.09 arbitrary units) compared to untreated controls (1±0.09 arbitrary units) (Figure 3.8.D).

3.2.5.1 The effect of TNFA on gene expression and collagen production by mammary fibroblasts from high and low MD breast tissue.

When the results were separated according to the MD score of each patient sample, were no differences in expression of CAF related genes were observed between fibroblasts from breast tissue with high or low MD when treated with TNFA (Figure 3.9.A). There were no differences in expression of genes involved in ECM regulation between fibroblasts from high or low MD patient samples when treated with TNFA (Figure 3.9.B). There was no difference in collagen I production or insoluble collagen production between fibroblasts from breast tissue with high or low MD when treated with TNFA (Figure 3.9.C,D).

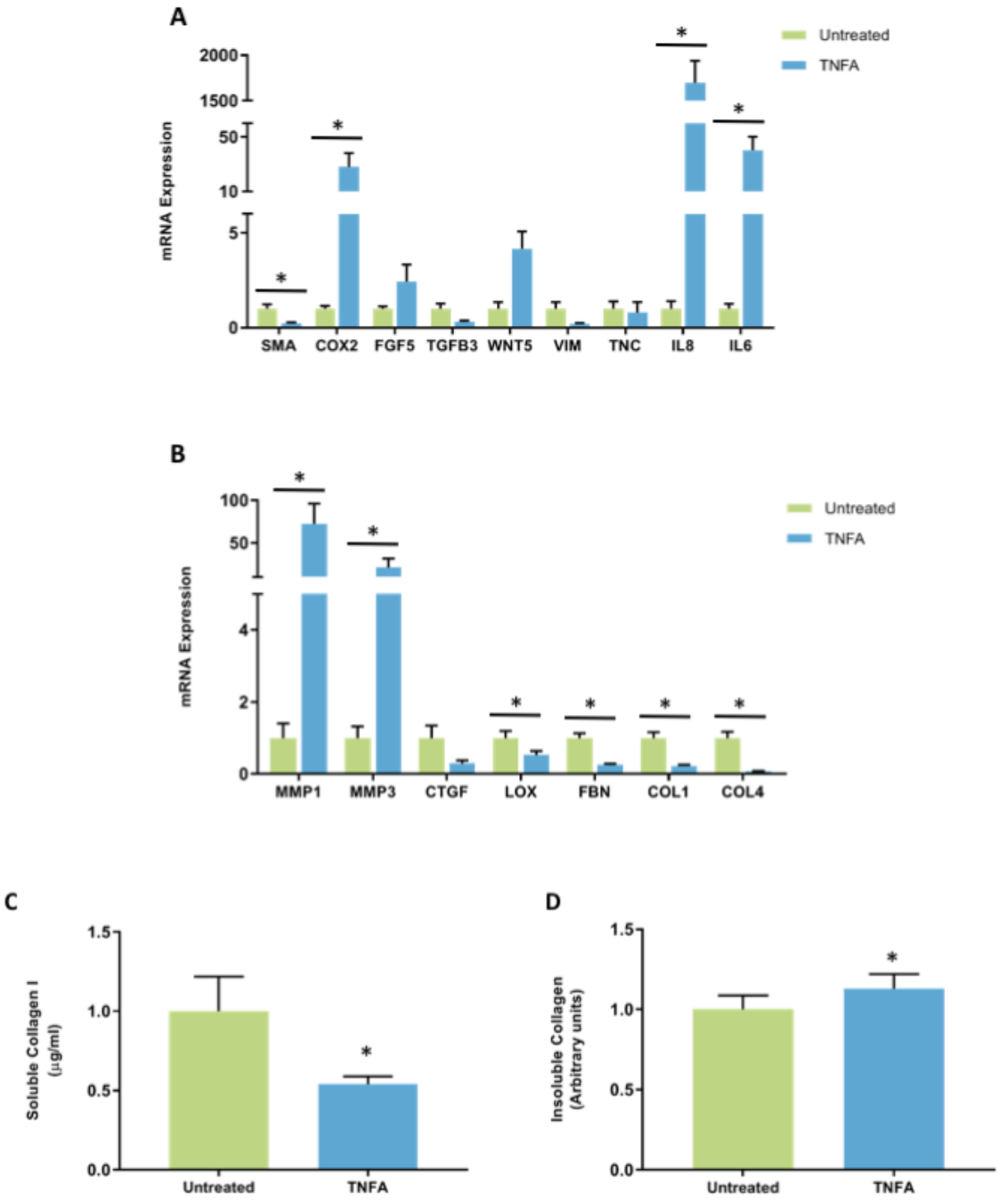

Figure 3.8: The effect of TNFA on mRNA expression and collagen production in mammary fibroblasts. Messenger RNA expression of cancer associated genes (A) and genes involved in extracellular matrix regulation and collagen production (B) measured by RT-PCR in human mammary fibroblasts following treatment with 10ng/mL of TNFA for 72hrs (n=16). mRNA expression normalised to HPRT1 expression, and presented as relative expression where the average for untreated control is 1. Collagen production was measured using collagen 1 ELISA (C) and insoluble collagen measured by sirius red staining (D). Data presented as mean + SEM with statistical analysis performed using a Linear Mixed-Effects model Tukey's post-hoc comparison. Statistical significance indicated by * when $p<0.05$.

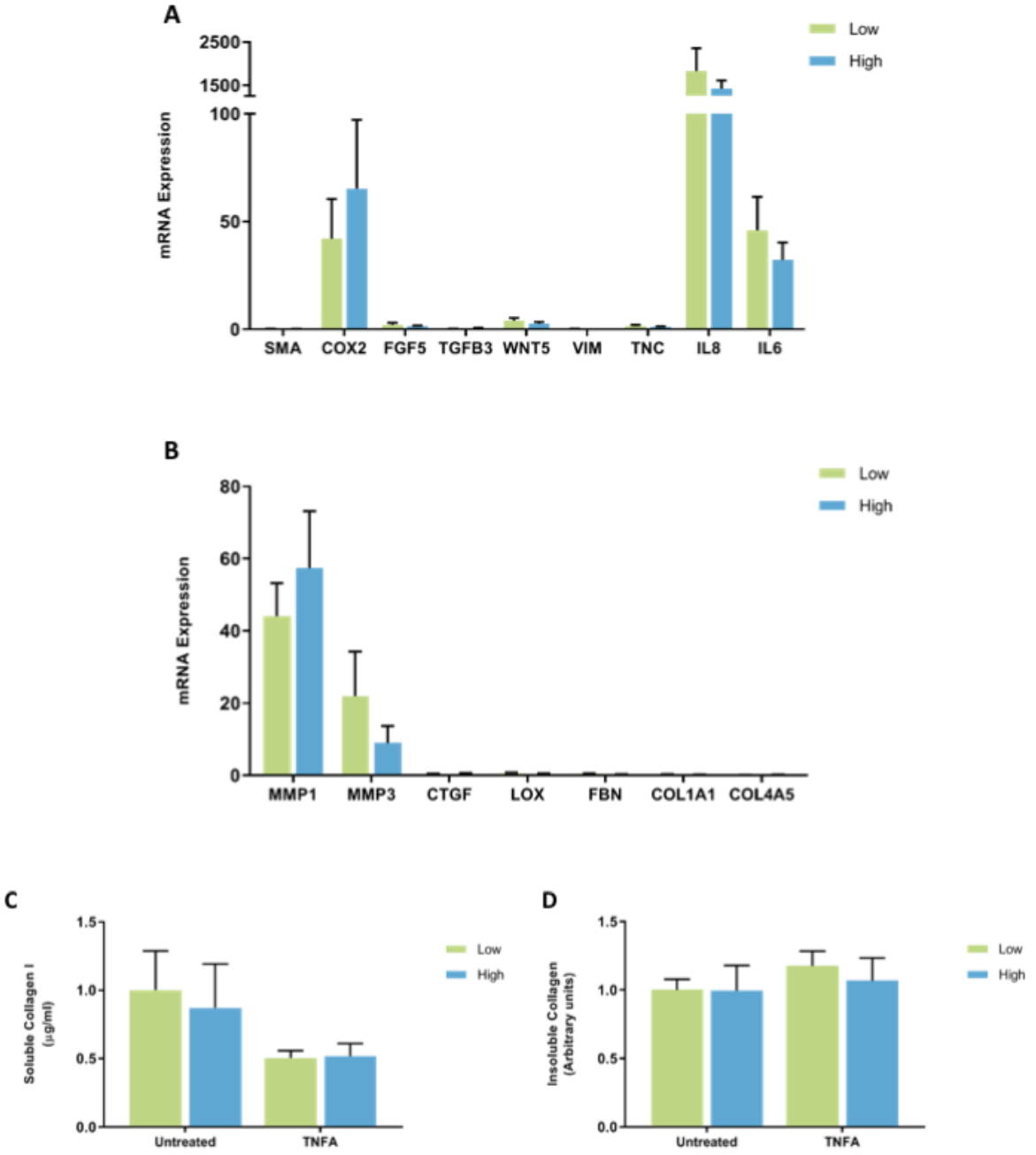

Figure 3.9: The effect of TNFA on mRNA expression and collagen production in mammary fibroblasts isolated from women with high and low mammographic density.
Messenger RNA expression of cancer associated genes (A) and genes involved in extracellular matrix regulation and collagen production (B) measured by RT-PCR in human mammary fibroblasts from women with high and low mammographic density (n=8 per group) following treatment with 10ng/mL of TNFA for 72 hours. mRNA expression normalised to HPRT1 expression, and presented as relative expression where the average for untreated control is 1. Collagen production was measured using collagen 1 ELISA (C) and insoluble collagen measured by sirius red staining (D). Data presented as mean + SEM with statistical analysis performed using a Linear Mixed-Effects model Tukey's post-hoc comparison.

3.3 DISCUSSION

The underlying biological mechanisms that contribute to mammographic density and the associated breast cancer risk are largely unknown. As fibroblasts are a prominent cellular component of the mammary stroma, which is highly abundant in tissue with high mammographic density, it is hypothesised that they may play a role in the development of mammographic density.

3.3.1 Mammary fibroblasts isolated from high MD tissue are not inherently different from those isolated from low MD tissue

High MD breasts exhibit high abundance of stromal fibroblasts, however previous studies have not investigated the potential of fibroblasts as drivers of MD. It was hypothesised that fibroblasts from high MD breast tissue may exhibit altered gene expression like that of CAFs that promote a more favourable environment for tumour development, or have greater expression of genes involved in production of the ECM, and in this way, act as drivers of mammographic density. However, the results here suggest that fibroblasts from high MD breasts are not inherently different to those from low MD breasts as there were no differences in ECM and CAF gene expression or collagen production between fibroblasts from breast tissue with high or low MD. Therefore, fibroblasts alone are unlikely to be driving mammographic density through their inherent fibrotic activities, or contributing to breast cancer risk through greater expression of CAF genes. In addition, when these fibroblasts were stimulated with immune proteins and cytokines, there were still no differences in gene expression or collagen production between fibroblasts from high or low density breast tissue. This suggests that fibroblasts isolated from high density breast tissue do not have different responsiveness to immune stimulus compared to fibroblasts from low density breast tissue. However, these studies were subject to limitations, and only measured a select subset of gene and protein expressions. Measures of other genes and

proteins related to fibroblast functions could reveal differences between high and low MD fibroblasts.

3.3.2 Modulation of extracellular matrix regulation and collagen production in mammary fibroblasts by peroxidase enzymes

Production of soluble collagen I was significantly increased in primary mammary fibroblasts when treated with myeloperoxidase or eosinophil peroxidase. However, there was no increase in mRNA expression of *COL1A1* in response to myeloperoxidase or eosinophil peroxidase. This is consistent with previous studies that reported that peroxidase enzymes stimulate production of collagen I in fibroblasts derived from various tissue sites, as well as production of collagen IV *in vitro*. This suggests that peroxidase enzymes have important roles in regulating extracellular matrix at the post translational level. However, our studies found no change in collagen fibre staining in response to peroxidase enzymes. Therefore, peroxidase enzymes may be involved in intracellular post-translational modifications prior to extracellular collagen fibril assembly.

Interestingly, eosinophil peroxidase significantly increased the mRNA expression of *COX2*. *COX2* is the gene encoding cyclooxygenase, an enzyme that catalyses the production of prostaglandins, and is expressed during inflammation [208]. COX2 has been implicated in mammographic density and breast cancer risk in previous studies. In a study by Yang et al. in 2009 chipseq analysis of normal breast tissue demonstrated that expression of COX2 was increased in tissues from women with high mammographic density, and this was further confirmed by immunohistochemistry [120]. In women, expression of *COX2* has been found to be upregulated in 56% of mammary tumours, and COX2 inhibitors have been trialled as chemoprevention therapies [209, 210]. Therefore, peroxidase enzymes may have a role in mammographic density and the associated breast

cancer risk through promoting the production of collagen 1 by mammary fibroblasts and also in the induction of COX2 expression.

3.3.3 TGFB1 signalling modulates extracellular matrix regulation and collagen production in mammary fibroblasts

Our studies found that mammary fibroblasts treated with TGFB1 displayed increased mRNA expression of genes involved in ECM regulation such as *MMP3*, *CTGF* and *LOX*, as well as alterations in collagen production. TGFB is a key regulator of fibrosis and is upregulated in most fibrotic diseases through excessive production of ECM components including collagen [119].

Connective tissue growth factor (*CTGF*), was highly expressed in fibroblasts treated with TGFB. CTGF is expressed by fibroblasts following activation by TGFB [118], however it has also been shown that CTGF alone can induce production of collagen by fibroblasts [211, 212]. Studies have suggested that CTGF, through TGFB signalling, is a key regulator of fibrosis [213]. In mice, CTGF can drive fibrosis in the lungs, and inhibition of CTGF signalling can prevent liver fibrosis in rats [214, 215]. Overexpression of CTGF has been linked to increased tumour size in breast cancer, and together with MMPs, can contribute to the tissue remodelling required for metastasis and angiogenesis [216, 217].

While production of soluble collagen I was decreased in TGFB-treated fibroblasts, an increase in sirius red staining for insoluble collagen fibres was observed in these cells. This may be the result of an increase in expression of *LOX,* which encodes the enzyme lysyl oxidase required to maintain the structural integrity of collagen fibres by facilitating the covalent cross-linking of collagen and elastin into insoluble fibres, and protecting collagen fibres from being degraded [207, 218]. Expression of LOX is upregulated in several fibrotic diseases associated with an accumulation of collagen and ECM

components, such as pulmonary fibrosis, skin tissues, hepatic fibrosis and cardiac fibrosis [219-223]. These fibrotic effects of LOX are mediated through interactions with TGFB [221, 222]. LOX has also been implicated in breast cancer risk. In a study by Levental and colleagues, overexpression of LOX in the mammary glands of MMTV-Neu mice lead to increased tumour growth with more invasive properties. Similarly, inhibition of LOX expression resulted in reduced ECM stiffness in the mammary gland, preventing fibrosis and reduced tumour susceptibility [92].

Treatment with TGFB induced an increase in expression of *MMP3*, a matrix metalloproteinase which is commonly thought to degrade components of the extracellular matrix [224]. However, studies have reported that MMP3 can promote the transformation of latent TGFB to its active form, and can therefore promote fibrotic processes [225]. These functions of MMP3 are poorly understood, and further investigation is required to understand the role of MMP3 in fibrotic processes and TGFB signalling.

Our studies demonstrate that TGFB can induce expression of ECM genes with pro-fibrotic activities, and increase production of insoluble collagen fibres. This suggests that TGFB could contribute to the increased stroma and collagen deposition seen in high density breast tissue [57, 70]. However, previous studies in women with high mammographic density have found a decrease in TGFB signalling in breast tissue samples using Chipseq [120]. Therefore, further studies are required to understand the role of TGFB in mammographic density.

3.3.4 TNFA Signalling and fibroblast function

Our studies investigating the effects of TNFA on mammary fibroblast function demonstrated that TNFA has profound effects of mammary fibroblast gene expression. TNFA significantly decreased mRNA expression of genes involved in ECM deposition and

including *LOX*, *FBN*, *COL1A1* and *COL4A5* as well as decreased production of soluble collagen I. This suggests that TNFA is imposing anti-fibrotic effects on mammary fibroblasts. Further, TNFA increased expression of *MMP1* and *MMP3*, which encode matrix metalloproteinases that have the primary function of degrading collagen and other ECM components [224]. These MMPs have been identified for use as potential therapeutics for fibrotic diseases, due to their capacity for breaking down the excessive deposits of ECM components [225]. These results are consistent with studies that investigated the role of TNFA in the skin, where TNFA induced expression of both *MMP1* and *MMP3* in skin tissue explants and accelerated degradation of collagen 1 [226]. Other studies have also reported that TNFA inhibits production of collagen 1 and promotes expression of collagenases such as MMP's [196, 227]. This suggests that inflammation driven by TNFA may not promote the increased collagen and pro-fibrotic environment seen in high MD breast tissue. However, an increase in insoluble collagen deposition was observed in TNFA treated fibroblasts, and there are some studies that suggest TNFA can promote collagen deposition [195]. Therefore, the effects of TNFA on collagen production in the breast require further investigation to be understood.

TNFA induced high expression of inflammatory genes *IL6*, *IL8* and *COX2* in mammary fibroblasts. In the breast, inflammation mediated by TNFA, IL6 and IL8 can favour a pro-tumorigenic environment, and promote tumour initiation, growth and progression [228]. As previously discussed, COX2 expression is increased in breast tissue of women with high MD [120, 229]. In mice with high collagen content in the mammary gland, pharmacological COX2 inhibition is associated with a decrease in tumour development and metastasis [150].

Although TNFA promoted expression of inflammatory genes that could promote a pro-tumour environment, it did not induce a CAF-like phenotype, as one of the standard markers of CAFs, *SMA* was decreased in TNFA treated fibroblasts [77]. Therefore, TNFA

may contribute to the inflammation which is associated with MD and breast cancer risk, but more studies are required. There is some evidence that there is increased mRNA expression of TNFA in breast tissue from women with high MD [192]. To understand the role of TNFA in establishing MD, future studies should investigate which cells are producing TNFA in the microenvironment of high MD breast tissue.

3.3.5 Limitations

The experiments performed in this chapter have several limitations that affect the results and the subsequent conclusions drawn from them. Specifically, low sample sizes, inter-patient variability and the specific culture methods used could have affected the results obtained.

These studies were limited by the availability of patient tissues of high and low mammographic density. Most women have breasts in the mid-range of density, either scattered density or heterogeneously dense, so there were limited number of samples obtained from the extreme ends of the spectrum of mammographic density. Higher sample sized could allow for the confounding of factors which can influence mammographic density such as age or BMI, and potentially reduce the variability in the results.

The treatment conditions in this experiment were limited, the 72-hour time point was investigated, which may not accurately represent how mammary fibroblasts respond to these immune factors. These experiments are more reflective of an acute response to stimulation, and the environment that contributes to mammographic density may be a more chronic response whereby the fibroblasts are more largely affected by longer exposure to stimuli such as immune signalling proteins. Analysing the mRNA expression and collagen production from mammary fibroblasts in response to immune proteins would be more meaningful if RNA had been collected at multiple time points. The experiments performed

in this chapter were in 2-dimensional culture and may not accurately represent how fibroblasts act within human tissue. Future studies may consider 3-dimensional culture models or tissue explants to further analyse cellular functions in MD. The concentration of immune proteins used in these experiments were the lowest concentration which yielded the highest affect as determined by previous studies. While this may yield the greatest effect of the treatment, it may not be the physiologically relevant concentration found in human tissues [177, 230, 231]. Therefore, analysis of fibroblasts response to immune proteins at various concentrations would be meaningful. While studies of gene expression and collagen production are valuable, there are many other features of mammary fibroblasts that could be measured to characterise their behaviour in high and low density breast tissue such as genome wide studies, protein expression, migration and interactions with other cells. In particular, it would be valuable to see if the changes in mRNA expression measured here lead to changes in protein expression both in the cell supernatant and in human tissue samples of high and low MD. Further, changes in activity of the enzymes of interest in this chapter such as MMP1, MMP3, and LOX should be measured at a post-translational level.

The experiments described in this chapter are subject to inter-patient variability in gene expression analyses from primary mammary fibroblasts. There was a very large degree of variability in expression of some genes that suggest other unknown factors apart from MD have great influence on gene expression in mammary fibroblasts. While these studies examine very specific subsets of genes by isolated cells, it is important to note that the cells were derived from tissues within a full body system that have been exposed to environmental, lifestyle and epigenetic factors that may influence the baseline functions of the cells within each patient.

3.4 CONCLUSION

By utilising primary mammary fibroblasts from patients with high and low mammographic density, we have shown that fibroblasts isolated from high density breast tissue are not inherently different to those isolated from low density breast tissue regarding their gene expression and collagen production. However, the sample size was small and there was a large amount of variability between patients. We have also demonstrated that peroxidase enzymes and other immune regulatory proteins such as TGFB and TNFA can have profound effects on the behaviour of mammary fibroblasts and can induce pro-fibrotic gene expression and collagen production, and promote an inflammatory microenvironment that might be more favourable for tumour development. The roles of peroxidases and immune proteins in mammographic density are complex, and further studies are required to elucidate the cellular and molecular interactions that drive breast cancer risk.

CHAPTER FOUR

MACROPHAGE-FIBROBLAST INTERACTIONS THAT CONTRIBUTE TO A PRO-TUMOUR MICROENVIRONMENT

4.1 INTRODUCTION

Whilst fibroblasts are a significant cell type abundant in high MD tissue, studies in Chapter 3 suggest that they are not drivers of high MD. Whether or not mammary fibroblasts are derived from high or low MD tissue, their activity is affected by immune mediators including peroxidases, TGFB and TNFA. This suggests that immune cells, such as macrophages, in the breast could be part of the regulatory mechanism that determines abundance of stromal fibroblasts and ECM deposition that is a key feature of high MD. Indeed, macrophages are in greater abundance in breast tissue from areas of high MD compared to low MD tissues [123].

Macrophages are key regulators of mammary gland development, facilitating proliferation of epithelial cells, as well as tissue remodelling [130]. However, they also play a role in breast cancer susceptibility. Previous studies have identified that macrophage infiltration is associated with poor prognosis in breast cancer patients [232]. Macrophages can also promote mammary tumour progression by immune suppression, tumour growth, metastasis and angiogenesis [232, 233]. On the other hand, macrophages can also be protective against cancer through immune surveillance functions and production of inflammatory signals that facilitate anti-tumour immune responses [122].

Macrophages and fibroblasts exist together within the breast stroma and cell-to-cell interactions may affect abundance of stroma and deposition of ECM. Macrophages can directly promote tissue remodelling by producing enzymes that break down collagen such

as MMPs, or prevent collagen breakdown such as TIMPs, as well as other growth factors [135, 140]. Macrophages can also influence tissue remodelling by stimulating fibroblast functions, and promote the production of collagen [234-236].

Interactions between fibroblasts and macrophages can also regulate the tumour micro-environment in cancer. Cancer associated fibroblasts (CAFs) can recruit macrophages to the tumour site through expression of chemoattractant signals such as CCL2 [237, 238]. They then can regulate the immune response to tumour cells by driving polarisation of macrophages have pro or anti-tumorigenic phenotypes [201, 239]. Similarly, expression of soluble factors from macrophages can induce expression of CAF markers in fibroblasts [238, 240].

CCL2 is a chemotactic cytokine that recruits macrophages to sites of inflammation [156]. Previous studies in our laboratory have demonstrated that high density breast tissue samples have increased CCL2 staining in the epithelium compared to low density tissues [157]. Currently, it is unknown how CCL2-stimaulted macrophages interact with surrounding stromal cells such as fibroblasts in the breast, and how it may contribute to MD. However, there is some evidence that CCL2 is associated with fibrotic diseases and can contribute to fibrosis by promoting survival of fibroblasts [241-243]. CCL2 has also been implicated in breast cancer, high expression of CCL2 in breast cancer tissues is associated with macrophage infiltration and poor prognosis [162, 244].

The effects of macrophages and CCL2 on both tissue remodelling, inflammation and CAF marker expression could suggest that the crosstalk between these cells and fibroblasts in the mammary stroma may play a contributing role in mammographic density and the associated breast cancer risk. The experiments described in this chapter investigate how CCL2 directly affects CAF and ECM gene expression, and collagen production in

mammary fibroblasts. Further, cell-to-cell interactions between mammary fibroblasts and macrophages were investigated in a co-culture model. Fibroblast mRNA expression of CAF, ECM and inflammatory genes, and collagen production were examined. And macrophage phenotype and expression of cytokines and ECM genes were investigated.

4.2 RESULTS

4.2.1 The effect of CCL2 on CAF and ECM mRNA expression and collagen production by mammary fibroblasts

To investigate the effects on CCL2 and on mammary fibroblasts, primary mammary fibroblasts were isolated from human breast tissue and cultured for 72 hours with 500ng/mL of CCL2 in serum free media (n=16). mRNA expression of CAF genes including SMA, *COX2*, *FGF5*, *TGFB3*, *WNT5*, *VIM*, *TNC*, *IL6* and *IL8*, as well as genes involved in ECM regulation and collagen production; *MMP1*, *MMP3*, *CTGF*, *LOX*, *FBN*, *COL1A1* and *COL4A5* were measured using quantitative real time PCR relative to expression of housekeeping gene *HPRT1* from the same patient. Results are expressed in arbitrary units, were the data were normalised so that the average expression of each gene in untreated controls was equal to 1.

The expression of mRNA encoding CAF related genes, or genes that are markers of CAFs was variable between patients. A 50% decrease was observed in expression of mRNA encoding COX2 in CCL2 treated fibroblasts (0.51±0.09 arbitrary units) compared to untreated controls (1±0.15 arbitrary units) ($p<0.05$). A significant 60% decrease in expression of mRNA encoding VIM in CCL2 treated fibroblasts (0.42±0.11 arbitrary units) compared to untreated controls (1±0.35 arbitrary units) ($p<0.05$). A trending 70% increase in expression of mRNA encoding FGF5 in CCL2 treated fibroblasts (1.72±0.77 arbitrary units) compared to untreated controls (1±0.12 arbitrary units) was observed ($p=0.08$).

There were no other significant differences in mRNA expression between CCL2 treated fibroblasts and untreated controls (Figure 4.1.A).

Expression of mRNA encoding genes involved in extracellular matrix regulation and collagen production was also variable between patients when treated with CCL2. There were no statistically significant differences in expression of these genes when treated with CCL2 compared to untreated controls. However, a trending 50% decrease in expression was observed in expression of mRNA encoding CTGF in CCL2 treated fibroblasts (0.47±0.12 arbitrary units) compared to untreated controls (1±0.35 arbitrary units) ($p=0.053$) (Figure 4.1.B).

Collagen production was measured by ELISA to detect production of soluble collagen I, and Sirius red dye to measure insoluble collagen fibres. Results were normalised so that the collagen production of untreated controls was equal to 1. Collagen I production was significantly decreased in fibroblasts treated with CCL2 (0.56±0.09µg/mL) compared to untreated controls (1±0.22µg/mL) ($p<0.05$) (Figure 4.1.C). Production of insoluble collagen fibres, as measured with Sirius red dye was significantly increased in fibroblasts treated with CCL2 (1.21±0.07 arbitrary units) compared to untreated controls (1±0.08 arbitrary units) ($p<0.05$) (Figure 4.1.D).

4.2.1.1 The effect of CCL2 on mammary fibroblasts from women with high and low MD

When gene expression was analysed according to the patient samples mammographic density, there were no significant differences in expression of CAF or ECM and collagen genes between high and low density patient fibroblasts when treated with CCL2 (Figure 4.2.A,B). No difference in collagen I production was observed between fibroblasts from high and low MD patient samples when treated with CCL2 (Figure 4.2.C). There was no

significant difference in Sirius red staining in fibroblasts from patients with high and low density when treated with CCL2 (Figure 4.2.D).

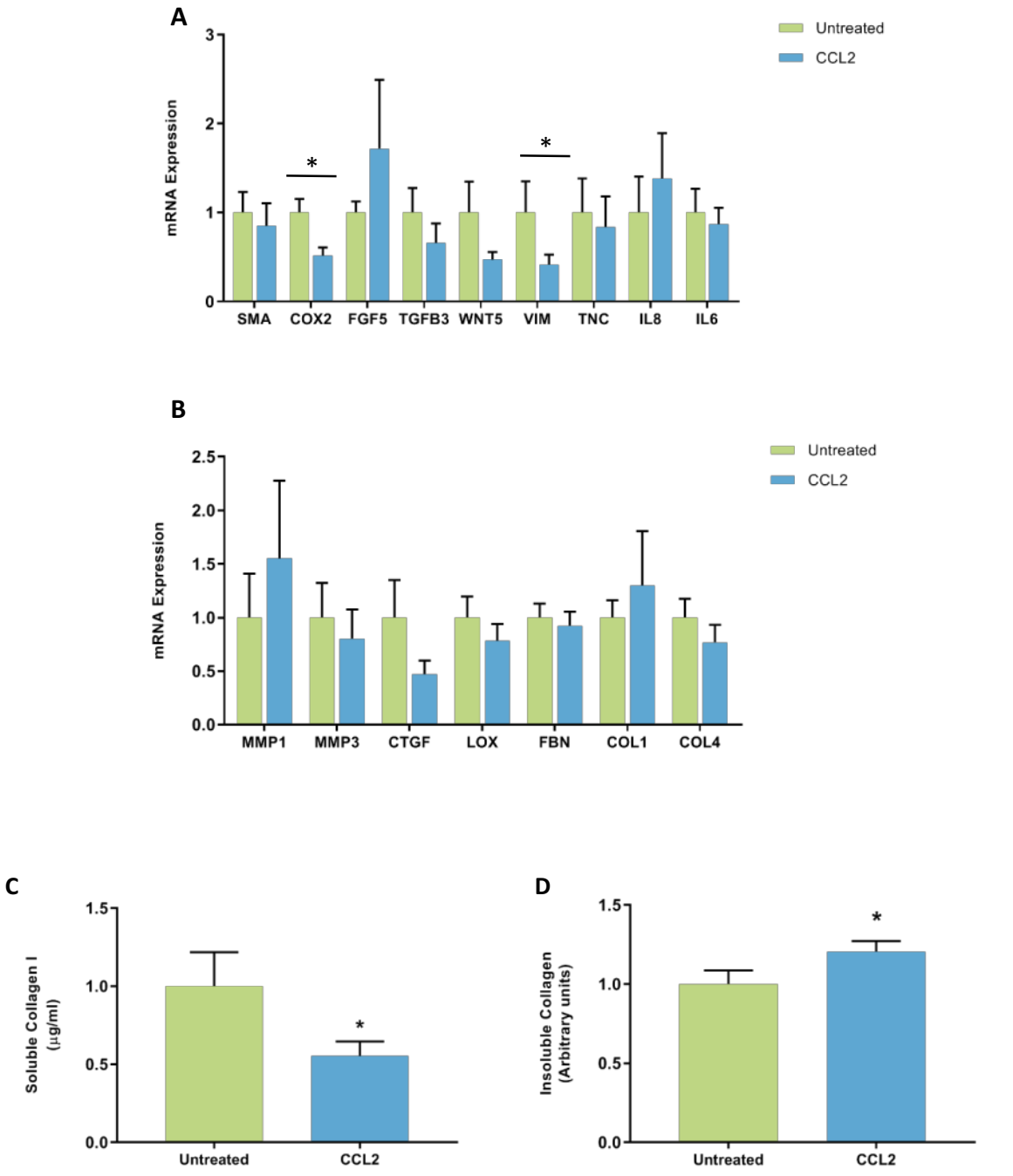

Figure 4.1: The effect of CCL2 on gene expression and collagen production in mammary fibroblasts. Messenger RNA expression of cancer associated genes (A) and genes involved in extracellular matrix regulation and collagen production (B) measured by RT-PCR in human mammary fibroblasts following treatment with 500ng/mL of CCL2 for 72hrs. mRNA expression normalised to HPRT1 expression, and presented as relative expression where the average for untreated control is 1. Collagen production was measured using collagen 1 ELISA (C) and insoluble collagen measured by sirius red staining (D). Data presented as mean + SEM with statistical analysis performed using a linear mixed effects model with Tukey's post-hoc comparison. Statistical significance indicated by * when $p<0.05$

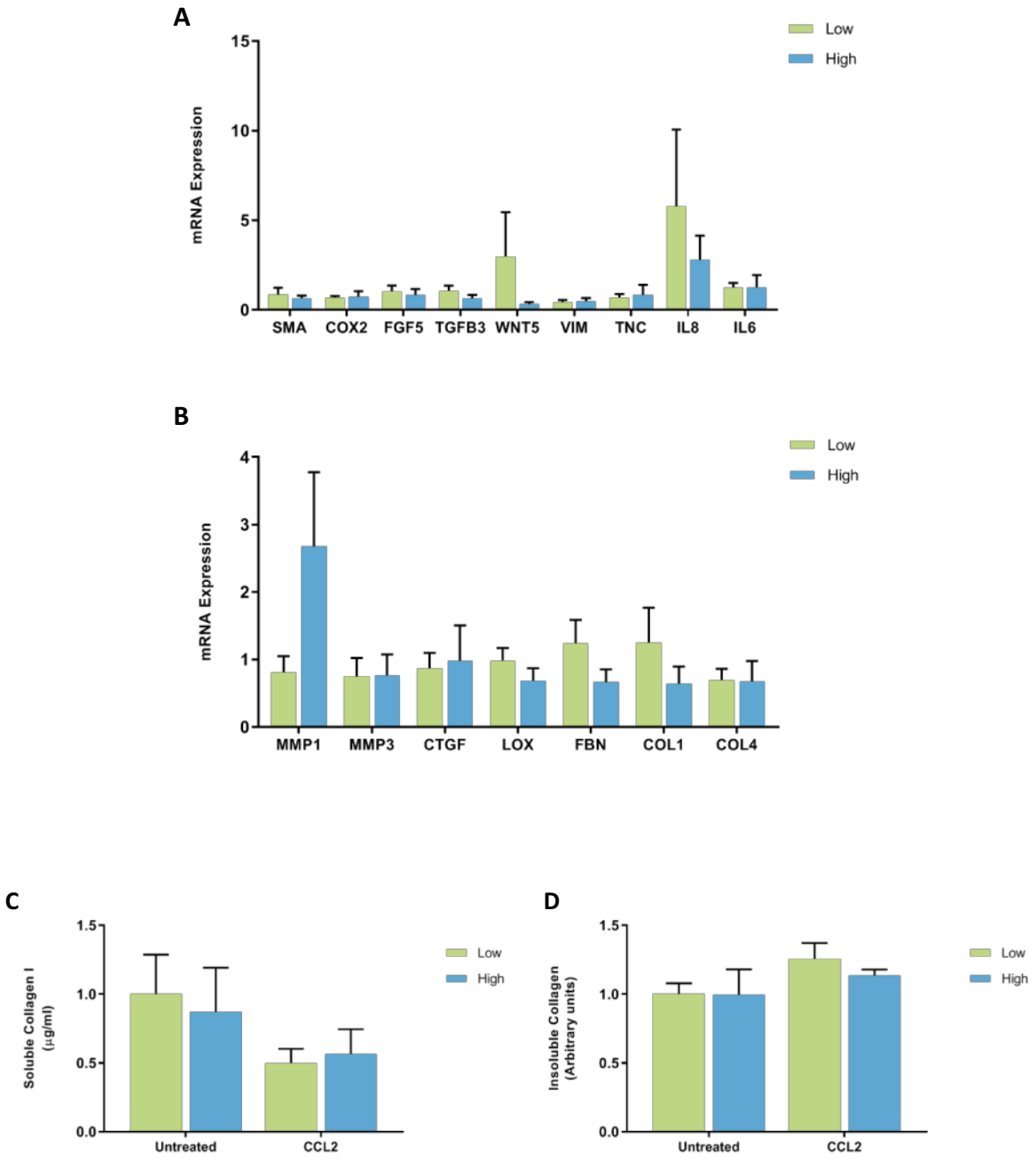

Figure 4.2: mRNA expression and collagen production in mammary fibroblasts isolated from women with high and low mammographic density.
Messenger RNA expression of cancer associated genes (A) and genes involved in extracellular matrix regulation and collagen production (B) measured by RT-PCR in human mammary fibroblasts from women with high and low mammographic density (n=8 per group) following treatment with 500ng/mL of CCL2 for 72 hours. mRNA expression normalised to HPRT1 expression, and presented as relative expression where the average for untreated control is 1. Collagen production was measured using collagen 1 ELISA (C) and insoluble collagen measured by sirius red staining (D). Data presented as mean + SEM with statistical analysis performed using a linear mixed effects model with Tukey's post-hoc comparison. Statistical significance indicated by * when $p<0.05$

4.2.2 The effect of mammary fibroblasts and CCL2 on THP-1 derived macrophage phenotype in co-culture

To investigate the effect of mammary fibroblasts and CCL2 on THP-1 derived macrophages, PMA-treated macrophages were co-cultured with primary mammary fibroblasts in the presence or absence of 500ng/mL of CCL2 for 72 hours. Macrophages were then analysed by flow cytometry to determine macrophage phenotype. Macrophage phenotype was determined by expression of surface markers CD80 and CD163. M0 cells were classified as CD80-/CD163- cells, M1 macrophages were classified as CD80+/CD163- cells, and M2 macrophages were classified as CD163+/CD80- negative cells based on isotype control gating strategy (Figure 2.3) [131, 138]. PMA-treated macrophages alone in culture were 40% M2 phenotype, 8% M1 phenotype, with the remainder in M0. The population of M1 CD80+/CD163- macrophages was significantly decreased by 6% in THP-1 derived macrophages in co-culture with mammary fibroblasts (1.45±0.24%) compared to macrophage only controls (7.75±1.00%) ($p<0.01$) (Figure 4.3.E). The population of M2 CD163+/CD80- macrophages was significantly increased from 44.03±2.3% in macrophage only controls to 61.69±0.67% in macrophages co-cultured with mammary fibroblasts ($p<0.01$ (Figure 4.3.F). However, there was no difference in M1 or M2 surface marker expression when treated with CCL2 in both macrophages alone or in co-culture.

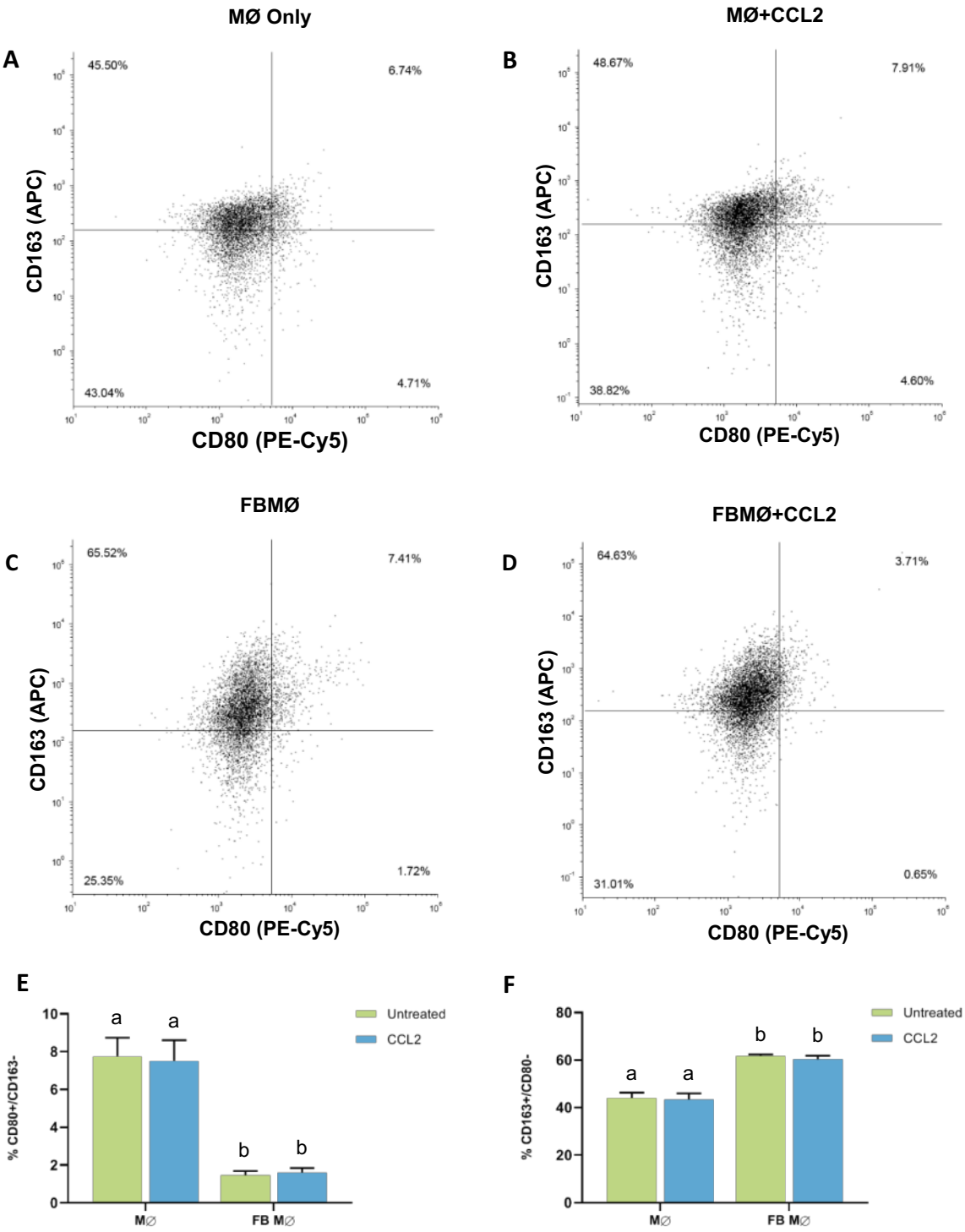

Figure 4.3: THP-1 derived macrophage phenotype following indirect co-culture with mammary fibroblasts and CCL2 for 72 hours.
Cell surface marker expression of CD163 and CD80 on THP-1 derived macrophages were detected using flow cytometry in macrophage only (MØ) (A), macrophages treated with CCL2 (MØ + CCL2) (B), macrophages in co-culture with mammary fibroblasts (FB MØ) (C), and macrophages in co-culture with mammary fibroblasts treated with CCL2 (FB MØ + CCL2) (D). Bar graphs represent the percentage of viable cells which are CD80+/CD163- (E), and CD163+/CD80- (F) in each culture condition. Data presented as mean percentage cells ±SEM (n=6). Statistical analysis was performed using one-way ANOVA with Tukey's Post hoc comparison. Statistical significance is indicated by different letters (a,b,c) when $p<0.05$.

4.2.3 The effect of mammary fibroblasts and CCL2 on THP-1 derived macrophage gene expression.

To investigate the effects of primary mammary fibroblasts and CCL2 on THP-1 derived macrophage gene expression, PMA-treated THP-1 cells were indirectly co-cultured with primary mammary fibroblasts in the presence or absence of 500ng/mL of CCL2 for 72 hours (n=3). The mRNA expression of cytokines *TGFB1*, *IL10*, *IFNG* and *TNFA* were detected by RT-PCR as well as expression of the CCL2 receptor *CCR2*. Genes involved in tissue remodelling and growth factors such as *MMP2*, *MMP9*, *TIMP1*, *PDGF* and *VEGF* were also measured using quantitative real time PCR relative to expression of housekeeping gene *HPRT1* from the same patient. Results are expressed in arbitrary units, were the data were normalised so that the average expression of each gene in untreated controls was equal to 1.

Expression of mRNA encoding TGFB1 appeared to be increased in THP-1 derived macrophages treated with CCL2, however this was highly variable and not significant (Figure 4.4.A). There was a trending 2-fold increase in expression of *IL10* mRNA in fibroblast co-cultured THP-1 derived macrophages (2.08±0.21 arbitrary units) ($p=0.063$), and a significant 3-fold increase in *IL10* expression in fibroblast co-cultured macrophages treated with CCL2 (3.15±0.62 arbitrary units) compared to macrophage only controls (1.00±0.41 arbitrary units) ($p<0.05$). However, there was no significant difference between co-cultured macrophages treated with CCL2 and those without (Figure 4.4.B). It was observed that *IFNG* mRNA expression was significantly increased 4-fold in fibroblast co-cultured macrophages treated with CCL2 (3.92±0.78 arbitrary units) compared to macrophage only controls (1.00±0.49 arbitrary units) ($p<0.05$). A trending 3-fold increase in expression of *IFNG* in co-cultured macrophages without CCL2 was observed, however this was not significant (Figure 4.4.C). Expression of *TNFA* mRNA was not significantly attenuated in THP-1 derived macrophages in any of the culture conditions reported in this

experiment (Figure 4.4.D). Expression of mRNA encoding the CCL2 receptor CCR2 was increased 4-fold in fibroblast co-cultured THP-1 derived macrophages in the presence (4.31±1.02 arbitrary units) and absence (4.02±0.72 arbitrary units) of CCL2, compared to macrophage only controls (1.00±0.11 arbitrary units) (Figure 4.4.E).

Expression of mRNA encoding MMP2 was significantly increased 11-fold in co-cultured THP-1 derived macrophages (11.23±2.11 arbitrary units), and 7-fold in co-cultured macrophages treated with CCL2 (7.13±0.68 arbitrary units), compared to macrophage only controls (1±0.10 arbitrary units) ($p<0.01$) (Figure 4.5.A). Expression of mRNA encoding MMP9 was significantly decreased in THP-1 derived macrophages when co-cultured with mammary fibroblasts (0.22±0.04 arbitrary units) compared to macrophage only controls (1.00±0.12 arbitrary units) ($p<0.05$). This result was unchanged by the addition of CCL2 (Figure 4.5.B). Expression of mRNA encoding TIMP1 was significantly increased 3-fold in co-cultured macrophages (3.48±1.00 arbitrary units) compared to macrophage only controls (1.00±0.20 arbitrary units) ($p<0.01$). Expression of *TIMP1* was also increased in co-cultured macrophages treated with CCL2, however this increase was only 2-fold (1.98±0.47 arbitrary units) ($p<0.01$) (Figure 4.5.C). A trending reduction in expression of mRNA encoding PDGF was observed in co-cultured macrophages with and without CCL2 compared to macrophage only controls, however this was not significant ($p=0.09$) (Figure 4.5.D). It was observed that mRNA expression of *VEGF* was significantly increased 4-fold in THP-1 derived macrophages when co-cultured with mammary fibroblasts (3.87±0.15 arbitrary units), in the presence and absence of CCL2 compared to macrophage only controls (1.00±0.05 arbitrary units) ($p<0.05$) (Figure 4.5.E).

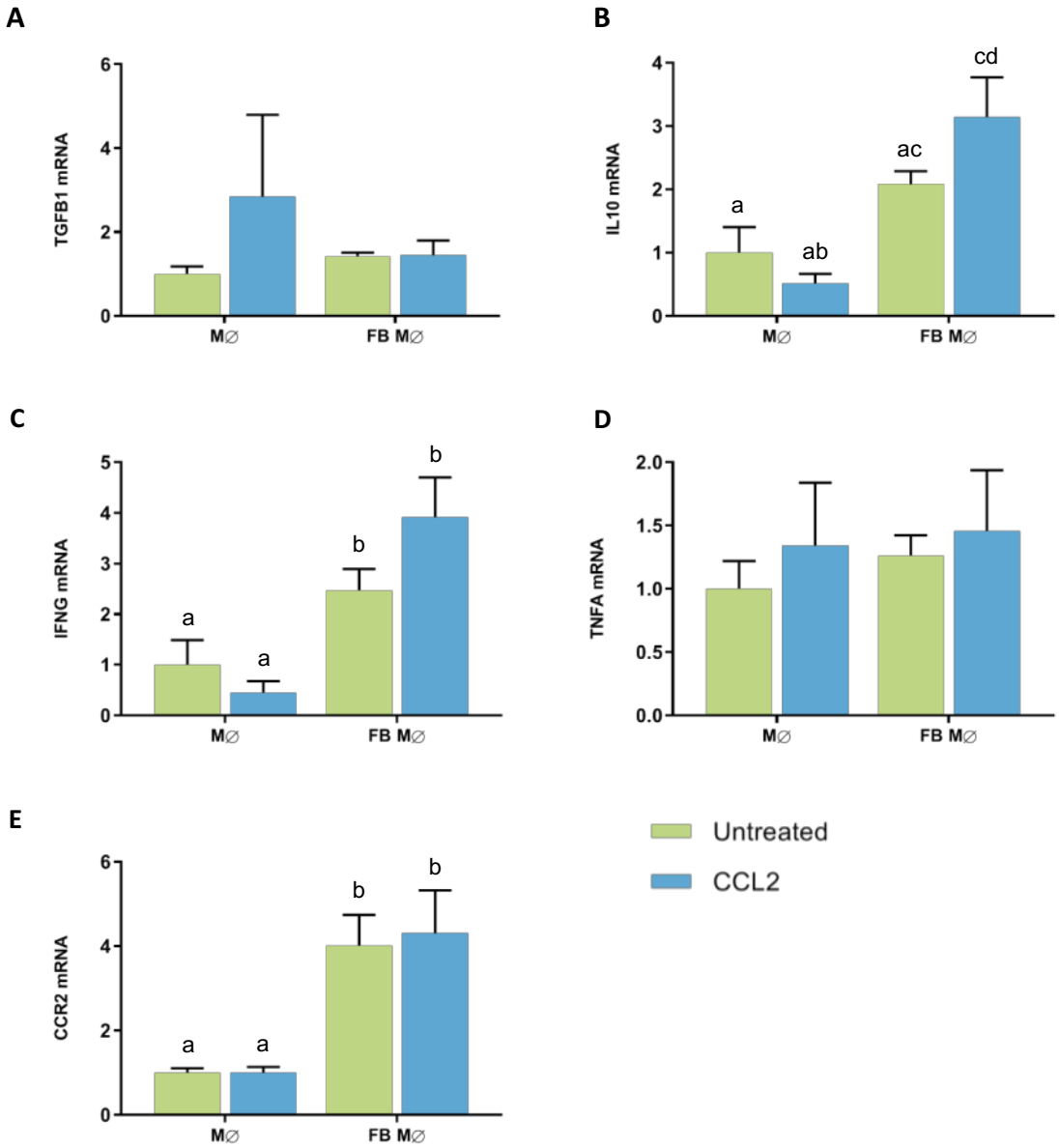

Figure 4.4: Cytokine gene expression in THP-1 derived macrophages following indirect co-culture with mammary fibroblasts and CCL2 for 72 hours.
Messenger RNA expression of genes A) *TGFB1*, B) *IL10*, C) *IFNG*, D) *TNFA* and E) *CCR2* in THP-1 derived macrophages upon co-culture with mammary fibroblasts and/or treatment with 500ng/mL of CCL2 for 72 hours (n=3). Culture conditions were macrophage only (MØ) and macrophages in co-culture with mammary fibroblasts (FB MØ). Results were normalised to housekeeping gene HPRT1 so average expression in macrophage only control samples is 1. Data presented as mean + SEM with statistical analysis performed using a linear mixed effects model with Tukey's post-hoc comparison. Statistical significance is indicated by different letters (a,b,c,d) when $p<0.05$.

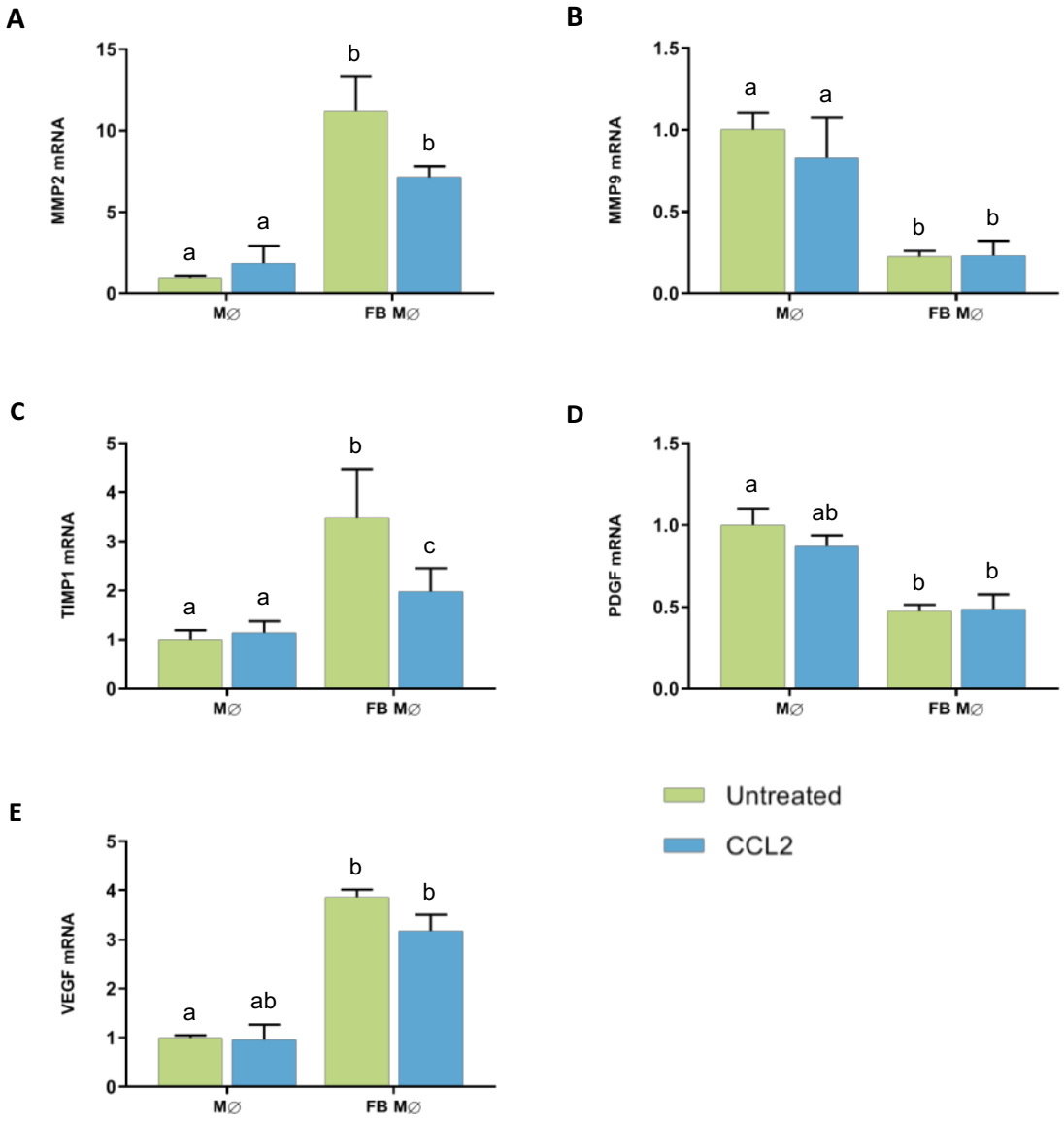

Figure 4.5: Tissue remodelling gene expression in THP-1 derived macrophages following indirect co-culture with mammary fibroblasts and CCL2 for 72 hours.
Messenger RNA expression of genes A) *MMP2*, B) *MMP9*, C) *TIMP1*, D) *PDGF* and E) *VEGF* in THP-1 derived macrophages upon co-culture with mammary fibroblasts and/or treatment with 500ng/mL of CCL2 for 72 hours (n=3). Culture conditions were in macrophage only (MØ) and macrophages in co-culture with mammary fibroblasts (FB MØ). Results were normalised to housekeeping gene HPRT1 so average expression in macrophage only control samples is 1. Data presented as mean + SEM with statistical analysis performed using a linear mixed effects model with Tukey's post-hoc comparison. Statistical significance is indicated by different letters (a,b,c) when $p<0.05$.

4.2.4 The effect of THP-1 derived macrophages and CCL2 on mammary fibroblast gene expression in co-culture

To investigate the effects of THP-1 derived macrophages and CCL2 on primary mammary fibroblast gene expression, PMA-treated THP-1 cells were indirectly co-cultured with primary mammary fibroblasts in the presence or absence of 500ng/mL of CCL2 for 72 hours (n=6). Expression of mRNA encoding genes which are markers of CAFs such as *SMA*, *FGF5*, *TNC*, *WNT5, TGFB3* and *VIM* were measured by RT-PCR. Genes involved in extracellular remodelling including *MMP1*, *MMP3*, *MMP9*, *TIMP1*, *LOX*, *FBN* and *CTGF* were also measured for mRNA expression as well as inflammatory markers *IL6*, *IL8* and *COX2*. Data presented is relative expression to the housekeeping gene *HPRT1* for each culture condition, and results were normalised so the average expression of fibroblast only controls is 1 arbitrary unit.

The average expression of *SMA* mRNA in fibroblasts co-cultured with THP-1 derived macrophages with and without CCL2 was 80% lower (0.18±0.04 arbitrary units) than in fibroblast only controls (1.00±0.36 arbitrary units) ($p=0.01$) (Figure 4.6.A). Expression of *FGF5* mRNA was observed to be increased 3-fold in mammary fibroblasts in co-culture with THP-1 derived macrophages with and without treatment with CCL2 (3.43±0.24 arbitrary units) compared to fibroblast only controls (1.00±0.24 arbitrary units) ($p<0.01$) (Figure 4.6.B). In mammary fibroblasts in co-culture with THP-1 derived macrophages, mRNA expression of *TGFB3* was significantly decreased by approximately 85% (0.13±.03) compared to fibroblast only controls (1.00±0.23 arbitrary units), this reduction was unchanged with treatment with CCL2 (0.15±0.04 arbitrary units) ($p<0.01$) (Figure 4.6.D). Co-culture of primary mammary fibroblasts with THP-1 derived macrophages did not have any significant effects on mRNA expression on *VIM*, *TNC* or *WNT5* (Figure 4.6.C,E-F).

In mammary fibroblasts in co-culture with THP-1 derived macrophages, mRNA expression of *MMP1* was significantly increased by approximately 80-fold in the absence (80.42±16.69 arbitrary units) and presence of CCL2 (88.26±18.62 arbitrary units) compared to fibroblast only controls (1.00±0.33 arbitrary units) ($p<0.01$ in both culture conditions) (Figure 4.7.A). Expression of mRNA encoding MMP3 was also significantly increased in co-cultured mammary fibroblasts, by approximately 19-fold both in the presence (19.47±3.57 arbitrary units) and absence (19.21±4.07 arbitrary units) of CCL2 compared to fibroblast only controls (1.00±0.59 arbitrary units) ($p<0.01$) (Figure 4.7.B). A significant 90-fold increase in mRNA expression encoding MMP9 was observed in mammary fibroblasts co-cultured with THP-1 derived macrophages (0.87±56.58 arbitrary units) compared to fibroblast only controls (1.00±0.46 arbitrary units) ($p<0.05$). In co-cultured fibroblasts treated with CCL2, expression of *MMP9* was also significantly increased (68.87±35.89 arbitrary units) ($p<0.05$). There was no significant difference between co-cultured fibroblasts treated with CCL2 compared to those without CCL2 (Figure 4.7.C). In mammary fibroblasts in co-culture with THP-1 derived macrophages, expression of mRNA encoding TIMP1 was significantly increased by approximately 60% (1.57±0.16 arbitrary units) compared to fibroblast only controls (1.00±0.23 arbitrary units), and this was not altered by treatment with CCL2 (1.59±0.13 arbitrary units) ($p<0.05$) (Figure 5.7.D).

It was observed that the average mRNA expression of *FBN* was decreased by approximately 60% in fibroblasts when co-cultured with THP-1 derived macrophages (0.39±.07 arbitrary units), compared to fibroblast only controls (1.00±0.28 arbitrary units) ($p<0.05$). This result was not further attenuated by treatment with CCL2 (0.43±0.08 arbitrary units) ($p<0.05$) (Figure 4.7.E). Co-culture of mammary fibroblasts with THP-1

derived macrophages, with and without CCL2 did not have any significant effects on mRNA expression of *CTGF* and *LOX* (Figure 4.7.F-G).

Marked changes in mRNA expression of inflammatory genes was observed in mammary fibroblasts when indirectly co-cultured with THP-1 derived macrophages in the presence and absence of CCL2. Expression of mRNA encoding COX2 was significantly increased by approximately 35-fold in fibroblasts when co-cultured with THP-1 derived macrophages both with CCL2 treatment (38.78±7.51 arbitrary units) and without (34.79±4.73 arbitrary units) compared to fibroblast only controls (1.00±0.28 arbitrary units) ($p<0.01$ in both conditions). There was no difference between co-cultured fibroblasts treated with CCL2 and those without CCL2 (Figure 4.8.A). Expression of mRNA encoding IL6 was significantly increased approximately 30-fold in fibroblasts co-cultured with THP-1 derived macrophages both with CCL2 (26.06±2.44 arbitrary units) and without (28.04±3.55 arbitrary units) compared to fibroblast only controls (1.00±0.26 arbitrary units) ($p<0.01$) (Figure 4.8.B). Expression of mRNA encoding IL8 was highly increased in mammary fibroblast in co-culture with THP-1 macrophages with over 500-fold increase (541.9±180.6 arbitrary units) in expression compared to fibroblast only controls (1.00±0.52 arbitrary units) ($p<0.01$). Co-cultured fibroblasts with CCL2 treatment also exhibited highly increased expression of *IL8*, with approximately 400-fold increase (411.6±102.62 arbitrary units) compared to fibroblast only controls (1.00±0.52 arbitrary units) ($p<0.01$) (Figure 4.8.C).

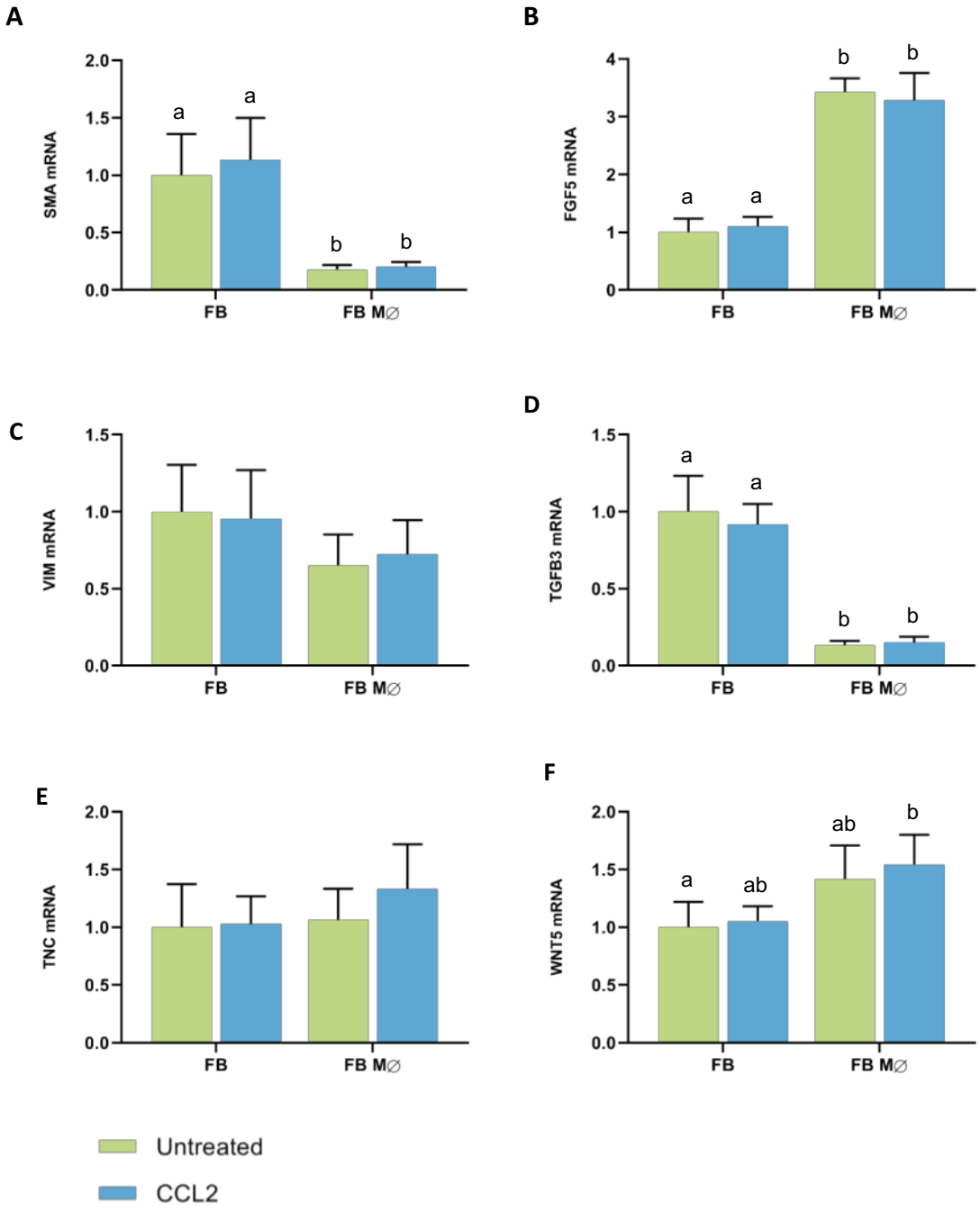

Figure 4.6: CAF marker gene expression in mammary fibroblasts following indirect co-culture with THP-1 derived macrophages and/or CCL2 for 72 hours.
Messenger RNA expression of genes A) *SMA*, B) *FGF5*, C) *VIM*, D) *TGFB3* E) *TNC* and F) WNT5 in mammary fibroblasts upon co-culture with THP-1 derived macrophages and/or treatment with 500ng/mL of CCL2 for 72 hours (n=6). Culture conditions were in fibroblast only (FB), and fibroblasts in co-culture with THP-1 derived macrophages (FB MØ). Results were normalised to housekeeping gene HPRT1 so average expression in fibroblast only control samples is 1. Data presented as mean + SEM with statistical analysis performed using a linear mixed effects model with Tukey's post-hoc comparison. Statistical significance is indicated by different letters (a,b,c) when $p<0.05$.

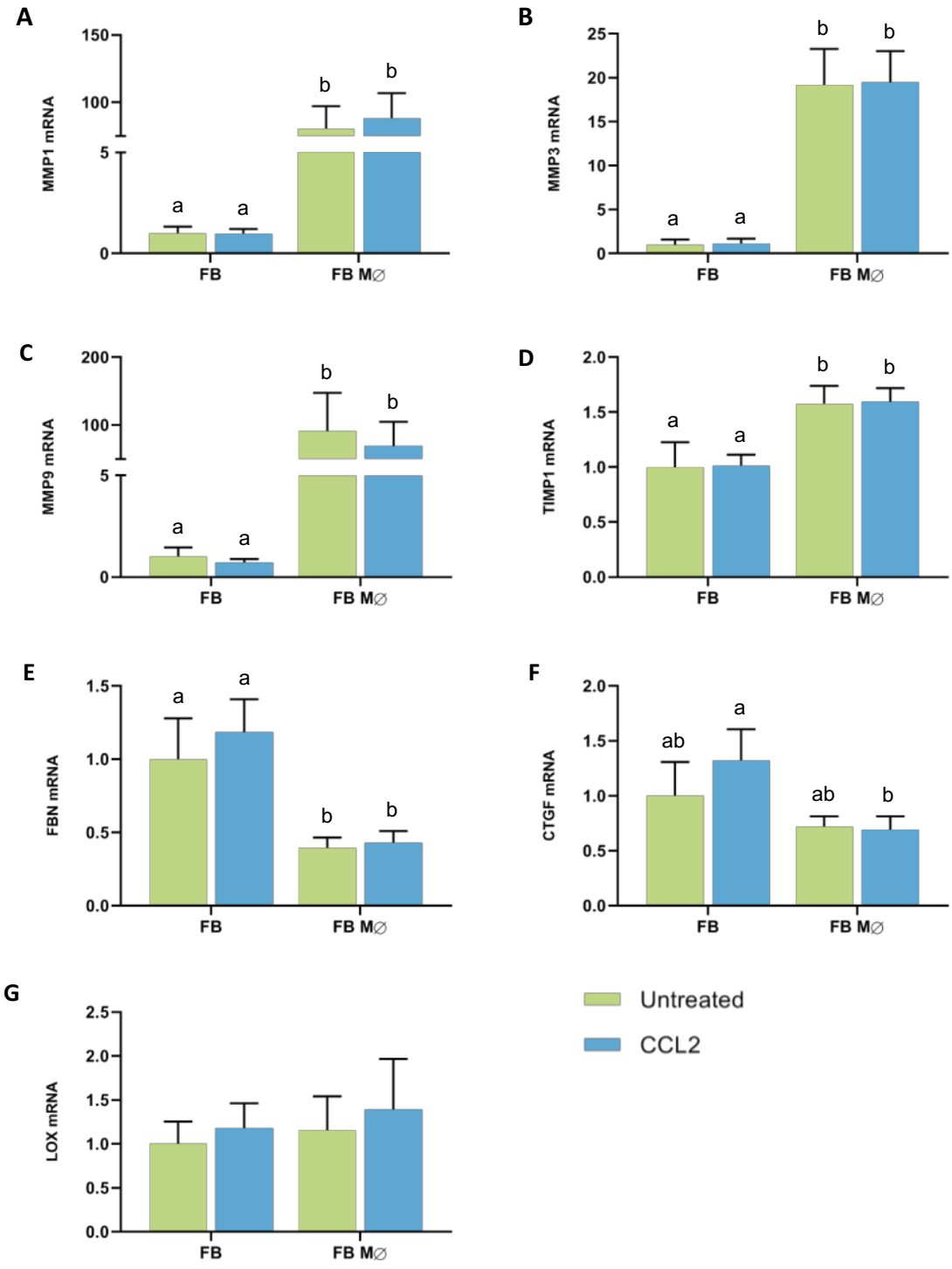

Figure 4.7: ECM remodelling gene expression in mammary fibroblasts following indirect co-culture with THP-1 derived macrophages and/or CCL2 for 72 hours.
Messenger RNA expression of genes A) *MMP1*, B) *MMP3*, C) *MMP9*, D) *TIMP1* E) *FBN*, F) *CTGF* and G) *LOX* in mammary fibroblasts upon co-culture with THP-1 derived macrophages and/or treatment with 500ng/mL of CCL2 for 72 hours (n=6). Culture conditions were in fibroblast only (FB), and fibroblasts in co-culture with THP-1 derived macrophages (FB MØ). Results were normalised to housekeeping gene HPRT1 so average expression in fibroblast only control samples is 1. Data presented as mean + SEM with statistical analysis performed using a linear mixed effects model with Tukey's post-hoc comparison. Statistical significance is indicated by different letters (a,b,c) when $p<0.05$.

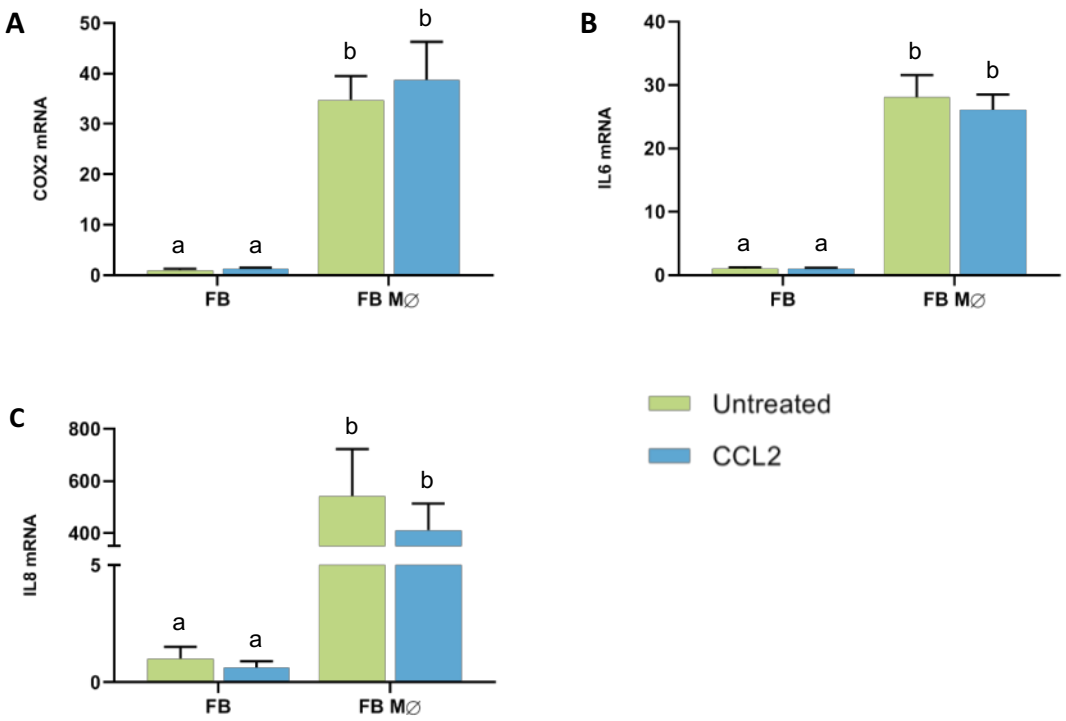

Figure 4.8: Inflammatory gene expression in mammary fibroblasts following indirect co-culture with THP-1 derived macrophages and/or CCL2 for 72 hours.
Messenger RNA expression of genes A) *COX2*, B) *IL6*, and C) *IL8* in mammary fibroblasts upon co-culture with THP-1 derived macrophages and/or treatment with 500ng/mL of CCL2 for 72 hours (n=6). Culture conditions were in fibroblast only (FB), and fibroblasts in co-culture with THP-1 derived macrophages (FB MØ). Results were normalised to housekeeping gene HPRT1 so average expression in fibroblast only control samples is 1. Data presented as mean + SEM with statistical analysis performed using a linear mixed effects model with Tukey's post-hoc comparison. Statistical significance is indicated by different letters (a,b,c) when $p<0.05$.

4.2.5 The effect of THP-1 derived macrophages and CCL2 on mammary fibroblast collagen production in co-culture

To investigate the effect of THP-1 derived macrophages and CCL2 on collagen production in primary mammary fibroblasts, fibroblasts were indirectly co-cultured with PMA-treated THP-1 cells in the presence or absence of 500ng/mL of CCL2 for 72 hours (n=6). Collagen production was measured by analysing mRNA expression of collagen genes *COL1A1* and *COL4A5* by RT-PCR in primary mammary fibroblasts, cell supernatants were analysed by ELISA to detect production of soluble collagen I, and Sirius red dye was used to measure insoluble collagen fibres (n=6). Results were adjusted to be relative to fibroblast only controls, where average level of collagen production was equal to 1 arbitrary units.

Expression of mRNA encoding COL1A1 was observed to be decreased by 60% in primary mammary fibroblasts when co-cultured with THP-1 derived macrophages both with (0.41±0.05 arbitrary units) and without CCL2 (0.43±0.06 arbitrary units) compared to fibroblast only controls (1.00±0.26 arbitrary units) ($p<0.01$) (Figure 4.9.A). In mammary fibroblasts co-cultured with THP-1 derived macrophages, mRNA expression of *COL4A5* was significantly decreased by 90% (0.13±0.03 arbitrary units) and with the addition of CCL2 (0.11±0.02 arbitrary units) compared to fibroblasts alone (1.00±0.25 arbitrary units) ($p<0.01$) (Figure 4.9.B).

It was observed that THP-1 derived macrophages (0.07±0.03 µg/mL) had significantly reduced collagen 1 production compared to fibroblast only controls (1±0.28µg/mL), and this was unchanged with the addition of CCL2 (0.09±0.04 µg/mL) ($p<0.01$). In primary mammary fibroblasts in co-culture with THP-1 derived macrophages, soluble collagen 1 production was significantly decreased by 40% (0.61±0.2 µg/mL) compared to fibroblast

only controls (1±0.28 µg/mL), and this result was unchanged with the addition of CCL2 (0.65±0.23 µg/mL) (p<0.05) (Figure 4.9.C).

Our studies observed that THP-1 derived macrophages had a significant 25% reduction in Sirius red staining (0.77±0.04 arbitrary units) compared to fibroblast only controls (1.00±0.02 arbitrary units) (p<0.01) this result was unchanged by treatment with CCL2 (0.83±0.04 arbitrary units). Sirius red staining was significantly increased in mammary fibroblasts alone treated with CCL2 (1.06±0.04 arbitrary units) compared to fibroblast only controls (1.00±0.02 arbitrary units). In mammary fibroblasts in co-culture with THP-1 derived macrophages treated with CCL2 there was a small but significant 10% increase in Sirius red staining (1.10±0.03 arbitrary units) compared to fibroblast only controls (1.00±0.02 arbitrary units) (p<0.01) (Figure 4.9.D). No other significant differences in Sirius red staining were identified (Figure 4.9.D).

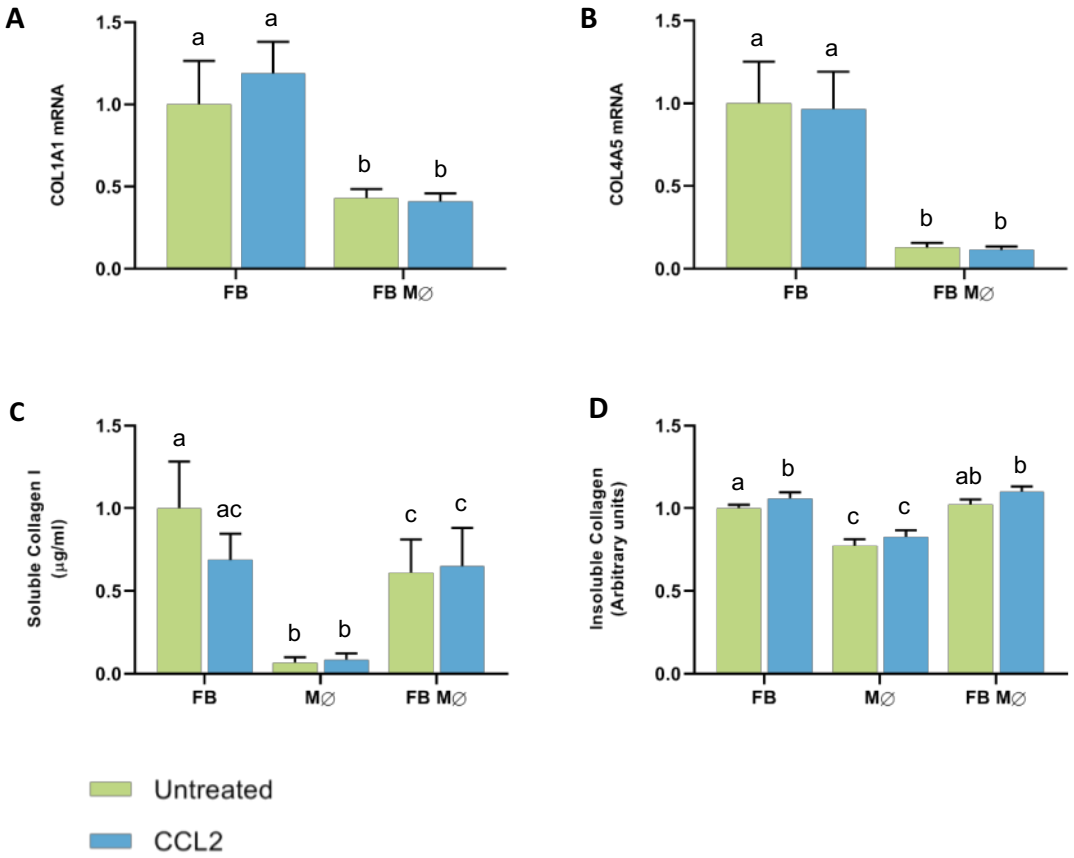

Figure 4.9: Collagen production in mammary fibroblasts following indirect co-culture with THP-1 derived macrophages and/or CCL2 for 72 hours.
Messenger RNA expression of genes A) *COL1A1* and B) *COL4A5* in mammary fibroblasts upon co-culture with THP-1 derived macrophages and/or treatment with 500ng/mL of CCL2 for 72 hours (n=6). Results were normalised to housekeeping gene HPRT1 so average expression in fibroblast only control samples is 1. Collagen production was measured using collagen 1 ELISA (C) and insoluble collagen measured by sirius red staining (D) normalised so that collagen production of fibroblast only controls was 1. Culture conditions were in fibroblast only (FB), macrophage only (MØ), and fibroblasts in co-culture with THP-1 derived macrophages (FB MØ). Data presented as mean + SEM with statistical analysis performed using a linear mixed effects model with Tukey's post-hoc comparison. Statistical significance is indicated by different letters (a,b,c) when $p<0.05$.

4.3 DISCUSSION

While the role of macrophages in the mammary gland have been extensively investigated, the crosstalk between primary fibroblasts and macrophages in the mammary gland are not well understood. In this chapter, we have demonstrated that THP-1 derived macrophages have significant roles in modulating fibroblast gene expression and collagen production, and the crosstalk between mammary fibroblasts and macrophages can influence macrophage phenotype. This research suggests that cell-to-cell communication between mammary fibroblasts and local macrophages can have a profound effect on both normal functioning of the mammary gland as well in breast cancer risk and progression.

4.3.1 The effect of CCL2 on ECM regulation in mammary fibroblasts

Our studies reported that although CCL2 did not affect expression of genes involved in ECM regulation in mammary fibroblasts, it did reduce the abundance of soluble collagen 1 in the culture supernatant and increase deposition of insoluble collagen fibres. The increase in insoluble collagen in response to CCL2 is consistent with previous observations in the literature. CCL2 has been investigated for its involvement in fibrotic diseases, which are characterised by excessive deposition of collagen and ECM. CCL2 is upregulated by hepatic monocytes during liver fibrosis, and production of CCL2 is elevated in both the serum and lungs of patients with pulmonary fibrosis [243, 245, 246]. In the mammary gland, it has been demonstrated that mice overexpressing CCL2 in the mammary glands exhibited greater thickness of stromal collagen in the mammary glands compared to wildtype controls [157]. The study by Sun et al also found an increase in mRNA expression of ECM genes *Lox* and *Timp3* in the mammary glands of CCL2 overexpressing mice.

However, our studies found no changes in mRNA expression of genes involved in ECM remodelling and collagen production by fibroblasts in response to treatment with CCL2.

This suggests that the role of CCL2 in collagen deposition in the mammary gland could be through post-translational processes, whereby the synthesis of soluble collagen monomers is not affected. This would explain why there was a decrease in soluble collagen accompanied by an increase in insoluble fibres.

On the other hand, while many studies have linked CCL2 to fibrosis and excess collagen deposition, some studies have reported that CCL2 can have anti-fibrotic functions. It has also been observed that CCL2 downregulates expression of collagen I in pulmonary fibroblasts [247]. Another study reported a reduction in liver fibrosis in CCL2 knockout mice [248]. Some studies have reported no effect of CCL2 on collagen production in fibroblasts [249]. This suggests that the role of CCL2 in collagen production is complex and requires further studies to be understood. Overall, these results suggest that CCL2 may play a role in increasing collagen deposition. However the role of CCL2 in the breast may be dependent on signalling from the surrounding microenvironment.

4.3.2 Mammary fibroblasts drive differentiation of THP-1 derived macrophages

The functions of macrophages are largely dependent on their phenotype. M1 macrophages are involved in inflammatory responses and have anti-tumour activities [131, 134]. M2 macrophages are anti-inflammatory and can have tumour promoting functions [138, 139, 142]. Our study of crosstalk between mammary fibroblasts and THP-1 derived macrophages demonstrated that there is an increase in CD163+ M2, or alternatively activated macrophages when in an indirect co-culture with primary mammary fibroblasts. Further, the co-cultured macrophages exhibited greater expression of *IL10* and reduced *TNFA.*

Our findings of increased percentages of CD163 positive M2 macrophages when co-cultured with mammary fibroblasts is supported by Ferrer et al who co-cultured human dermal fibroblasts with M1 macrophages. This promoted expression of CD163 surface marker and skewed macrophages to an M2 phenotype [250]. Further, the authors observed low secretion of TNFA and high levels of IL10 from co-cultured macrophages which is consistent with our gene expression studies, which demonstrated that THP-1 derived macrophages expressed higher abundance of IL10, and baseline levels of TNFA when in the presence of mammary fibroblasts [250].

Previous studies have demonstrated that alternatively activated M2 macrophages have tumour promoting functions, and tumour associated macrophages (TAMs) have a similar phenotype to M2 macrophages [131, 142, 251]. One study observed that CD14+ human peripheral blood mononuclear cells (PBMCs), when co-cultured with fibroblasts from pancreatic cancer tissue, exhibited increased expression of M2 macrophage phenotype markers CD163 and CD206 [239]. Both M2 and TAM subtypes produce immunosuppressive cytokines such as IL10 so that cancer cells can avoid immune surveillance, as well as producing growth factors and angiogenesis promoting factors to drive tumour progression such as VEGF and PDGF [132, 136, 252, 253]. Our studies found that macrophages in co-culture with mammary fibroblasts produce greater VEGF and IL10 than macrophages alone.

Alternatively activated macrophages have been implicated in breast cancer. Previous studies have demonstrated that CD163+ macrophages in the tumour stroma of breast cancer tissues correlated to high tumour grade, larger tumour size, triple negative cancers, and suggest that CD68+ macrophages in the tumour stroma is an independent prognostic marker for cancer free survival [136, 254]. Our results show that mammary fibroblasts stimulate the polarisation of macrophages to an alternatively activated M2 phenotype,

expressing high abundance of immune suppressive cytokines and pro-angiogenic factors that could favour tumour development and progression in breast cancer. However, the role of fibroblasts-macrophage interactions in mammographic density is still unclear. Previous studies of have reported there to be less CD206+ alternatively activated macrophages in the stroma of high density breast tissue areas compared to low density breast tissue areas [57]. Therefore, further studies are required to elucidate the role of macrophages, and their interactions with mammary fibroblasts in mammographic density and the associated breast cancer risk.

4.3.3 M2 polarised macrophages promote tissue remodelling in mammary fibroblasts

M2 macrophages have roles in tissue remodelling and are found in fibrotic conditions where there is an abundance of collagen and extracellular matrix. Our gene expression studies reported that macrophages have higher expression of *MMP2* and *TIMP1,* and reduced expression of *MMP9* when in co-culture with mammary fibroblasts. A balance of expression of MMP's and their inhibitors, TIMPs, are important in the production and degradation of collagen and the extracellular matrix. Studies have reported that mice with macrophages overexpressing MMP9 had a reduction in collagen deposition in a model of pulmonary fibrosis [255]. Expression of TIMP1 has also been implicated in multiple fibrotic conditions. Previous studies have reported that TIMP1 promotes liver fibrosis, and is upregulated in mouse models of liver fibrosis [256, 257]. Therefore, macrophages can directly influence the production of collagen and extracellular matrix through expression of MMPs and TIMPs.

Alternative activated M2 macrophages can also influence tissue remodelling and collagen production through their effects on fibroblasts. Our studies demonstrated that when in co-culture with THP-1 derived macrophages, mammary fibroblasts upregulated fibrotic genes

MMP1, *MMP3*, *MMP9* and *TIMP1*, and increased deposition of insoluble collagen fibres. Previous studies on dermal fibroblasts have shown that M2 macrophages promote fibrotic activity of dermal fibroblasts in co-culture by increasing collagen production and expression of TIMP1 [236]. Other studies have reported that stimulation of human dermal fibroblasts with M2 macrophage conditioned media resulted in upregulation of collagen production, however, contradictory to our studies, it was also reported that MMP gene expression was downregulated [234]. This could be due to the mixed population of macrophage subtypes in our studies, as not all macrophages were polarised to M2 phenotypes. The role of macrophages in the fibrotic activity of mammary fibroblasts is complex, further studies that delineate each subtype of macrophage, and examine their effects on tissue remodelling and collagen production would help to gain understanding how these interactions may contribute to the collagen rich environment in high density breast tissue.

4.3.4 Limitations

The experiments described in this chapter possess a number of limitations, which may affect the interpretation of the results. The limitations of fibroblast only RT-PCR analysis and collagen analysis in mammary fibroblasts from women with high and low mammographic density have been previously described in Chapter 3 (section 3.3.4). Other limitations are related to the use of the macrophage cell line THP-1 cells.

THP-1 cells are a monocyte cell line derived from acute monocytic leukaemia, and are therefore an immortal cell line and may not reflect the function and responsiveness of macrophages that reside in the mammary gland stroma. Further, as this cell line was being co-cultured with primary fibroblasts from human breast tissue samples, there is a possibility for HLA mismatching to occur, which may influence the gene expression and other behaviour of the THP-1 derived cells. Due to the limited amount of human tissues

we can obtain, it is not feasible to use human samples with only specific HLA types. Greater sample size of human mammary fibroblasts would be required to ensure there is no HLA mismatching.

Our studies found that PMA-treated THP-1 macrophages were differentiated into M2 macrophages when in the presence of mammary fibroblasts, our study utilised a basic analysis of M2 macrophage phenotype by identifying CD163+, CD80 negative cells as well as mRNA expression of cytokines such as IL10. However, M2 macrophages have multiple subtypes including M2a, M2b, M2c and tumour associated macrophages (TAMs) which all have different functions, making the investigation of crosstalk between mammary fibroblasts and M2 macrophages more complex, future studies may identify proportions of each M2 subtype in the our population to better understand the functional role of M2 macrophages in modulating fibroblast activity.

4.4 CONCLUSION

Using an indirect co-culture of primary mammary fibroblasts with THP-1 derived macrophages, we have shown that the crosstalk between these cells have many effects on gene expression and collagen production. Co-culture with mammary fibroblasts promotes the polarisation of macrophages to the alternatively-activated M2 phenotype, and increases expression of anti-inflammatory cytokines and pro-angiogenic factors that may contribute to the development and progression of breast cancer. However, the role of these interactions in mammographic density is still unclear. While macrophages stimulated a production of insoluble collagen by fibroblasts, an upregulation of pro-fibrotic TIMP1 in both macrophages and fibroblasts, there was also upregulation of collagen degrading MMPs. Future experiments are required to further understand the interactions between macrophages and fibroblasts in the mammary gland, how those interactions contribute to mammographic density and breast cancer risk.

CHAPTER FIVE

THE EFFECT OF CCL2 ON MAMMARY TUMORIGENESIS AND GLOBAL GENE EXPRESSION IN MICE

5.1 INTRODUCTION

Chemokine Ligand 2 (CCL2) is a chemotactic cytokine that acts as a chemoattractant for monocytes and macrophages to sites of inflammation [156]. Expression of CCL2 is largely induced by oxidative stress or cell activation by growth factors and cytokines [258]. The main target of CCL2 is macrophages and the primary receptor, CCR2, is expressed on leukocytes, monocytes and macrophages. CCL2 is expressed by several different cell types including fibroblasts, epithelial, smooth muscle, endothelial cells [153, 154].

CCL2 has been implicated in tumour development and progression. Studies have demonstrated that CCL2 is highly expressed by tumour cells in the primary tumour and contribute to the development and progression of breast cancer. CCL2 promotes recruitment of tumour associated macrophages (TAMs) and increases the invasive properties of cancer cells, thereby promoting metastasis to the lungs and bone [162, 163, 259, 260]. Further, high expression of CCL2 is associated with poor prognosis in women with breast cancer [162, 260].

Previous studies have implicated CCL2-mediated inflammation in mammographic density and the associated breast cancer risk. A study in 2017 utilised mice constitutively expressing CCL2 in the mammary gland, under the control of the MMTV promoter to investigate the role of CCL2 in mammary gland development and cancer risk. This study reported that 12-week-old MMTV-Ccl2 mice exhibited a greater proportion of stroma and density of collagen surrounding epithelial ducts compared to wildtype controls [157]. This

is characteristic of high mammographic density [57, 70]. When these mice were subsequently challenged with the chemical carcinogen DMBA, CCL2 overexpressing mice exhibited increased susceptibility to cancer with decreased tumour latency and decreased tumour-free survival [157]. These studies suggest that chronic inflammation, mediated by CCL2, may contribute to mammographic density and the associated cancer risk in these mice. In humans, analysis of paired high and low MD samples of healthy breast tissue demonstrated that elevated CCL2 expression is associated with high MD regions [157].

While CCL2 is associated with increased susceptibility to mammary tumours using the DMBA model, this has not yet been confirmed in other animal models of mammary tumorigenesis, and the role of CCL2 in mammary tumour development and progression has not been investigated. Expression of the polyomavirus middle T-antigen (PyMT) under the control of the mouse mammary tumour virus promotor (Mmtv) in mice creates a model of mammary tumorigenesis of an epithelial cell origin with 100% penetrance [261]. Use of this model allows for investigation of multiple stages of mammary tumorigenesis and progression.

In this chapter, we used a transgenic mouse model that constitutively expresses CCL2 in the mammary gland (Mmtv-Ccl2) crossed with the Mmtv-Pymt mouse tumour model to create a PyMT/CCL2 cohort. These mice spontaneously develop tumours from 6 weeks of age and this enables analysis of disease progression and metastasis. Using these mice, we investigated the role of CCL2 in mammary tumourigenesis by examining the hyperplasia, tumour latency, development, progression and metastasis of tumours using a PyMT/CCL2 transgenic mouse model. RNAseq analysis was performed on mammary glands from 12 week old Mmtv-Ccl2 mice to elucidate the biological pathways that are affected by CCL2 overexpression, which may contribute to mammographic density and breast cancer risk.

5.2 RESULTS

5.2.1 The effect of CCL2 on early tumorigenesis in 9 week old PyMT mice

Mice that carry the Mmtv-Pymt transgene spontaneously develop mammary gland tumours from 6 weeks of age. In this study, Mmtv-Ccl2 and FVB wild type control mice were cross-bred with Mmtv-Pymt transgenic mice to generate the PyMT/CCL2 cohort. We first sought to investigate the impact of CCL2 overexpression on very early tumorigenesis. Prior to the emergence of palpable tumours, there are early tumorigenic events such as hyperplasia in this mouse model. The 4th pair mammary glands, where there were no palpable tumours, were collected from 9 week old mice and carmine alum stained for whole mount analysis of early tumorigenesis.

All dissected mammary glands from both PyMT/CCL2 and PyMT controls exhibited extensive areas of early tumorigenesis at 9 weeks of age. It was observed that the largest tumorigenic area was at the nipple end of the mammary gland (Figure 5.1.A,C). These areas may be more advanced tumours. These areas were measured using Image J and there was no significant difference in nipple area or percentage nipple area between PyMT controls and PyMT/CCL2 mice. These nipple areas were excluded from the further analysis of early tumorigenesis.

Several measures were used to assess the early tumorigenic areas of PyMT/CCL2 and PyMT control mice. The average tumorigenic area as a percentage of total mammary gland area was 15.95±1.56% and 18.81±2.71% for PyMT controls and PyMT/CCL2 mice respectively, and there was no significant difference between these groups ($p=0.325$) (Figure 5.1.E). However, when the number of individual tumorigenic areas per mouse was manually counted, there was a significant increase in the number of tumorigenic areas per

mm^2 of mammary gland for PyMT/CCL2 compared to PyMT controls (0.557±0.04 and 0.455±0.03 areas per mm^2 respectively (p=0.047) (Figure 5.1.F).

5.2.2 The effect of CCL2 on tumour latency

To investigate the effect of CCL2 on tumour latency in the Mmtv-PyMT mouse model, PyMT controls and PyMT/CCL2 mice were monitored for emergence of palpable tumours weekly from 6 weeks of age, and sacrificed at 9 and 12 week for analysis. A Kaplan-Meier plot was constructed to analyse the percentage of mice that were tumour-free in each week of monitoring. By 10 weeks of age 100% of the mice had developed tumours. The average tumour latency of the PyMT controls and PyMT/CCL2 mice was 8 and 7.5 weeks respectively (Figure 5.2). There was no significant difference in tumour latency between groups as determined using SPSS Log Rank (n=19 mice per group).

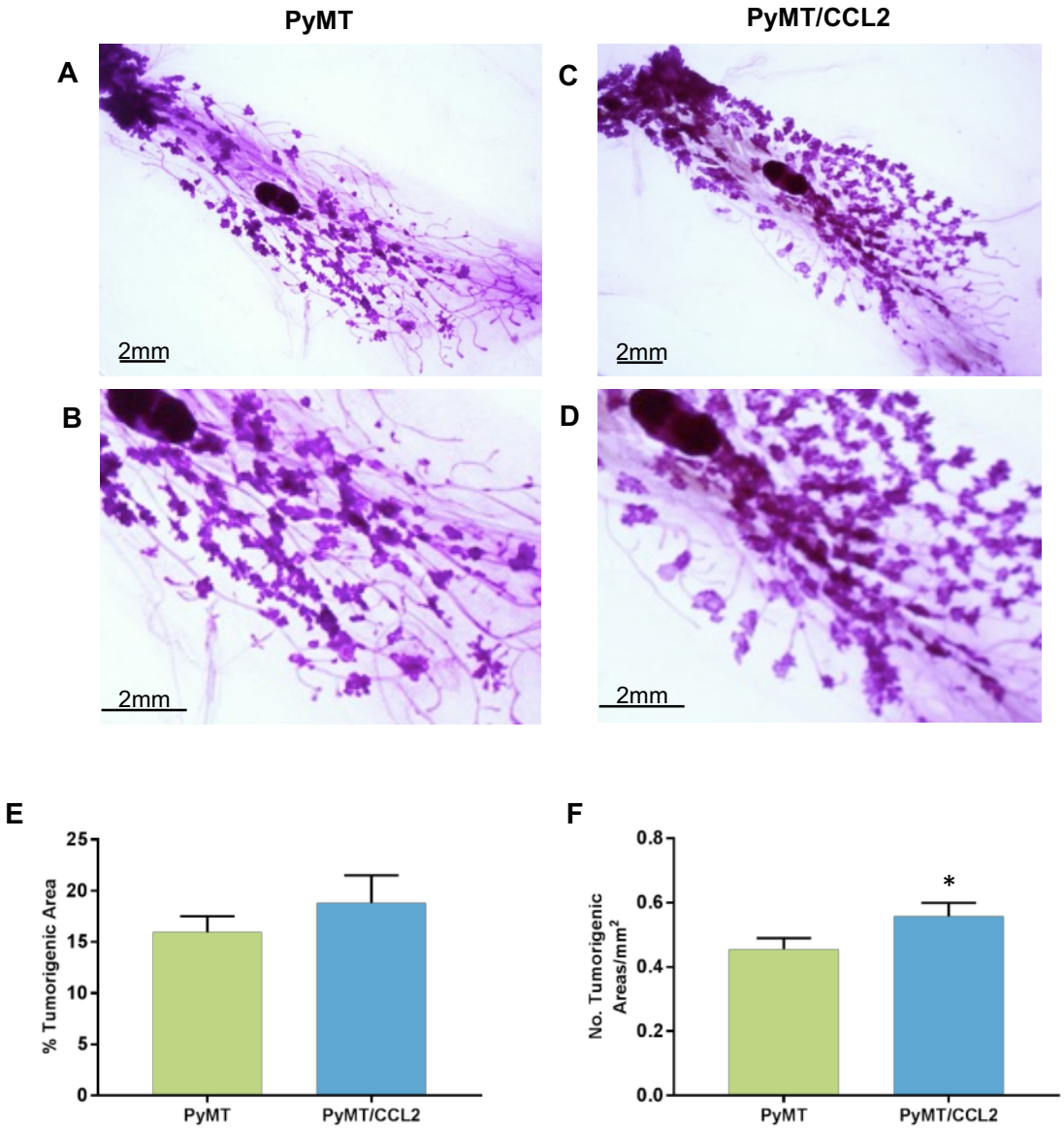

Figure 5.1: The effect of CCL2 overexpression on early mammary gland tumorigenesis in 9 week old PyMT transgenic mice
Representative images of carmine alum stained whole mounted 4th pair mammary glands of 9 week old PyMT (A, low magnification, B, high magnification) and PyMT/CCL2 (C, low magnification, D, high magnification) mice. Tumorigenic areas first start in the nipple area (indicated by open arrows). Growth of smaller tumorigenic, areas can be seen at the distal end of the mammary gland. Tumorigenic areas were measured and analysed for tumorigenic areas as a percentage of the gland area (E), and number of tumorigenic areas per mm^2 of gland (F). Data presented as mean + SEM (n= 9 per group). Measured data was analysed using a simple linear regression, and number of tumours was analysed using a negative binomial regression with Wald Chi-square post-hoc comparison * when $p<0.05$

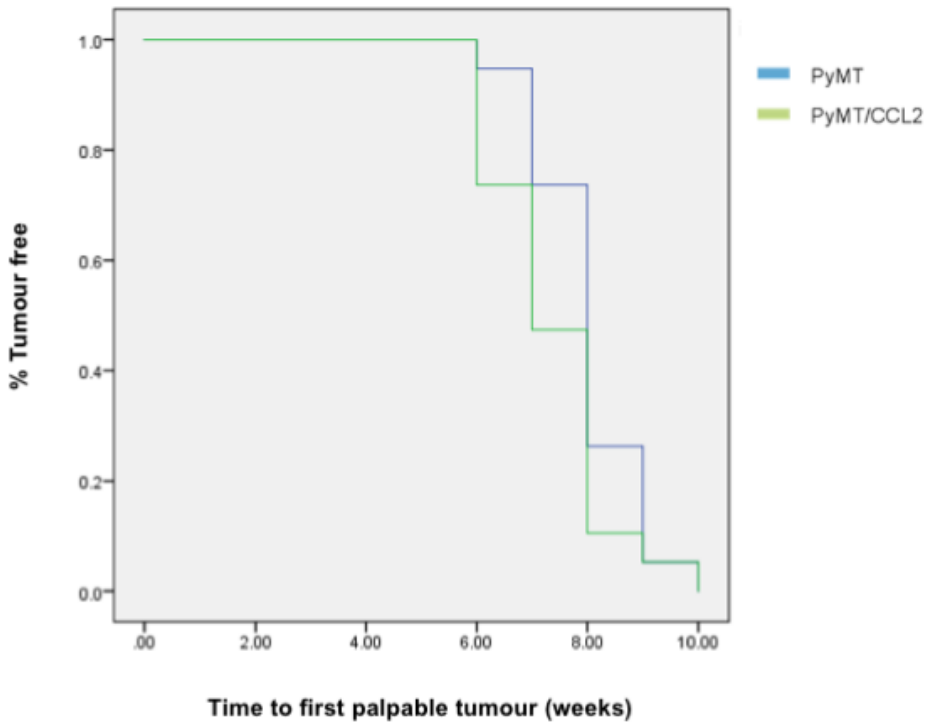

Figure 5.2: The effect of CCL2 overexpression on tumour latency in PyMT transgenic mice
PyMT and PyMT/CCL2 mice were palpated weekly to monitor for tumour latency from 6 weeks of age (n=28 per group). Kaplan-Meier survival plot of the percentage of tumour free mice for each week of monitoring (A) Statistical analysis was performed using SPSS, mean survival was tested using Log Rank test.

5.2.3 The effect of CCL2 on mammary tumour burden

To investigate the effect of CCL2 on mammary tumour burden, PyMT controls and PyMT/CCL2 mice were monitored for tumour development and sacrificed at 9 and 12 weeks. At this time, both the primary tumour and all other tumours were dissected and weighed to investigate tumour burden.

At 9 weeks age, the average primary tumour weight was 124.28±15.48mg for PyMT controls and 145.33±41.62mg in PyMT/CCL2 mice. At 12 weeks of age, the average primary tumour weight was 588.39±64.30mg in PyMT control mice and 613.29±104.01mg in PyMT/CCL2 mice. There was no significant difference in primary tumour weight between PyMT/CCL2 and PyMT control mice at 9 ($p=0.586$) and 12 ($p=0.885$) weeks of age (Figure 5.3.A).

The total tumour number for each mouse was counted. The average number of tumours in PyMT control mice was 3.36±0.26 tumours and in PyMT/CCL2 mice, there were 2.8±0.21 tumours at 9 weeks of age. At 12 weeks of age, the average number of tumours in PyMT control mice was 6.95±0.73 tumours, and in PyMT/CCL2 mice there were 8.24±0.26 tumours. There was no significant difference in tumour number between PyMT and PyMT/CCL2 mice at 9 ($p=0.187$) and 12 ($p=0.364$) weeks of age (Figure 5.3.B).

Tumour burden was measured as the total weight of all mammary tumours in each mouse. The average total tumour burden at 9 weeks of age was 268.67±19.04mg for PyMT controls and 211.93±45.43mg for PyMT/CCL2 mice. The average total tumour burden at 12 weeks of age was 1,611.79±154.57mg for PyMT controls and 1,695±169.46mg in PyMT/CCL2 mice. There was no significant difference in total tumour burden between PyMT/CCL2 and PyMT control mice at 9 ($p=0.187$) and 12 ($p=0.706$) weeks of age (Figure 5.3.D). Total tumour burden was also calculated as percentage of each mouse's total body

weight. The average percentage tumour burden at 9 weeks age was 1.15±0.08% in PyMT controls and 0.93±0.20% in PyMT/CCL2 mice. At 12 weeks of age, the average percentage tumour burden was 6.20±0.53% in PyMT control mice and 6.56±0.53% in PyMT/CCL2 mice. There was no significant difference in percentage tumour burden between PyMT/CCL2 and PyMT control mice at 9 ($p=0.243$) and 12 ($p=0.837$) weeks of age (Figure 5.3.C).

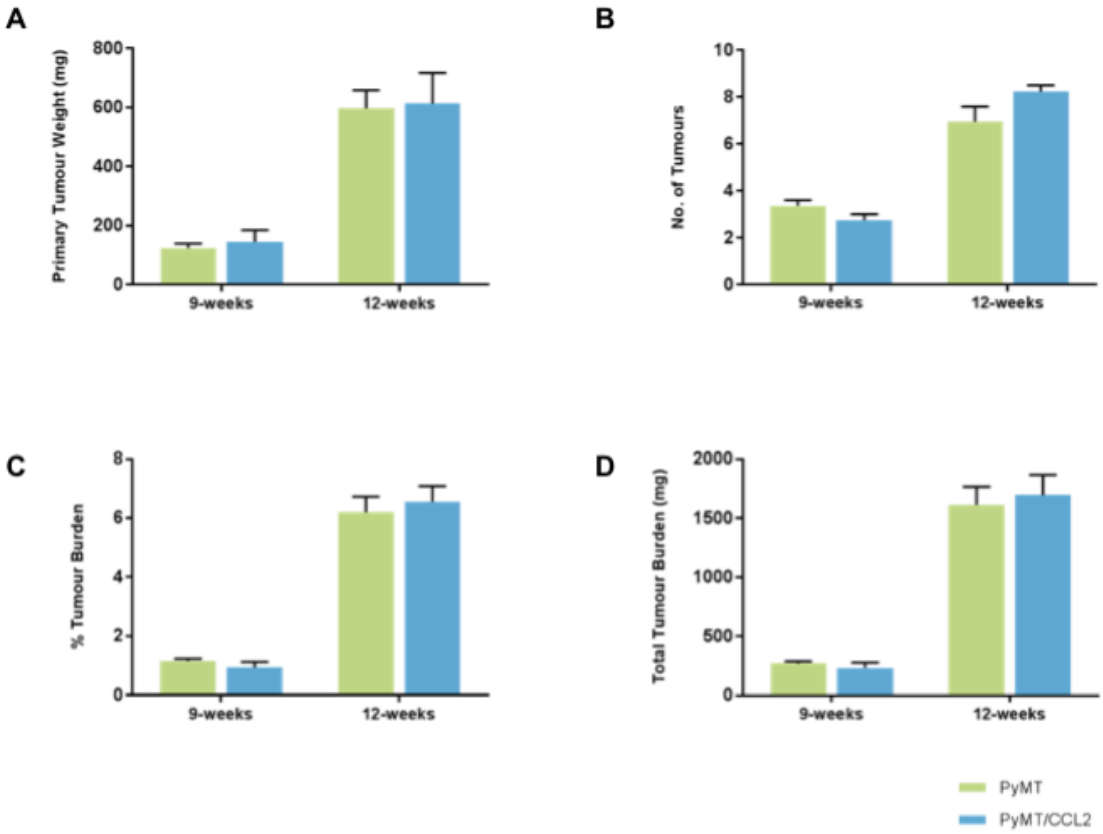

Figure 5.3: The effect of CCL2 overexpression on mammary tumour burden in PyMT transgenic mice. Primary and secondary tumours were collected from FVB/PyMT and PyMT/CCL2 mice at 9 (n=10) and 12 (n=19) weeks of age and weighed. The Primary tumour weight was determined as the first palpable tumour with the highest weight (A), total number of mammary tumours for each mouse was calculated (B). Tumour burden was calculated as a percentage of each animals total weight (C). Total tumour burden was determined by the sum of the weight of all tumours for each mouse (D). Data presented as mean + SEM with statistical analysis performed on measured data simple linear regression model, tumour number was analysed using a negative binomial regression model. Post-hoc comparison was performed using Wald Chi square test.

5.2.4 The effect of CCL2 on primary tumour progression

To investigate the effect of CCL2 on primary tumour progression, primary tumours from PyMT and PyMT/CCL2 mice were dissected at 9 and 12 weeks age (n=10 per genotype and 18 per genotype respectively). Primary tumours were formalin fixed and paraffin embedded, stained with haematoxylin and eosin and analysed for tumour grade and other pathological markers by veterinary pathologist Dr Lucy Woolford. The statistics of this pathological analysis can be found summarised in Table 5.3.A-B.

Primary tumours were classified into 4 tumour grades according to their morphology; hyperplasia (Figure 5.4.A), adenoma (Figure 5.4.B), early carcinoma (Figure 5.4.C) and late carcinoma (Figure 5.4.D). Late carcinoma is the most advanced tumour stage. At 9 weeks of age 100% of the primary tumours were late carcinoma, and there was no difference between PyMT and PyMT/CCL2 tumours (Figure 5.4.E). Primary tumours collected from PyMT mice at 12 weeks were 16.67% early carcinoma (3 out of 18 mice) and 83.33% late carcinoma (15 out of 18 mice). In PyMT/CCL2 mice, 10.53% of primary tumours were early carcinoma (2 out of 19 mice) and 89.47% were late carcinoma (17 out of 19 mice). There were no statistically significant differences in tumour grade between PyMT control mice and PyMT/CCL2 mice (Figure 5.4.F)

Primary tumours were also evaluated for cytological atypia, indicating the degree of abnormality to the cells appearance, with larger nuclear size compared to cytoplasm and variation in cell size. Cytological atypia is graded from none or minimal (Figure 5.5.A), mild (Figure 5.5.B), moderate (Figure 5.5.C) and marked (Figure 5.5.D). Primary tumours from PyMT/CCL2 and PyMT controls exhibited a marked degree of cytological atypia in all primary tumours, with no difference between mouse genotypes (Figure 5.5.E). Primary tumours collected from PyMT control mice at 12 weeks age had 11.11% moderate atypia (2 out of 18 mice) and 88.89% marked atypia (16 out of 18 mice). Tumours from

PyMT/CCL2 mice at 12 weeks age exhibited 5.26% moderate atypia (1 out of 19 mice) and 94.74% marked atypia (18 out of 19 mice). No significant differences in cytological atypia were observed between PyMT/CCL2 and PyMT control mice at 12 weeks age (Figure 5.5.F).

Primary tumours from PyMT/CCL2 and PyMT control mice were assessed for presence of tumour necrosis. The degree of tumour necrosis was categorised into none (5.6.A), rare (Figure 5.6.B), infrequent multifocal (Figure 5.6.C) and frequent multifocal (Figure 5.6.D). Primary tumours collected from PyMT/CCL2 and PyMT control mice at 9 weeks age had rare presence of tumour necrosis in 100% of tumours, with no difference between mouse genotype (Figure 5.6.E). Primary tumours collected from PyMT control mice at 12 weeks of age had 38.89% rare necrosis (7 out of 18 mice), 16.67% infrequent multifocal necrosis (3 out of 18 mice) and 44.44% frequent multifocal necrosis (8 of 18 mice). Primary tumours collected from PyMT/CCL2 mice at 12 weeks age had 10.53% with no necrosis observed (2 of 19 mice), 26.32% rare necrosis (5 of 19 mice), 36.84% infrequent multifocal necrosis (7 of 19 mice) and 26.32% frequent multifocal necrosis (5 of 19 mice). There was no significant difference in the distribution of tumours across the different classifications of necrosis between PyMT/CCL2 and PyMT controls (Figure 5.6.F).

In the Mmtv-Pymt mouse model, mammary gland tumours progress to pulmonary metastasis. To investigate the effect of CCL2 on pulmonary metastasis in Mmtv-Pymt mice, PyMT control and PyMT/CCL2 mice were sacrificed at 12 weeks of age. Lungs were dissected and were formalin fixed paraffin embedded and frozen in liquid nitrogen for histological and RNA analysis. Haematoxylin and eosin stained lung sections were analysed for the presence of pulmonary metastasis by veterinary pathologist Dr Lucy Woolford. Approximately 40% of both PyMT control and PyMT/CCL2 mice showed presence of metastatic lesions, the occurrence of metastasis was not affected by the

mouse genotype (Figure 5.7.C). Histological analysis shows the presence of mammary tumour cells in the lung to confirm metastasis (Figure 5.7.A-B).

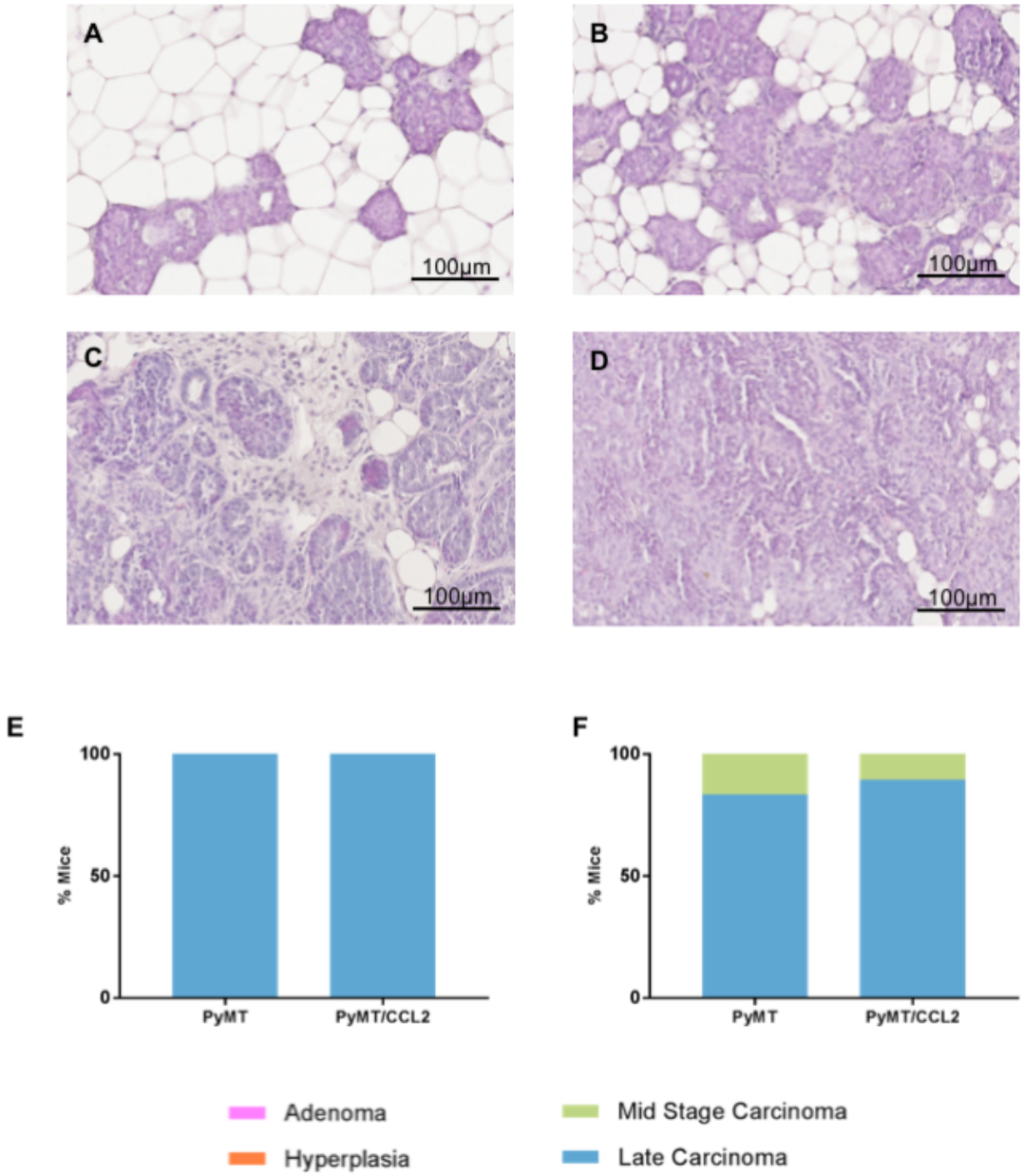

Figure 5.4: The effect of CCL2 on mammary tumour progression in PyMT transgenic mice
Representative images of haematoxylin and eosin stained primary mammary tumours at the four stages of tumour classification hyperplasia (A), adenoma (B), early carcinoma (C), and late carcinoma (D), taken at 40x magnification. Histological tumour staging was performed on primary mammary tumours from PyMT and PyMT/CCL2 mice at 9 (n=10) and 12 (n=19) weeks of age. Graph depict the percentage distribution of tumours at each histological grade at 9 weeks (E), and 12 weeks (F). Statistical analyses performed using Fisher's Exact test.

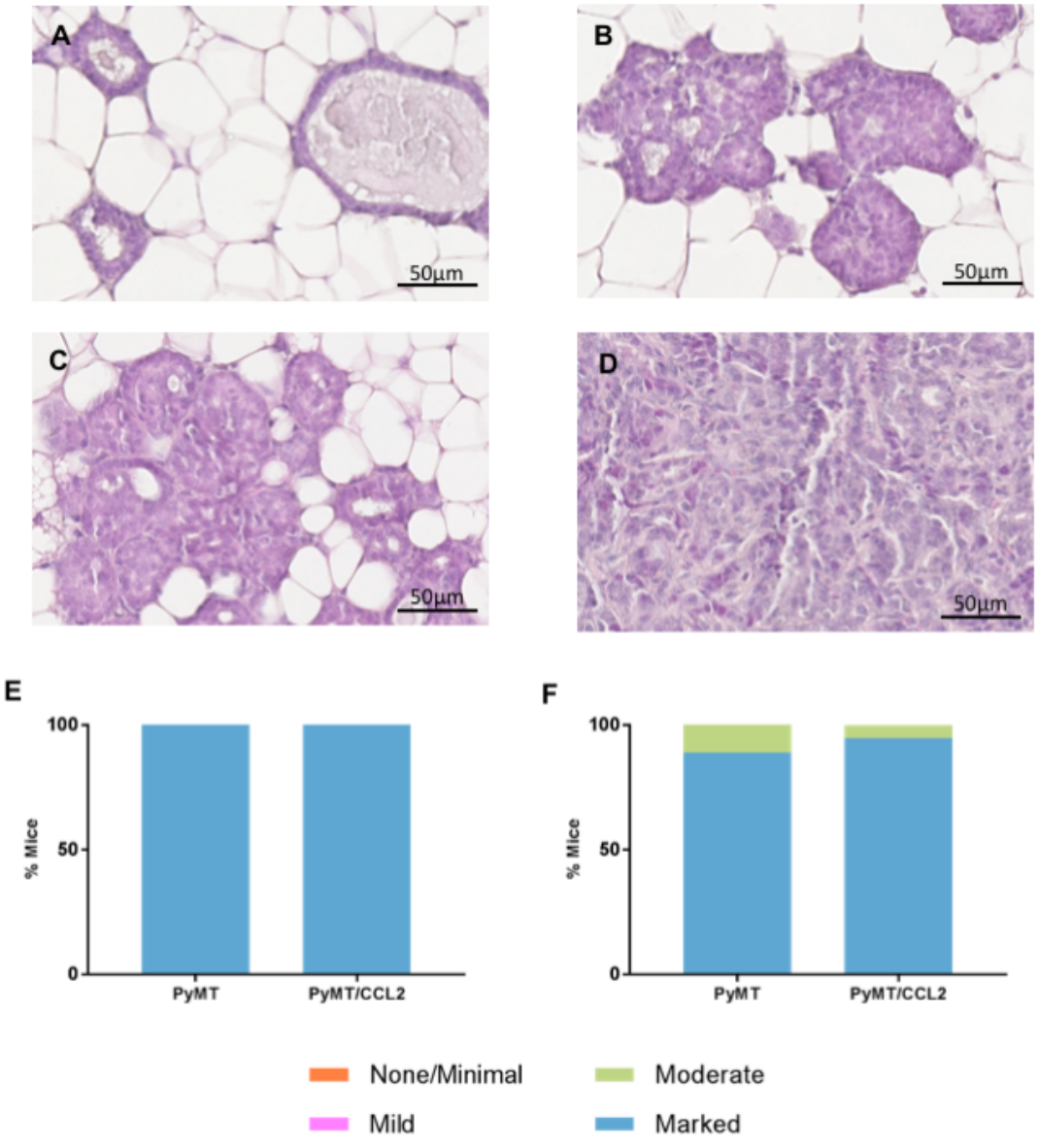

Figure 5.5: The effect of CCL2 overexpression on cytological atypia in PyMT transgenic mice
Representative images of haematoxylin and eosin stained primary mammary tumours with no atypia (A), mild atypia (B), moderate atypia (C), and marked atypia (D), taken at 40x magnification. Cytological atypia characterisation was performed on primary mammary tumours from PyMT and PyMT/CCL2 mice at 9 (n=10) and 12 (n=19) weeks of age. Graph depict the percentage distribution of tumours at each atypia grade at 9 weeks (E), and 12 weeks (F). Statistical analyses performed using Fisher's Exact test.

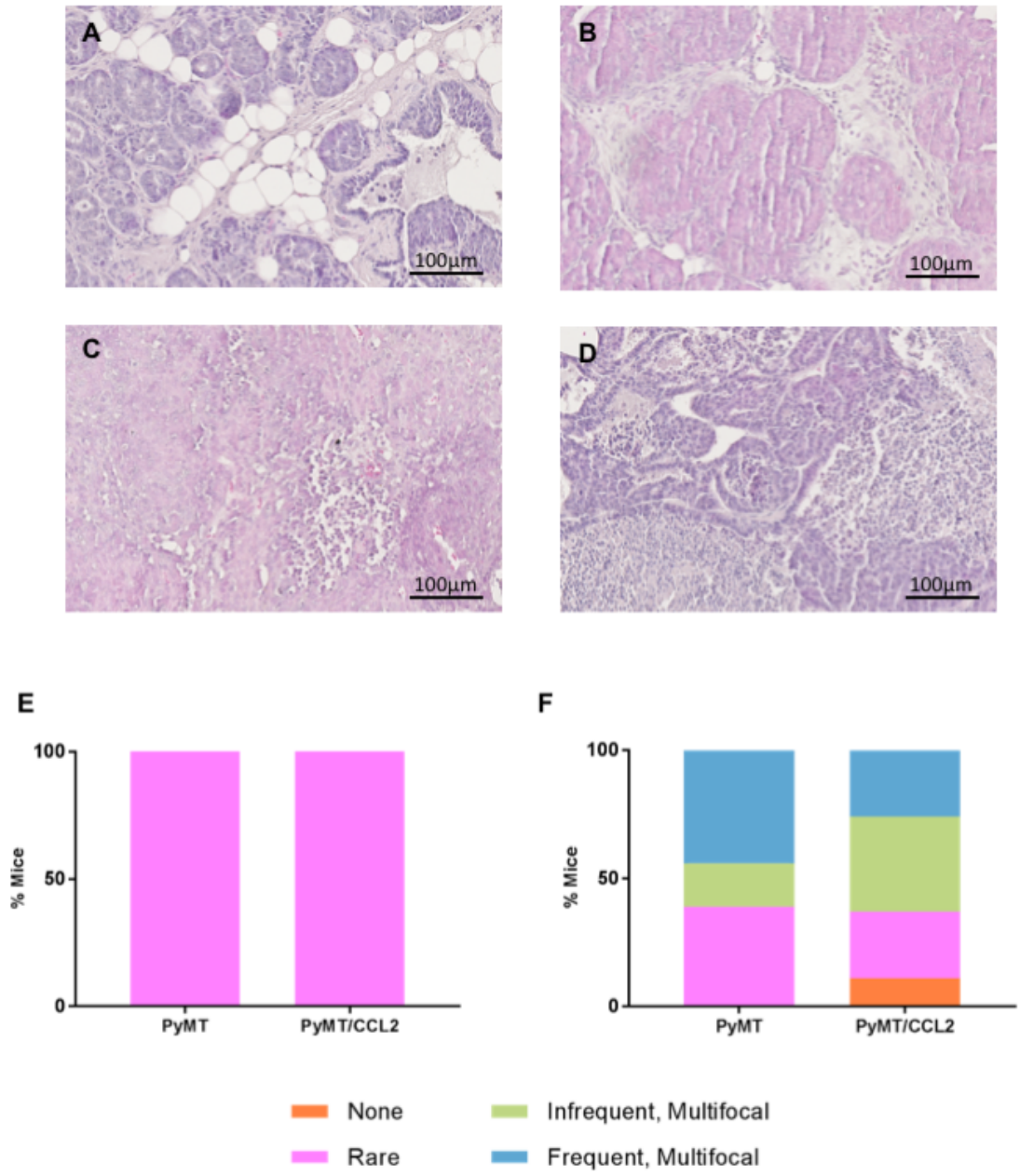

Figure 5.6: The effect of CCL2 overexpression of tumour necrosis in PyMT transgenic mice
Representative images of haematoxylin and eosin stained primary mammary tumours with no necrosis (A), rare necrosis (B), infrequent necrosis (C), and frequent necrosis (D), taken at 40x magnification. Characterisation of necrosis was performed on primary mammary tumours from PyMT and PyMT/CCL2 mice at 9 (n=10) and 12 (n=19) weeks of age. Graph depict the percentage distribution of tumours at each stage of necrosis at 9 weeks (E), and 12 weeks (F). Statistical analyses performed using Fisher's Exact test.

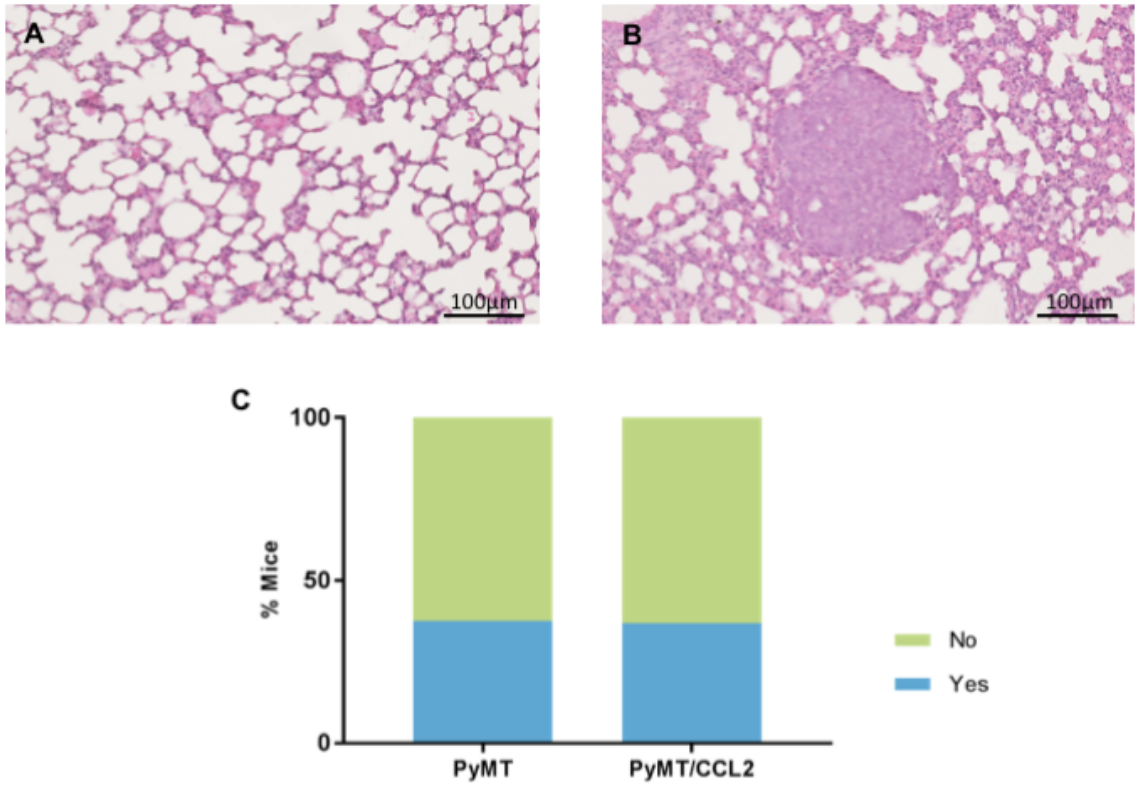

Figure 5.7: The effect of CCL2 overexpression on pulmonary metastasis in PyMT transgenic mice
Representative images of haematoxylin and eosin stained lung tissues from PyMT and PyMT/CCL2 mice at 12 weeks of age (n=19). Images represent normal lung tissue (A) and lung tissue with pulmonary metastases present (B). Graphs represent the percentage distribution of mice with presence or absence of pulmonary metastases in PyMT and PyMT mice (C). Data presented as mean +SEM with statistical analyses performed by Fischer's Exact test.

5.2.5 The effect of CCL2 on macrophage infiltration

To investigate the effect of CCL2 on macrophage infiltration during early tumorigenesis in the Mmtv-PyMT mouse model, 4th pair mammary glands were dissected at 9 weeks' age from PyMT and PyMT/CCL2 and formalin fixed paraffin embedded tissue sections were stained with pan macrophage marker F4/80. Three areas of early tumorigenesis were randomly identified, with assessor blinded to mouse genotype, in each mammary gland and the number of F4/80+ cells were manually counted around the perimeter of this area.

In mammary glands of 9 week of PyMT and PyMT/CCL2 mice, F4/80 stained macrophages were identified around the edges of regions of early tumorigenic and more advanced tumorigenic tissue regions (Figure 5.8.A-B). In PyMT mice, the average number of F4/80 stained macrophages per mm^2 was 3.87±0.413, and in PyMT/CCL2 mice there was an average of 7.67±0.961 macrophages per mm^2. There were significantly more macrophages infiltrating early tumorigenic tissue in PyMT/CCL2 mice compared to PyMT controls at 9 weeks of age ($p<0.001$) (Figure 5.8.C).

To investigate the role of CCL2 on macrophage infiltration of mammary tumours in the Mmtv-PyMT mouse model. Primary tumours were collected at 9 and 12 weeks of age from PyMT controls and PyMT/CCL2 mice, and formalin fixed paraffin embedded tissue sections were stained with F4/80. Areas of macrophage infiltration were measured and F4/80+ cells manually counted to determine the average macrophages per mm^2.

In primary tumours of PyMT and PyMT/CCL2 mice, F4/80 stained macrophages were identified around the borders of the primary tumours, and in the interstitial spaces between tumours regions (Figure 5.9,10. A-D). At 9 weeks of age, primary tumours collected from PyMT control mice had an average number of 338.44±58.34 macrophages per mm^2, and PyMT/CCL2 mice had an average of 697.13±145.23 macrophages per mm^2. PyMT/CCL2

mice had significantly greater number of macrophages per mm^2 than PyMT control mice at 9 weeks of age (p=0.008) (Figure 5.9.E). At 12 weeks of age, primary tumours collected from PyMT control mice had an average of 497.54±85.02 macrophages per mm^2, and PyMT/CCL2 mice had an average of 683.00±97.81 macrophages per mm^2. There was no significant difference in macrophage abundance in primary tumours collected from PyMT/CCL2 and PyMT control mice at 12 weeks of age (p=0.143) (Figure 5.10.E).

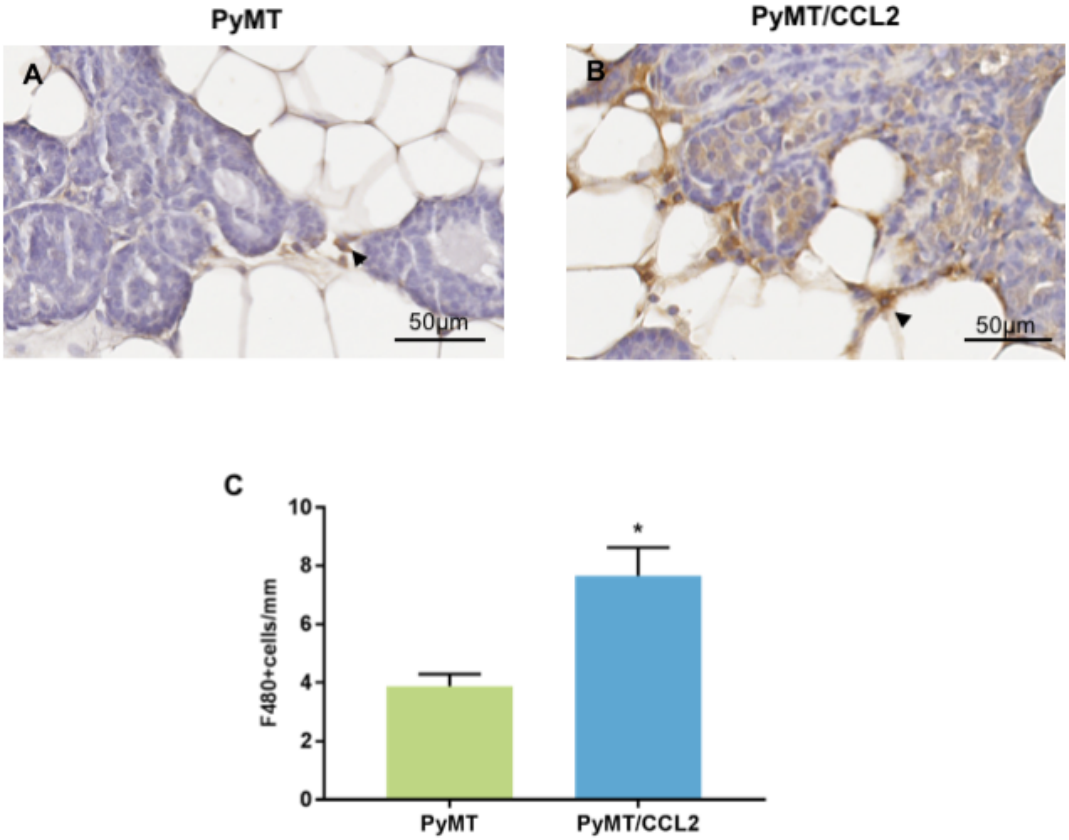

Figure 5.8: The effect of CCL2 overexpression on macrophage infiltration during early mammary tumorigenesis in 9 week old PyMT transgenic mice
Representative images of F4/80 stained mammary glands of 9 week old PyMT (A) and PyMT/CCL2 (B) mice taken at 40x magnification (n=10 per group). F4/80+ cells were manually counted in 3 areas of early tumorigenesis per mammary gland (C). Arrows indicate F4/80+ stained cells. Data presented as mean F4/80+ cells per mm + SEM with statistical analysis performed using a simple linear regression with Wald Chi square post hoc comparison. Statistical significance indicated by * when $p<0.05$.

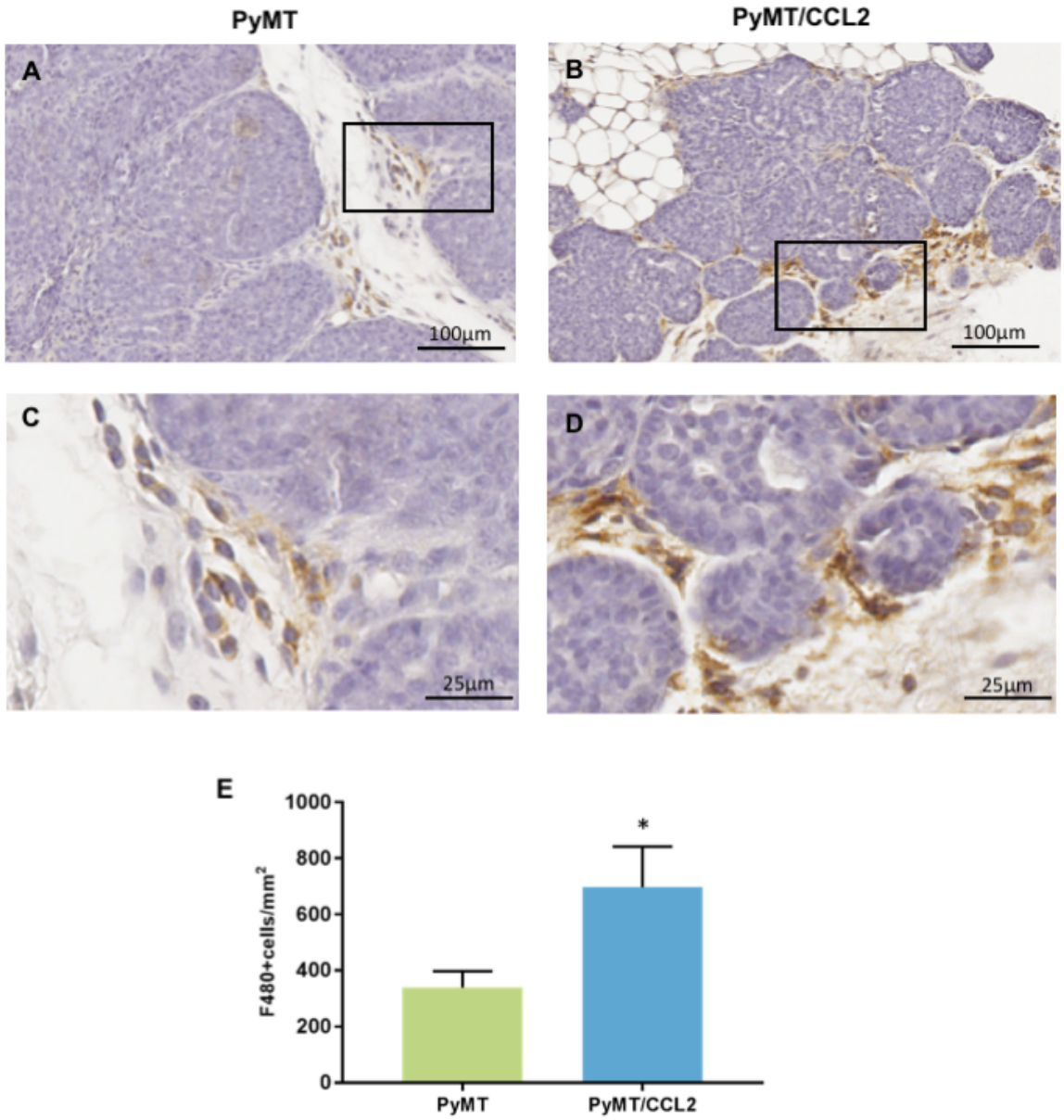

Figure 5.9: The effect of CCL2 overexpression on macrophage density in primary tumours of PyMT transgenic mice at 9 weeks age.
Representative images of F4/80 stained primary mammary tumours from PyMT (A low, C high magnification) and PyMT/CCL2 (B low, D high magnification) mice at 9 weeks age (n=10 per group). Graph represent the average macrophage density of PyMT and PyMT/CCL2 mice at 9 weeks (E). Data presented as mean +SEM with statistical analyses performed by simple linear regression model with Wald Chi square post hoc comparison (*, $p<0.05$).

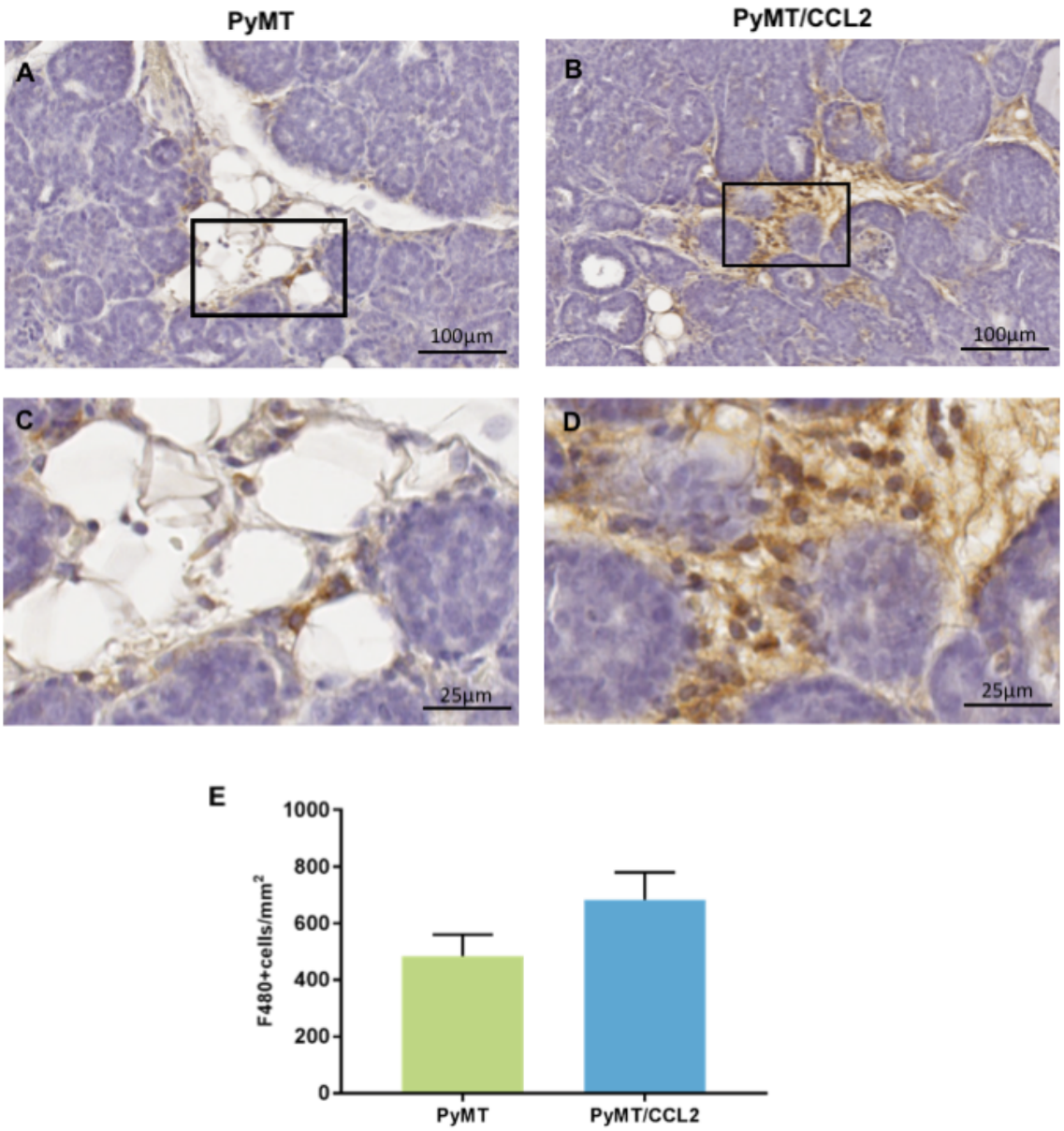

Figure 5.10: The effect of CCL2 overexpression on macrophage density in primary tumours of PyMT transgenic mice at 12 weeks age.
Representative images of F4/80 stained primary mammary tumours from PyMT (A low, C high magnification) and PyMT/CCL2 (B low, D high magnification) mice at 12 weeks age (n=18 per group). Graph represent the average macrophage density of PyMT and PyMT/CCL2 mice at 12 weeks (E). Data presented as mean +SEM with statistical analyses performed by simple linear regression model with Wald Chi square post hoc comparison.

5.2.6 The effect of CCL2 on global gene expression in the mammary gland

To investigate the effect of CCL2 on mammary gland gene expression, mammary glands from Mmtv-Ccl2 and FVB control mice were collected at 12 weeks age and analysed for global gene expression by RNAseq. These were healthy normal mammary glands, not tumorigenic as these mice did not carry the PyMT oncogene. The results of the RNAseq analysis showed 6,149 genes that were differentially expressed in mammary glands of Mmtv-Ccl2 mice.

Of the 6,149 genes identified using RNAseq, 2,783 genes (45%) were upregulated in mice overexpressing CCL2 in their mammary glands. Functional enrichment analysis of those genes using DAVID revealed cellular pathways significantly upregulated in Mmtv-Ccl2 mouse mammary glands, these pathways are summarised in Table 5.1. A number of pathways involved in cancer and cell survival were upregulated in Mmtv-Ccl2 mice compared to wildtype controls including proteoglycans in cancer (p=1.39E-08), cell cycle (p=7.36E-05), pathways in cancer (p=4.4E-04), Ras signalling (p=0.0162) and PI3K-Akt signalling (p=4.23E-04). In addition, a number of pathways involved in DNA damage and repair were upregulated such as DNA replication (p=5.57E-05), mRNA surveillance (p=0.0012), nucleotide excision repair (p=0.0033), mismatch repair (p=0.0102), p53 signalling (p=0.0155) and transcriptional mis-regulation in cancer (p=0.0425). Other upregulated pathways were involved in the extracellular matrix (p=0.0077) and TGFB signalling (p=0.0389). Endocrine pathways upregulated in Mmtv-Ccl2 mice include prolactin signalling (p=0.0345) and estrogen signalling pathways. Angiogenic genes involved VEGF signalling (p=0.051), and leukocyte migration (p=5.35E-04) were also upregulated (Table 5.1).

Of the 6,149 genes identified using RNAseq, 3,366 genes (55%) were downregulated in mice overexpressing CCL2 in their mammary glands. Functional enrichment analysis using DAVID of those genes revealed cellular pathways which were significantly downregulated in Mmtv-Ccl2 mouse mammary glands, these pathways are summarised in Table 5.2. In Mmtv-Ccl2 mouse mammary glands, 386 genes involved in metabolic pathways were downregulated (p=5.83E-42). Specific metabolic pathways downregulated in these mice include those involved in glucose metabolism such as citric acid cycle (p=4.54E-17), insulin signalling pathway (p=6.58E-10), AMPK signalling (p=1.38E-09) and glycolysis and gluconeogenesis (p=1.21E-07). Fatty acid signalling pathways downregulated included fatty acid metabolism (p=1.26E-14), PPAR signalling (p=1.63E-11), fatty acid degradation (p=6.55E-10), fatty acid elongation (p=2.05E-06), fatty acid biosynthesis (p=1.25E-04), adipokine signalling (p=1.13E-06) and regulation of lipolysis (p=4.84E-05). Immune signalling pathways involved in T cell and B cell receptor signalling were also suppressed (p=0.004 and 0.016 respectively).

Table 5.1: Upregulation of functional pathways from RNAseq analysis of global mammary gland mRNA expression in 12 week old Mmtv-Ccl2 transgenic mice

KEGG Pathway	Count	P value
Proteoglycans in Cancer	62	1.39E-08
DNA Replication	16	5.57E-05
Cell Cycle	36	7.36E-05
PI3K-Akt Signalling Pathway	76	4.23E-04
Pathways in Cancer	84	4.40E-04
Leukocyte Migration	33	5.35E-04
mRNA Surveillance	27	0.0012
Nucleotide Excision Repair	15	0.0033
ECM Receptor Interaction	23	0.0077
Mismatch Repair	9	0.0102
Estrogen Signalling Pathway	24	0.0143
P53 Signalling Pathway	18	0.0155
Ras Signalling Pathway	47	0.0162
cAMP Signalling Pathway	41	0.0201
Prolactin Signalling Pathway	18	0.0345
TGFB Signalling Pathway	20	0.0389
Transcriptional Misregulation in Cancer	34	0.0425
VEGF Signalling Pathway	15	0.051

Table 5.2: Downregulation of functional pathways from RNAseq analysis of global mammary gland mRNA expression in 12 week old Mmtv-Ccl2 transgenic mice

KEGG Pathway	Count	P value
Metabolic Pathways	386	5.82E-42
Non-Alcoholic Fatty Liver Disease	88	1.71E-29
Citric Acid Cycle	28	4.54E-17
Fatty Acid Metabolism	34	1.26E-14
PPAR Signalling Pathway	40	1.63E-11
Fatty Acid Degradation	28	6.55E-10
Insulin Signalling Pathway	54	6.58E-10
AMPK Signalling Pathway	50	1.38E-09
Glycolysis/Gluconeogenesis	30	1.21E-07
Adipokine Signalling Pathway	30	1.13E-06
Fatty Acid Elongation	16	2.05E-06
Regulation of Lipolysis in Adipocytes	23	4.84E-05
Biosynthesis of Unsaturated Fatty Acids	14	1.25E-04
T Cell Receptor Signalling Pathway	29	0.004
B Cell Receptor Signalling Pathway	20	0.016
Fatty Acid Biosynthesis	7	0.018

5.3 DISCUSSION

CCL2 is an inflammatory chemoattractant with potential roles in cancer development and progression. Mice overexpressing CCL2 have been found to exhibit a number of features reminiscent of mammographic density and the associated breast cancer risk. We hypothesised that CCL2 over expression in mice, when cross bred with the Mmtv-PyMT mammary tumour model, may promote tumorigenesis and tumour progression. Our results suggest that CCL2 over expression has minimal effects on tumour development in the Mmtv-PyMT mouse model, however, these results may have been confounded by a number of external factors. Our studies of global mammary gland gene expression suggests that overexpression of CCL2 in the mammary gland results in a number of altered genetic pathways which may contribute to cancer risk.

5.3.1 The role of CCL2 in mammographic density

Our studies investigated how constitutive expression of CCL2 in the mammary glands affected overall gene expression using RNAseq. Pathway analysis of differentially expressed genes revealed that Mmtv-Ccl2 mice have upregulated expression of genes involved in extracellular matrix and collagen deposition at 12 weeks of age. CCL2 has been implicated in numerous fibrotic diseases characterised by high levels of collagen deposition such as pulmonary fibrosis, liver fibrosis and renal fibrosis [242, 246, 262, 263]. This is consistent with previous studies which reported that Mmtv-Ccl2 mice have increased stromal density and collagen thickness surrounding epithelium [157]. These characteristics are reminiscent of the increase proportion of stroma and collagen deposition seen in human breast tissue with high mammographic density, and CCL2 expression is increased in the epithelium of high density breast tissue [57, 157]. These results support the notion that CCL2 mediated inflammation may be a driver of mammographic density.

5.3.2 The role of CCL2 in tumour development and progression

Our results suggest that CCL2 overexpression in the mammary gland increases expression of genes involved in cancer and PyMT/CCL2 mice had a greater number of tumorigenic areas per mm^2 in the mammary gland at 9 weeks and suggesting that CCL2 may promote mammary tumorigenesis. However, this did not continue to enhance tumour development or progression to metastasis in the Mmtv-PyMT mouse model. In many previous studies, CCL2 has been implicated in promoting tumour progression and metastasis. Previous studies in our lab have demonstrated that CCL2 overexpression reduces tumour latency and tumour-free survival in a carcinogen-induced mammary tumour model [157]. However, it appears that the role of CCL2 in tumour development and progression is complex and multifaceted. Another study by Li et al, reported that tumour growth was reduced in CCL2 null mutant mice, and anti-CCL2 antibody treatment reduced pulmonary metastasis in mice bearing mammary tumours, supporting the role of CCL2 in tumour promotion [166]. However, this study also reported that CCL2 null mutant mice exhibited increased metastatic spread, and that treatment with anti-CCL2 antibody during early tumorigenesis resulted in a spike in tumour growth [166]. This suggests that CCL2 may play multiple opposing roles during different stages of tumour development and progression. The role of CCL2 may be dependent on the level of CCL2 production by tumours on surrounding tissues. Previous studies in melanoma have reported that low concentration of CCL2 promoted survival of tumour cells, while high concentration of CCL2 resulted in destruction of tumour mass and high infiltration of immune cells [264, 265].

Although inflammation is one of the hallmarks of cancer, the role of CCL2 mediated inflammation in tumour development and progression is more complex. It is suggested that the pro-tumorigenic effects of CCL2 is a result of the chemoattractant properties of CCL2 in recruitment of cells that suppress immune surveillance or recruit tumour associated macrophages (TAMs) to tumour sites [253, 260, 266]. TAMs then produce several factors

to support tumour growth as well as tissue remodelling to promote angiogenesis and metastasis [162, 163]. TAMs recruited by CCL2 also play roles in immune surveillance and can inhibit tumour development and progression [143]. Our results showed an increase in infiltration of macrophages to tumour sites in CCL2 overexpressing mice, however our studies did not delineate the phenotype or functions of these macrophages. Further, the chemoattractant properties of CCL2 are not exclusive to tumour promoting macrophages. CCL2 also recruits a number of other immune cells such as natural killer cells, immature B cells and CD4+ T cells, through the CCL2 receptor CCR2 and binding of CCL2 to the CCR4 receptor [156, 267, 268]. Recruitment of these cells to the tumour microenvironment may influence immune surveillance and tumour progression. Studies have reported that CCL2 recruits cytotoxic $\gamma\delta$ T lymphocytes *in vitro*, and to tumour sites *in vivo* [165, 269]. These cells have been reported to have cytotoxic effects against breast cancer cell lines both *in vitro* and in mouse models [270]. The balance of different cell types recruited to the tumour site by CCL2 may determine the rate of tumour growth and progression.

Surprisingly, CCL2 overexpression in the Mmtv-Pymt tumour mouse model did not result in a greater rate of metastases to the lung. Previous studies have highlighted that CCL2 drives metastasis of cancer cells through recruitment of TAMs which encourage angiogenesis and metastasis [166, 244, 260]. Our studies found that CCL2 increased infiltration of macrophages to tumorigenic areas at 9 weeks age in PyMT/CCL2 mice. And in our RNAseq analysis of CCL2 over expressing mammary glands found an increase in expression of genes involved in VEGF pathways which are major regulators of breast cancer angiogenesis and metastasis [163, 271, 272]. Tumour development in the Mmtv-Pymt model was very aggressive, and it is possible that tumour progression was too swift for any effect of CCL2 in promoting metastasis to be observable.

5.3.3 Constitutive CCL2 expression downregulates fatty acid synthesis and metabolism

Interestingly, our studies observed an overall downregulation of genes involved in fatty acid synthesis and metabolism, particularly fatty acid synthase (*FASN*) in mammary glands with constitutive CCL2 expression. This result was unexpected as there is extensive literature reporting increased fatty acid metabolism during inflammation, and CCL2 expression is associated with diseases with increased fatty acid synthesis and metabolism such as fatty liver disease [273-275]. Further, fatty acid synthesis and lipid metabolism in increased in breast cancer [276, 277]. Increased fatty acid metabolism can play a supporting role in proliferation and survival of breast cancer cells [278, 279]. In particular, fatty acid synthase is highly expressed in breast cancer, and has been used as a predictor of decreased tumour-free survival and is associated with risk of recurrence in breast cancer [280-283]. A number of studies have investigated the potential of inhibitors of fatty acid synthase as a potential therapy in cancer [279]. However, expression of fatty acid synthase is also necessary for normal mammary gland development [284]. Currently, there is no literature that implicates CCL2 in the downregulation of fatty acid metabolism. Preliminary studies in our lab have observed that the adipose tissue in the mammary glands of Mmtv-Ccl2 mice contain a greater abundance of highly eosinophilic multi-lobular lipid droplets in the mammary gland compared to wild type mice (Hodson et al, unpublished). Currently, it is unknown if the function of this adipose tissue is perturbed, and further investigation into the function of these cells may shed light on the role of CCL2 in downregulation of fatty acid and lipid metabolism.

5.3.4 Limitations

There are a number of limitations that may have influenced the results of this study. Firstly, the rate of tumour development in the Mmtv-PyMT tumour model is greatly affected by the background strain of the mice. Previous studies have reported that Mmtv-PyMT mice on

an FVB background have a reduced tumour latency and greater incidence of pulmonary metastases compared to mice on a C57B6 background [261, 285]. In the current study, primary tumours were first palpable around 7-8 weeks of age, and the tumours dissected when the mice were 9 weeks of age were already all late stage carcinomas. The aggressiveness of this tumour development limited our analysis of the effect of CCL2 on early tumourigenesis and hyperplasia. Collection of tumours and mammary glands at earlier time points may reveal differences in PyMT/CCL2 and FVB control mice. It is worth noting also that during the course of this study there was a lot of construction occurring in the building the animals were housed in, and the mice were exposed to a number of external stressors such as noise and vibrations that could have affected the rate of tumour development.

5.4 CONCLUSION

In this study, we have reported that CCL2 overexpression in the mammary gland increases expression of genes involved in cancer development and progression, and in collagen synthesis. CCL2 increased the number of tumorigenic areas in the mammary gland, and infiltration of macrophages to tumour sites in 9-week-old PyMT/CCL2 mice, however there was no difference in tumour progression and metastasis between PyMT/CCL2 mice and PyMT controls. Our results, combined with the literature, support the notion that CCL2 may be a driver of mammographic density through increase collagen production and effects on early tumour initiation. However, the role of CCL2 in tumour development, progression and metastasis may be dependent on the level of expression, cell types present in the microenvironment, and the stage of progression. Further studies are necessary to further elucidate the role of CCL2 in mammary tumorigenesis.

CHAPTER SIX

GENERAL DISCUSSION AND CONCLUSIONS

6.1 BREAST CANCER PREVENTION

Breast cancer is an incredibly common disease, and affects 1 in 7 women before the age of 85 [1]. A breast cancer diagnosis leads to morbidities associated with surgery and adjuvant chemotherapy, and mortality due to cancer metastasis to sites such as the bone, liver, or brain [286]. Reducing the number of women diagnosed with breast cancer would have a significant impact on the health burden of this disease.

Currently, there is a lack of preventative measures that can reduce the incidence of breast cancer. Radical surgery such as prophylactic mastectomy can reduce breast cancer risk, however this is not a suitable approach for the majority of women. In contrast to our lack of success in preventing breast cancer, we are now able to dramatically reduce risk of cervical cancer through a strategy based on understanding the biological mechanism that led to increased risk. It was identified that 99% of cervical cancers can be attributed to sexually-transmitted infection with human papilloma virus (HPV) [287]. This discovery led to a vaccination strategy against this virus to reduce cervical cancer risk [288]. The barrier to progress in preventing breast cancer is our lack of knowledge of the biological mechanisms that drive increased risk. Mammographic density (MD) is a strong risk factor for breast cancer [14] with thirty percent of breast cancer cases are attributable to mammographic density (MD) [199]. Through a better understanding of why some women have high MD, we can develop new interventions to reduce the incidence of breast cancer.

High MD is the result of many different contributing biological factors. There is some evidence that inflammation in the breast, mediated by cytokines such as CCL2, may be

driving the increased collagen and breast cancer risk seen in high MD [123, 157]. The relationship between MD and breast cancer risk is an association, therefore the factors that cause increased MD do not necessarily also increase breast cancer risk and vice versa. And there may also be common causes that increase both MD and breast cancer risk leading to a spurious association. It is important to understand the nature of the relationships between contributing factors, MD and breast cancer risk. The studies described in this thesis explored some of the inflammatory and cellular interactions which could be contributing to MD and breast cancer risk. These interactions hold potential to determining targets for preventative therapeutics to decrease breast cancer risk, and reduce the incidence of breast cancer in the future. Opportunities for further research to understand how inflammation and immune processes in the mammary gland influence the activity of different cellular components of the breast and cancer development, and how that may contribute to mammographic density are discussed.

6.2 Cellular and Inflammatory Interactions Driving Mammographic Density and Breast Cancer Risk

While the underlying biological mechanisms that mediate MD are largely unknown, the literature and the results described in this thesis suggest that it is the result of many different contributing factors. The different factors that influence the proportions of MD in the breast include hormones, immune cells, fibroblasts, inflammatory signals, and extracellular matrix [9, 289, 290]. The studies in this thesis focused on the interactions between inflammatory signals, immune cells and fibroblasts which could contribute to MD. A summary of the findings of these studies is illustrated in Figure 6.1.

Immune cells are a key component of the mammary epithelium and stroma [62]. Immune cells are vital in regulating the normal function of the mammary gland and cancer risk [122, 291]. Therefore, the immune cell environment has been a focus of previous studies and

this thesis, to understand how they contribute to mammographic density. Analysis of the immune cell profile of high and low MD breast tissue has demonstrated that high MD breast tissue has greater cell infiltration of vimentin+/CD45+ leukocytes, CD11c+ dendritic cells, B cells and CD4+ T cells [57]. High MD breast tissue also exhibited an increase in infiltration of CD68+ macrophages compared to low MD breast tissue [123]. Our studies found that undifferentiated macrophages polarised to an M2 phenotype when in co-culture with mammary fibroblasts. This polarisation may occur in high MD, where there is a high abundance of fibroblasts. It is also suggested that the macrophages found in high MD breast tissue are of the M2 phenotype, as there is increased expression of IL6, which is expressed by M2 polarised macrophages [123].

These M2 macrophages are known to have roles in tissue remodelling and have a high level of expression of ECM remodelling genes such as MMPs and TIMPs [135]. They also promote expression of ECM remodelling genes by mammary fibroblasts. Expression of these genes can directly affect the proportions of collagen and ECM in the breast and therefore contribute to MD. These macrophages may also be driving increased breast cancer risk. M2 macrophages produce express cytokines such as IL10 and TGFB that promote a more tolerogenic environment for immune evasion by breast cancer cells. Further there is high expression of pro-tumour factors such as VEGF that promotes tumour invasion, progression and metastasis.

Chronic inflammation is a hallmark of cancer, and is associated with several risk factors for breast cancer [292, 293]. Our co-culture studies also revealed that macrophages promoted a high level of expression of inflammatory markers IL6 and COX2 by mammary fibroblasts. IL6 has been implication in mammographic density and breast cancer risk. Previous studies have reported that circulating IL6 is positively correlated with breast density [294]. Studies of genetic variation identified 9 single nucleotide polymorphisms in

the IL6 gene which were associated with high mammographic density [149]. And both gene and protein expression of IL6 has been found to be upregulated in high MD than low MD breast tissue in women [123, 295]. Inflammation mediated by IL6 is associated with increased breast cancer risk, and circulating IL6 is associated with poor prognosis in breast cancer patients [296]. IL6 plays roles in proliferation, therapeutic resistance and metastasis in breast cancer [296]. Multiple studies have identified inflammatory COX2 as a potential driver of MD. In a study by Yang et al, COX2 expression was increased in the stroma of women with high MD [120]. This finding was further confirmed by paired sample analyses of high and low MD breast tissue that found elevated expression of COX2 in high MD breast tissue [148]. COX2 is highly expressed in pre-malignant legions in the breast, and is highly expressed during all stages of breast cancer development [297]. Therefore, the interactions between macrophages and fibroblasts both contribute to the histological features of MD, as well as promote an inflammatory environment that may drive increased breast cancer risk.

Macrophages can be recruited to regions of high MD in response to inflammatory signals from the chemotactic cytokine CCL2 [156]. CCL2 can also contribute to macrophage polarisation towards an M2 phenotype [298]. Previous studies have demonstrated that high MD breast tissue has a greater expression of CCL2 than low MD tissue. Mice that overexpress CCL2 in the mammary gland also exhibit greater stromal density and collagen deposition, and increased susceptibility to mammary carcinogenesis reminiscent of high MD [157]. Our studies further implicate CCL2 as a driver of MD and breast cancer risk, as CCL2 promoted deposition of insoluble collagen by mammary fibroblasts *in vitro*. Further, our RNAseq studies in Mmtv-Ccl2 transgenic mouse mammary glands revealed that over expression of CCL2 upregulated expression of genes involved in collagen production and ECM regulation. Genes involved in fatty acid metabolism were also perturbed, suggesting there may be impaired metabolism in the adipose tissue that may contribute to MD.

Expression of genes involved in cancer and DNA damage were also upregulated in CCL2 overexpressing mammary glands, suggesting an increase in breast cancer risk. Mmtv-Ccl2 mice have previously been demonstrated to have an increased susceptibility to mammary tumorigenesis in a chemical carcinogen model of breast cancer [157]. Our studies utilising PyMT/CCL2 mice suggested that CCL2 overexpression is associated with an increase in early tumorigenic areas in the mammary gland, and an increase in macrophage infiltration to tumours.

Our studies demonstrate that there are several biological mechanisms that contribute to increased MD, and the interactions between the cells and immune signalling factors in the breast microenvironment that mediate high MD are complex. However our studies highlight that inflammation may be a key factor. Combined, our studies suggest that inflammation could drive both increased MD and breast cancer risk. Therefore, the association between MD and breast cancer risk might be a spurious association, with inflammation as the common cause of both. If this is indeed the case, a strategy that dampens inflammation could be most effective in reducing breast cancer risk associated with high MD.

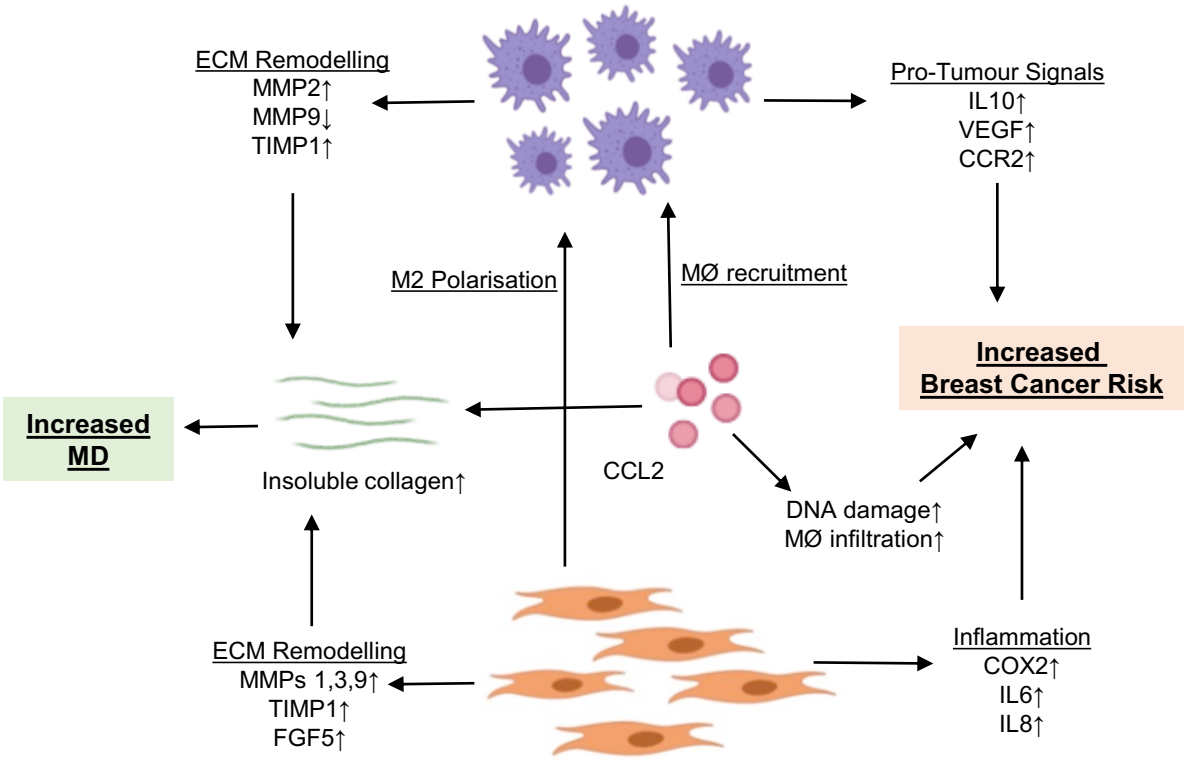

Figure 6.1: Schematic representation of the suggested interactions between fibroblasts, macrophages and CCL2 in mammographic density and breast cancer risk.
Our studies demonstrated that fibroblasts (orange) drive polarisation of macrophages to the M2 phenotype (purple) when in co-culture conditions. Macrophages are recruited to the breast by CCL2. These macrophages exhibit high expression of ECM remodelling genes. Macrophages induces expression of ECM remodelling genes by mammary fibroblasts. These interactions, with the addition of CCL2, resulted in an increase in deposition of insoluble fibres which could lead to increased MD. M2 macrophages can promote tumour development and progression through suppression of anti-tumour immunity and expression of tumour promoting factors. Macrophages drive expression of inflammatory genes by mammary fibroblasts which could increase breast cancer risk.

6.3 Use of Anti-inflammatories to Prevent Breast Cancer

The literature, combined with studies described in this thesis, have implicated inflammatory signals as drivers of MD and breast cancer risk. This reveals a potential target for strategies that could possibly reduce the risk of breast cancer that is associated with high MD.

Non-steroidal anti-inflammatory drugs (NSAIDs) are a class of drugs that inhibit the action of COX2 [299]. As discussed previously, inflammatory COX2 is elevated in breast tissue samples with high MD, and interactions between macrophages and mammary fibroblasts promote expression of COX2. In studies of mouse models with excessive collagen in the mammary glands, inhibition of COX2 signalling reduced collagen deposition and tumour development [150]. This suggests that anti-inflammatory treatment may reduce both MD and the associated breast cancer risk.

Two studies have investigated the potential for NSAIDS to reduce mammographic density in women. One study matched pharmacy records to evaluate NSAID usage alongside two screening mammograms in nearly 30,000 postmenopausal women. This study reported that women who initiated NSAID use between their two mammograms showed no change in MD, but those who were continuous users of NSAIDs were more likely to have no increase in MD. However, the mammograms used in this study were taken at an average of two years apart, and does not demonstrate the long term effects of NSAID use and changes in MD [152]. A second study analysed mammograms from 26,000 women who were either users or non-users of the NSAID aspirin. This study found that aspirin use was associated with lower MD, and women with high MD were less likely to be users of aspirin. Further, the probability of having dense breasts was lower in women who consumed higher dosages of aspirin [300]. Suggesting that the effect of NSAIDs on MD may be dose dependant. However, this study only analysed aspirin usage with one screening

mammogram. NSAID use in MD appears promising, however more studies of long term NSAID use and changes in MD and breast cancer incidence are needed to determine their potential as a preventative treatment for women with high MD.

While there are very few studies examining the use of NSAIDs and MD, the role of NSAID use has been well studied in cancer. Meta-analyses have reported that there is an inverse relationship between use of NSAIDs such as aspirin and risk of breast cancer [301]. Case control studies have reported that NSAID use is associated with a 14-18% reduction in breast cancer incidence [302, 303]. The use of NSAIDs as a preventative treatment for MD and breast cancer risk is appealing, as they are easily accessible, cost effective and have very few side effects [304]. However, it is important to note that continuous use of aspirin can result in increased risk for bleeding disorders and gastric ulcers [305, 306]. Therefore, patient history of such disorders must be evaluated before NSAID use for MD reduction can be considered. Nonetheless, using reduction of MD and breast cancer risk by use of NSAIDs may reduce incidence of breast cancer and burden of disease, and prevent breast cancer related deaths in the future.

6.4 Future Research to Understand the Biological Drivers of Breast Cancer Risk

The findings reported in this thesis help to build an understanding of some of the cellular processes that may be contributing to MD and breast cancer risk. These studies further emphasise that mammographic density and the associated breast cancer risk are a result of complex interactions between many contributing factors including crosstalk between the inflammatory immune microenvironment and stromal cells. However, inflammatory immune processes that mediate mammographic density and breast cancer risk are still largely unknown.

In our studies of CCL2 in mammary tumour development and progression, the tumours in the PyMT mice were highly aggressive and progressed too quickly to truly identify the effects of CCL2 on tumour initiation and progression. Future studies could utilise Mmtv-PyMT derived mammary tumour cell lines such as Met1, and inject them into the mammary fat pad of Mmtv-Ccl2 mice. Tumours, mammary glands, lymph nodes, lungs and blood can then be collected at multiple time points from injection date to investigate early tumour development and metastasis. Studies could investigate whether inhibition of CCL2 signalling in Mmtv-Ccl2 mice could reduce the proportions of collagen and stroma in the mammary gland, and whether there is a reduction in mammary tumour susceptibility. To identify the effect of CCL2 on immune cell recruitment and immune surveillance during early tumour development, the populations of immune cells at the tumour site including macrophages and T cells and their phenotypes could be identified by flow cytometry and immunohistochemistry, as well as determining tumour stages. It would also be interesting to determine the immune cell populations and phenotypes in non-tumour burdened Mmtv-Ccl2 mice and determine if this immune cell profile is comparative to that in high density human breast tissue.

Our studies demonstrated that crosstalk between mammary fibroblasts and macrophages has several effects on gene expression, macrophage polarisation and collagen production. However, the phenotype of macrophages that are most abundant in high and low density breast tissue is currently unknown. Future studies should utilise paired samples of high and low density breast tissue to determine the phenotype and gene expression of these cells in human samples. These studies could utilise single cell analysis to determine the heterogeneity of both macrophage and other cell populations including fibroblasts from high and low MD breast tissue and how this heterogeneity may contribute to a dense microenvironment or breast cancer risk. Further *in vitro* studies could investigate the

pathways by which macrophages promote expression of inflammatory mediators and what soluble factors are released that might contribute to breast cancer risk and MD.

Studies of MD have largely focused on the stroma, collagen and immune components of the breast, while there is very little understanding of the role that adipose tissue plays in MD and the associated breast cancer risk. The RNAseq studies reported in this thesis identified that fatty acid metabolism, lipid metabolism and adipokine signalling pathways are downregulated in the mammary glands of Mmtv-Ccl2 mice, suggesting that there may be perturbed activity in adipocytes in high density. It would be interesting to further investigate this in paired samples of high and low density breast tissue and use immunohistochemistry to measure expression of key proteins involved in fat metabolism such as leptin, adiponectin and fatty acid synthase. *In vitro* studies could investigate how breast adipocytes interact with other cells in the breasts such as epithelial cells, fibroblasts and macrophages through gene and protein expression. This could help elucidate how adiposity in the breast can be protective from breast cancer in the context of MD.

To understand how inflammation may be driving MD and the associated breast cancer risk, it would be informative to obtain information on the history of NSAID use in women donating tissue from reduction mammoplasty and mastectomy surgeries. By doing this, it may help to determine whether NSAID use is linked to the histological characteristics of low MD, and whether there is reduced expression of inflammatory markers such as CCL2 in breast tissue. This may help to determine which biological pathways are altered by anti-inflammatory treatment and how this may reduce a woman's risk of breast cancer.

To understand how inflammation may be driving MD, research needs to focus on determining what could be causing some women to have higher expression of inflammatory markers such as CCL2 and COX2 in the breast. Many recent studies have

demonstrated that adult diseases can be linked to influences during fetal development [307]. These studies highlight that inherited and epigenetic factors, as well as environmental influences could lead to disease later in life. An autopsy study of women without clinically detectable breast cancer demonstrated that precancerous microscopic columnar cell lesions are found in 1 of 4 women with dense breasts [308], suggesting these breast cancers develop slowly over the woman's lifetime. Future studies should investigate whether there are certain environmental or epigenetic changes during fetal or pubertal development that lead to increased inflammation and high MD during adulthood. Understanding what may be driving increased expression of CCL2 and other inflammatory markers in women is complex, as expression of inflammatory markers including CCL2 are often elevated in women with obesity [309, 310]. While obesity and inflammation increase breast cancer risk, high BMI is associated with a decrease in mammographic density [15, 34, 311]. This factor needs to be considered when addressing the role of inflammation in both mammographic density and breast cancer risk.

6.5 CONCLUSIONS

Breast cancer is the most prevalent cancer in women, affecting 1 in 7 women before the age of 85. Understanding the biological drivers that increase breast cancer risk hold the potential for therapeutic targets for breast cancer prevention. Mammographic density is a strong risk factor for breast cancer that is a result of several contributing factors. Our studies have demonstrated that interactions between immune cells and fibroblasts can contribute to MD and create a favourable environment for tumour growth, and these processes can be driven by inflammatory signals such as CCL2. There is potential for medications that attenuate this inflammation, such as NSAIDs, to reduce MD-associated breast cancer risk in women. However, more studies are required to understand the biological mechanisms that underpin breast cancer risk. Understanding how inflammation drives MD can help to elucidate the underlying biological basic of breast cancer risk. Modification of the biological drivers of MD may reduce the incidence of breast cancer in the future.

REFERENCES

1. Australia, A.I.o.H.a.W.C., *Breast Cancer in Australia: An Overview.* Canberra: AIHW, 2012. **Cancer Series no. 71**(CAN 67).
2. Kotsopoulos, J., *BRCA Mutations and Breast Cancer Prevention.* Cancers (Basel), 2018. **10**(12).
3. Melvin, J.C., et al., *Family history of breast cancer and its association with disease severity and mortality.* Cancer Med, 2016. **5**(5): p. 942-9.
4. Ziegler, R.G., et al., *Migration patterns and breast cancer risk in Asian-American women.* J Natl Cancer Inst, 1993. **85**(22): p. 1819-27.
5. Boyd, N.F., et al., *Mammographic density and the risk and detection of breast cancer.* N Engl J Med, 2007. **356**(3): p. 227-36.
6. Engmann, N.J., et al., *Population-Attributable Risk Proportion of Clinical Risk Factors for Breast Cancer.* JAMA Oncol, 2017. **3**(9): p. 1228-1236.
7. Johns, P.C. and M.J. Yaffe, *X-ray characterisation of normal and neoplastic breast tissues.* Phys Med Biol, 1987. **32**(6): p. 675-95.
8. Hugo, H.J., et al., *InforMD: a new initiative to raise public awareness about breast density.* Ecancermedicalscience, 2018. **12**: p. 807.
9. Boyd, N.F., *Mammographic density and risk of breast cancer.* Am Soc Clin Oncol Educ Book, 2013.
10. Timmers, J.M., et al., *The Breast Imaging Reporting and Data System (BI-RADS) in the Dutch breast cancer screening programme: its role as an assessment and stratification tool.* Eur Radiol, 2012. **22**(8): p. 1717-23.
11. Sprague, B.L., et al., *Prevalence of mammographically dense breasts in the United States.* J Natl Cancer Inst, 2014. **106**(10).
12. Jeffers, A.M., et al., *Breast Cancer Risk and Mammographic Density Assessed with Semiautomated and Fully Automated Methods and BI-RADS.* Radiology, 2017. **282**(2): p. 348-355.

13. Astley, S.M., et al., *A comparison of five methods of measuring mammographic density: a case-control study.* Breast Cancer Research, 2018. **20**(1): p. 10.

14. Wolfe, J.N., *Risk for breast cancer development determined by mammographic parenchymal pattern.* Cancer, 1976. **37**(5): p. 2486-92.

15. Boyd, N.F., et al., *Body size, mammographic density, and breast cancer risk.* Cancer Epidemiol Biomarkers Prev, 2006. **15**(11): p. 2086-92.

16. McCormack, V.A. and I. dos Santos Silva, *Breast density and parenchymal patterns as markers of breast cancer risk: a meta-analysis.* Cancer Epidemiol Biomarkers Prev, 2006. **15**(6): p. 1159-69.

17. Vachon, C.M., et al., *Mammographic breast density as a general marker of breast cancer risk.* Cancer Epidemiol Biomarkers Prev, 2007. **16**(1): p. 43-9.

18. Eriksson, L., et al., *Mammographic density and molecular subtypes of breast cancer.* Br J Cancer, 2012. **107**(1): p. 18-23.

19. Yaghjyan, L., et al., *Mammographic breast density and subsequent risk of breast cancer in postmenopausal women according to tumor characteristics.* J Natl Cancer Inst, 2011. **103**(15): p. 1179-89.

20. Heusinger, K., et al., *Association of mammographic density with hormone receptors in invasive breast cancers: results from a case-only study.* Int J Cancer, 2012. **131**(11): p. 2643-9.

21. Ding, J., et al., *Mammographic density, estrogen receptor status and other breast cancer tumor characteristics.* Breast J, 2010. **16**(3): p. 279-89.

22. Bertrand, K.A., et al., *Mammographic density and risk of breast cancer by age and tumor characteristics.* Breast Cancer Res, 2013. **15**(6): p. R104.

23. Eriksson, L., et al., *Possible influence of mammographic density on local and locoregional recurrence of breast cancer.* Breast Cancer Res, 2013. **15**(4): p. R56.

24. Maskarinec, G., et al., *Mammographic density as a predictor of breast cancer survival: the Multiethnic Cohort.* Breast Cancer Res, 2013. **15**(1): p. R7.

25. Gierach, G.L., et al., *Relationship between mammographic density and breast cancer death in the Breast Cancer Surveillance Consortium.* J Natl Cancer Inst, 2012. **104**(16): p. 1218-27.

26. Chiu, S.Y., et al., *Effect of baseline breast density on breast cancer incidence, stage, mortality, and screening parameters: 25-year follow-up of a Swedish mammographic screening.* Cancer Epidemiol Biomarkers Prev, 2010. **19**(5): p. 1219-28.

27. Weigel, S., et al., *Digital mammography screening: sensitivity of the programme dependent on breast density.* Eur Radiol, 2017. **27**(7): p. 2744-2751.

28. Sandberg, M.E., et al., *Change of mammographic density predicts the risk of contralateral breast cancer--a case-control study.* Breast Cancer Res, 2013. **15**(4): p. R57.

29. Cil, T., et al., *Mammographic density and the risk of breast cancer recurrence after breast-conserving surgery.* Cancer, 2009. **115**(24): p. 5780-7.

30. Buist, D.S., et al., *Diagnosis of second breast cancer events after initial diagnosis of early stage breast cancer.* Breast Cancer Res Treat, 2010. **124**(3): p. 863-73.

31. Sung, H., et al., *Breast cancer risk factors and mammographic density among high-risk women in urban China.* NPJ Breast Cancer, 2018. **4**: p. 3.

32. Pankow, J.S., et al., *Genetic analysis of mammographic breast density in adult women: evidence of a gene effect.* J Natl Cancer Inst, 1997. **89**(8): p. 549-56.

33. Boyd, N.F., et al., *Heritability of mammographic density, a risk factor for breast cancer.* N Engl J Med, 2002. **347**(12): p. 886-94.

34. Reeves, K.W., et al., *Longitudinal association of anthropometry with mammographic breast density in the Study of Women's Health Across the Nation.* Int J Cancer, 2009. **124**(5): p. 1169-77.

35. Tamimi, R.M., et al., *Endogenous hormone levels, mammographic density, and subsequent risk of breast cancer in postmenopausal women.* J Natl Cancer Inst, 2007. **99**(15): p. 1178-87.

36. Boyd, N.F., et al., *The relationship of anthropometric measures to radiological features of the breast in premenopausal women.* Br J Cancer, 1998. **78**(9): p. 1233-8.

37. Hjerkind, K.V., et al., *Volumetric Mammographic Density, Age-Related Decline, and Breast Cancer Risk Factors in a National Breast Cancer Screening Program.* Cancer Epidemiol Biomarkers Prev, 2018. **27**(9): p. 1065-1074.

38. Checka, C.M., et al., *The relationship of mammographic density and age: implications for breast cancer screening.* AJR Am J Roentgenol, 2012. **198**(3): p. W292-5.

39. Burton, A., et al., *Mammographic density and ageing: A collaborative pooled analysis of cross-sectional data from 22 countries worldwide.* PLOS Medicine, 2017. **14**(6): p. e1002335.

40. Nguyen, T.L., et al., *Explaining variance in the cumulus mammographic measures that predict breast cancer risk: a twins and sisters study.* Cancer Epidemiol Biomarkers Prev, 2013. **22**(12): p. 2395-403.

41. Woolcott, C.G., et al., *Mammographic density, parity and age at first birth, and risk of breast cancer: an analysis of four case-control studies.* Breast Cancer Res Treat, 2012. **132**(3): p. 1163-71.

42. Lope, V., et al., *Obstetric history and mammographic density: a population-based cross-sectional study in Spain (DDM-Spain).* Breast Cancer Res Treat, 2012. **132**(3): p. 1137-46.

43. Bremnes, Y., et al., *Different types of postmenopausal hormone therapy and mammographic density in Norwegian women.* Int J Cancer, 2007. **120**(4): p. 880-4.

44. Couto, E., et al., *Hormone therapy use and mammographic density in postmenopausal Norwegian women.* Breast Cancer Res Treat, 2012. **132**(1): p. 297-305.

45. Lowry, S.J., et al., *Predictors of breast density change after hormone therapy cessation: results from a randomized trial.* Cancer Epidemiol Biomarkers Prev, 2011. **20**(10): p. 2309-12.

46. Azam, S., et al., *Hormone replacement therapy, mammographic density, and breast cancer risk: a cohort study.* Cancer Causes Control, 2018. **29**(6): p. 495-505.

47. Kerlikowske, K., et al., *Breast cancer risk by breast density, menopause, and postmenopausal hormone therapy use.* J Clin Oncol, 2010. **28**(24): p. 3830-7.

48. van Duijnhoven, F.J., et al., *Postmenopausal hormone therapy and changes in mammographic density.* J Clin Oncol, 2007. **25**(11): p. 1323-8.

49. Cecchini, R.S., et al., *Baseline mammographic breast density and the risk of invasive breast cancer in postmenopausal women participating in the NSABP study of tamoxifen and raloxifene (STAR).* Cancer Prev Res (Phila), 2012. **5**(11): p. 1321-9.

50. Cuzick, J., et al., *Tamoxifen-induced reduction in mammographic density and breast cancer risk reduction: a nested case-control study.* J Natl Cancer Inst, 2011. **103**(9): p. 744-52.

51. Cuzick, J., et al., *Tamoxifen and breast density in women at increased risk of breast cancer.* J Natl Cancer Inst, 2004. **96**(8): p. 621-8.

52. Chow, C.K., et al., *Effect of tamoxifen on mammographic density.* Cancer Epidemiol Biomarkers Prev, 2000. **9**(9): p. 917-21.

53. Li, J., et al., *Mammographic density reduction is a prognostic marker of response to adjuvant tamoxifen therapy in postmenopausal patients with breast cancer.* J Clin Oncol, 2013. **31**(18): p. 2249-56.

54. Henry, N.L., et al., *Aromatase inhibitor-induced modulation of breast density: clinical and genetic effects.* Br J Cancer, 2013. **109**(9): p. 2331-9.

55. Kim, J., et al., *Breast density change as a predictive surrogate for response to adjuvant endocrine therapy in hormone receptor positive breast cancer.* Breast Cancer Res, 2012. **14**(4): p. R102.

56. Vachon, C.M., et al., *Mammographic Breast Density Response to Aromatase Inhibition.* Clin Cancer Res, 2013. **19**(8): p. 2144-53.

57. Huo, C.W., et al., *High mammographic density is associated with an increase in stromal collagen and immune cells within the mammary epithelium.* Breast Cancer Res, 2015. **17**: p. 79.

58. Woolcott, C.G., et al., *Association between sex hormones, glucose homeostasis, adipokines, and inflammatory markers and mammographic density among postmenopausal women.* Breast Cancer Res Treat, 2013. **139**(1): p. 255-65.

59. Johansson, H., et al., *Relationships between circulating hormone levels, mammographic percent density and breast cancer risk factors in postmenopausal women.* Breast Cancer Res Treat, 2008. **108**(1): p. 57-67.

60. Richert, M.M., et al., *An atlas of mouse mammary gland development.* J Mammary Gland Biol Neoplasia, 2000. **5**(2): p. 227-41.

61. Russo, J., et al., *Chapter 1: Developmental, Cellular, and Molecular Basis of Human Breast Cancer.* JNCI Monographs, 2000. **2000**(27): p. 17-37.

62. Hovey, R.C., J.F. Trott, and B.K. Vonderhaar, *Establishing a framework for the functional mammary gland: from endocrinology to morphology.* J Mammary Gland Biol Neoplasia, 2002. **7**(1): p. 17-38.

63. Polyak, K. and R. Kalluri, *The role of the microenvironment in mammary gland development and cancer.* Cold Spring Harb Perspect Biol, 2010. **2**(11): p. a003244.

64. Wiseman, B.S. and Z. Werb, *Stromal effects on mammary gland development and breast cancer.* Science, 2002. **296**(5570): p. 1046-9.

65. Roozendaal, R. and R.E. Mebius, *Stromal cell-immune cell interactions.* Annu Rev Immunol, 2011. **29**: p. 23-43.

66. Boyd, N.F., et al., *Relationship between mammographic and histological risk factors for breast cancer.* J Natl Cancer Inst, 1992. **84**(15): p. 1170-9.

67. Bright, R.A., et al., *Relationship between mammographic and histologic features of breast tissue in women with benign biopsies.* Cancer, 1988. **61**(2): p. 266-271.

68. Bartow, S.A., et al., *Breast Mammographic Pattern: A Concatenation of Confounding and Breast Cancer Risk Factors.* American Journal of Epidemiology, 1995. **142**(8): p. 813-819.

69. Li, T., et al., *The association of measured breast tissue characteristics with mammographic density and other risk factors for breast cancer.* Cancer Epidemiol Biomarkers Prev, 2005. **14**(2): p. 343-9.

70. Lin, S.J., et al., *Image-guided sampling reveals increased stroma and lower glandular complexity in mammographically dense breast tissue.* Breast Cancer Res Treat, 2011. **128**(2): p. 505-16.

71. Ghosh, K., et al., *Tissue composition of mammographically dense and non-dense breast tissue.* Breast Cancer Res Treat, 2012. **131**(1): p. 267-75.

72. Khan, Q.J., et al., *Mammographic density does not correlate with Ki-67 expression or cytomorphology in benign breast cells obtained by random periareolar fine needle aspiration from women at high risk for breast cancer.* Breast Cancer Res, 2007. **9**(3): p. R35.

73. Conklin, M.W. and P.J. Keely, *Why the stroma matters in breast cancer: insights into breast cancer patient outcomes through the examination of stromal biomarkers.* Cell Adh Migr, 2012. **6**(3): p. 249-60.

74. Alowami, S., et al., *Mammographic density is related to stroma and stromal proteoglycan expression.* Breast Cancer Res, 2003. **5**(5): p. R129-35.

75. Kalluri, R. and M. Zeisberg, *Fibroblasts in cancer.* Nat Rev Cancer, 2006. **6**(5): p. 392-401.

76. Lühr, I., et al., *Mammary fibroblasts regulate morphogenesis of normal and tumorigenic breast epithelial cells by mechanical and paracrine signals.* Cancer Lett, 2012. **325**(2): p. 175-88.

77. Houthuijzen, J.M. and J. Jonkers, *Cancer-associated fibroblasts as key regulators of the breast cancer tumor microenvironment.* Cancer Metastasis Rev, 2018. **37**(4): p. 577-597.

78. Raz, Y. and N. Erez, *An inflammatory vicious cycle: Fibroblasts and immune cell recruitment in cancer.* Exp Cell Res, 2013. **319**(11): p. 1596-603.

79. Han, Y., et al., *Molecular mechanism underlying the tumor-promoting functions of carcinoma-associated fibroblasts.* Tumour Biol, 2015. **36**(3): p. 1385-94.

80. De Wever, O., et al., *Tenascin-C and SF/HGF produced by myofibroblasts in vitro provide convergent pro-invasive signals to human colon cancer cells through RhoA and Rac.* FASEB J, 2004. **18**(9): p. 1016-8.

81. O'Connell, J.T., et al., *VEGF-A and Tenascin-C produced by S100A4+ stromal cells are important for metastatic colonization.* Proc Natl Acad Sci U S A, 2011. **108**(38): p. 16002-7.

82. Olsen, C.J., et al., *Human mammary fibroblasts stimulate invasion of breast cancer cells in a three-dimensional culture and increase stroma development in mouse xenografts.* BMC Cancer, 2010. **10**: p. 444.

83. Hemalatha, S.K., et al., *Brca1 Defective Breast Cancer Cells Induce in vitro Transformation of Cancer Associated Fibroblasts (CAFs) to Metastasis Associated Fibroblasts (MAF).* Sci Rep, 2018. **8**(1): p. 13903.

84. Calon, A., D.V. Tauriello, and E. Batlle, *TGF-beta in CAF-mediated tumor growth and metastasis.* Semin Cancer Biol, 2014. **25**: p. 15-22.

85. Rasanen, K. and A. Vaheri, *Activation of fibroblasts in cancer stroma.* Exp Cell Res, 2010. **316**(17): p. 2713-22.

86. Last, J.A. and K.M. Reiser, *Collagen biosynthesis.* Environ Health Perspect, 1984. **55**: p. 169-77.

87. Insua-Rodriguez, J. and T. Oskarsson, *The extracellular matrix in breast cancer.* Adv Drug Deliv Rev, 2016. **97**: p. 41-55.

88. Uitto, J. and D. Kouba, *Cytokine modulation of extracellular matrix gene expression: relevance to fibrotic skin diseases.* J Dermatol Sci, 2000. **24 Suppl 1**: p. S60-9.

89. Verrecchia, F. and A. Mauviel, *TGF-beta and TNF-alpha: antagonistic cytokines controlling type I collagen gene expression.* Cell Signal, 2004. **16**(8): p. 873-80.

90. Provenzano, P.P., et al., *Collagen density promotes mammary tumor initiation and progression.* BMC Med, 2008. **6**: p. 11.

91. Ghajar, C.M. and M.J. Bissell, *Extracellular matrix control of mammary gland morphogenesis and tumorigenesis: insights from imaging.* Histochem Cell Biol, 2008. **130**(6): p. 1105-18.

92. Levental, K.R., et al., *Matrix crosslinking forces tumor progression by enhancing integrin signaling.* Cell, 2009. **139**(5): p. 891-906.

93. Chambers, A.F. and L.M. Matrisian, *Changing views of the role of matrix metalloproteinases in metastasis.* J Natl Cancer Inst, 1997. **89**(17): p. 1260-70.

94. Cheng, G., et al., *Higher levels of TIMP-1 expression are associated with a poor prognosis in triple-negative breast cancer.* Mol Cancer, 2016. **15**(1): p. 30.

95. Steude, J.S., et al., *Mammographic density and matrix metalloproteinases in breast tissue.* Cancer Microenviron, 2010. **3**(1): p. 57-65.

96. Radisky, E.S. and D.C. Radisky, *Matrix metalloproteinases as breast cancer drivers and therapeutic targets.* Front Biosci (Landmark Ed), 2015. **20**: p. 1144-63.

97. Duffy, M.J., et al., *Metalloproteinases: role in breast carcinogenesis, invasion and metastasis.* Breast Cancer Research, 2000. **2**(4): p. 252.

98. Lyons, R.M., et al., *Mechanism of activation of latent recombinant transforming growth factor beta 1 by plasmin.* J Cell Biol, 1990. **110**(4): p. 1361-7.

99. Todorovic, V., et al., *Latent TGF-beta binding proteins.* Int J Biochem Cell Biol, 2005. **37**(1): p. 38-41.

100. Massague, J., *How cells read TGF-beta signals.* Nat Rev Mol Cell Biol, 2000. **1**(3): p. 169-78.

101. Pierce, D.F., Jr., et al., *Mammary tumor suppression by transforming growth factor beta 1 transgene expression.* Proc Natl Acad Sci U S A, 1995. **92**(10): p. 4254-8.

102. Gorska, A.E., et al., *Transgenic mice expressing a dominant-negative mutant type II transforming growth factor-beta receptor exhibit impaired mammary development and enhanced mammary tumor formation.* Am J Pathol, 2003. **163**(4): p. 1539-49.

103. Bachman, K.E. and B.H. Park, *Duel nature of TGF-beta signaling: tumor suppressor vs. tumor promoter.* Curr Opin Oncol, 2005. **17**(1): p. 49-54.

104. Moses, H. and M.H. Barcellos-Hoff, *TGF-beta biology in mammary development and breast cancer.* Cold Spring Harb Perspect Biol, 2011. **3**(1): p. a003277.

105. Siegel, P.M. and J. Massague, *Cytostatic and apoptotic actions of TGF-beta in homeostasis and cancer.* Nat Rev Cancer, 2003. **3**(11): p. 807-21.

106. Heldin, C.H., M. Landstrom, and A. Moustakas, *Mechanism of TGF-beta signaling to growth arrest, apoptosis, and epithelial-mesenchymal transition.* Curr Opin Cell Biol, 2009. **21**(2): p. 166-76.

107. Shi, X.P., et al., *Resveratrol sensitizes tamoxifen in antiestrogen-resistant breast cancer cells with epithelial-mesenchymal transition features.* Int J Mol Sci, 2013. **14**(8): p. 15655-68.

108. Wendt, M.K., T.M. Allington, and W.P. Schiemann, *Mechanisms of the epithelial-mesenchymal transition by TGF-beta.* Future Oncol, 2009. **5**(8): p. 1145-68.

109. Muraoka-Cook, R.S., et al., *Conditional overexpression of active transforming growth factor beta1 in vivo accelerates metastases of transgenic mammary tumors.* Cancer Res, 2004. **64**(24): p. 9002-11.

110. Parvani, J.G., et al., *Targeted inactivation of beta1 integrin induces beta3 integrin switching, which drives breast cancer metastasis by TGF-beta.* Mol Biol Cell, 2013. **24**(21): p. 3449-59.

111. Miyazono, K., S. Ehata, and D. Koinuma, *Tumor-promoting functions of transforming growth factor-beta in progression of cancer.* Ups J Med Sci, 2012. **117**(2): p. 143-52.

112. Li, C., et al., *Angiogenesis in breast cancer: the role of transforming growth factor beta and CD105.* Microsc Res Tech, 2001. **52**(4): p. 437-49.

113. Sime, P.J., et al., *Adenovector-mediated gene transfer of active transforming growth factor-beta1 induces prolonged severe fibrosis in rat lung.* J Clin Invest, 1997. **100**(4): p. 768-76.

114. Sanderson, N., et al., *Hepatic expression of mature transforming growth factor beta 1 in transgenic mice results in multiple tissue lesions.* Proc Natl Acad Sci U S A, 1995. **92**(7): p. 2572-6.

115. Fukasawa, H., et al., *Treatment with anti-TGF-beta antibody ameliorates chronic progressive nephritis by inhibiting Smad/TGF-beta signaling.* Kidney Int, 2004. **65**(1): p. 63-74.

116. Nakamura, T., et al., *Inhibition of transforming growth factor beta prevents progression of liver fibrosis and enhances hepatocyte regeneration in dimethylnitrosamine-treated rats.* Hepatology, 2000. **32**(2): p. 247-55.

117. Teekakirikul, P., et al., *Cardiac fibrosis in mice with hypertrophic cardiomyopathy is mediated by non-myocyte proliferation and requires Tgf-beta.* J Clin Invest, 2010. **120**(10): p. 3520-9.

118. Denton, C.P. and D.J. Abraham, *Transforming growth factor-beta and connective tissue growth factor: key cytokines in scleroderma pathogenesis.* Curr Opin Rheumatol, 2001. **13**(6): p. 505-11.

119. Verrecchia, F. and A. Mauviel, *Transforming growth factor-beta and fibrosis.* World J Gastroenterol, 2007. **13**(22): p. 3056-62.

120. Yang, W.T., et al., *Decreased TGFbeta signaling and increased COX2 expression in high risk women with increased mammographic breast density.* Breast Cancer Res Treat, 2010. **119**(2): p. 305-14.

121. Lee, E., et al., *Genetic variation in Transforming Growth Factor beta 1 and mammographic density in Singapore Chinese women.* Cancer Res, 2013. **73**(6): p. 1876-82.

122. Bates, J.P., et al., *Mechanisms of immune evasion in breast cancer.* BMC Cancer, 2018. **18**(1): p. 556.

123. Huo, C.W., et al., *High mammographic density in women is associated with protumor inflammation.* Breast Cancer Res, 2018. **20**(1): p. 92.

124. Mahmoud, S.M., et al., *Tumor-infiltrating CD8+ lymphocytes predict clinical outcome in breast cancer.* J Clin Oncol, 2011. **29**(15): p. 1949-55.

125. Mamessier, E., et al., *Peripheral blood NK cells from breast cancer patients are tumor-induced composite subsets.* J Immunol, 2013. **190**(5): p. 2424-36.

126. Iwamoto, M., et al., *Prognostic value of tumor-infiltrating dendritic cells expressing CD83 in human breast carcinomas.* Int J Cancer, 2003. **104**(1): p. 92-7.

127. DeNardo, D.G. and L.M. Coussens, *Inflammation and breast cancer. Balancing immune response: crosstalk between adaptive and innate immune cells during breast cancer progression.* Breast Cancer Res, 2007. **9**(4): p. 212.

128. Hussein, M.R. and H.I. Hassan, *Analysis of the mononuclear inflammatory cell infiltrate in the normal breast, benign proliferative breast disease, in situ and*

infiltrating ductal breast carcinomas: preliminary observations. J Clin Pathol, 2006. **59**(9): p. 972-7.

129. Goto, S., et al., *Analysis of Th1 and Th2 cytokine production by peripheral blood mononuclear cells as a parameter of immunological dysfunction in advanced cancer patients.* Cancer Immunol Immunother, 1999. **48**(8): p. 435-42.
130. Chua, A.C., et al., *Dual roles for macrophages in ovarian cycle-associated development and remodelling of the mammary gland epithelium.* Development, 2010. **137**(24): p. 4229-38.
131. Shapouri-Moghaddam, A., et al., *Macrophage plasticity, polarization, and function in health and disease.* J Cell Physiol, 2018. **233**(9): p. 6425-6440.
132. Jetten, N., et al., *Anti-inflammatory M2, but not pro-inflammatory M1 macrophages promote angiogenesis in vivo.* Angiogenesis, 2014. **17**(1): p. 109-18.
133. Bashir, S., et al., *Macrophage polarization: the link between inflammation and related diseases.* Inflamm Res, 2016. **65**(1): p. 1-11.
134. Locati, M., A. Mantovani, and A. Sica, *Macrophage activation and polarization as an adaptive component of innate immunity.* Adv Immunol, 2013. **120**: p. 163-84.
135. Mantovani, A., et al., *Macrophage plasticity and polarization in tissue repair and remodelling.* J Pathol, 2013. **229**(2): p. 176-85.
136. Mukhtar, R.A., et al., *Tumor-associated macrophages in breast cancer as potential biomarkers for new treatments and diagnostics.* Expert Rev Mol Diagn, 2011. **11**(1): p. 91-100.
137. Wang, N., H. Liang, and K. Zen, *Molecular mechanisms that influence the macrophage m1-m2 polarization balance.* Front Immunol, 2014. **5**: p. 614.
138. Porta, C., et al., *Molecular and epigenetic basis of macrophage polarized activation.* Semin Immunol, 2015. **27**(4): p. 237-48.
139. Roszer, T., *Understanding the Mysterious M2 Macrophage through Activation Markers and Effector Mechanisms.* Mediators Inflamm, 2015. **2015**: p. 816460.

140. Braga, T.T., J.S. Agudelo, and N.O. Camara, *Macrophages During the Fibrotic Process: M2 as Friend and Foe.* Front Immunol, 2015. **6**: p. 602.

141. Sicari, B.M., et al., *The promotion of a constructive macrophage phenotype by solubilized extracellular matrix.* Biomaterials, 2014. **35**(30): p. 8605-12.

142. Mantovani, A., et al., *Macrophage polarization: tumor-associated macrophages as a paradigm for polarized M2 mononuclear phagocytes.* Trends Immunol, 2002. **23**(11): p. 549-55.

143. Allavena, P., et al., *The Yin-Yang of tumor-associated macrophages in neoplastic progression and immune surveillance.* Immunol Rev, 2008. **222**: p. 155-61.

144. Sica, A., et al., *Tumour-associated macrophages are a distinct M2 polarised population promoting tumour progression: potential targets of anti-cancer therapy.* Eur J Cancer, 2006. **42**(6): p. 717-27.

145. Pierce, B.L., et al., *Elevated biomarkers of inflammation are associated with reduced survival among breast cancer patients.* J Clin Oncol, 2009. **27**(21): p. 3437-44.

146. Cuzick, J., et al., *Aspirin and non-steroidal anti-inflammatory drugs for cancer prevention: an international consensus statement.* Lancet Oncol, 2009. **10**(5): p. 501-7.

147. Harris, R.E., et al., *Aspirin, ibuprofen, and other non-steroidal anti-inflammatory drugs in cancer prevention: a critical review of non-selective COX-2 blockade (review).* Oncol Rep, 2005. **13**(4): p. 559-83.

148. Chew, G.L., et al., *Dynamic changes in high and low mammographic density human breast tissues maintained in murine tissue engineering chambers during various murine peripartum states and over time.* Breast Cancer Res Treat, 2013. **140**(2): p. 285-97.

149. Ozhand, A., et al., *Variation in inflammatory cytokine/growth-factor genes and mammographic density in premenopausal women aged 50-55.* PLoS One, 2013. **8**(6): p. e65313.

150. Esbona, K., et al., *COX-2 modulates mammary tumor progression in response to collagen density.* Breast Cancer Res, 2016. **18**(1): p. 35.

151. Stone, J., et al., *The association between mammographic density measures and aspirin or other NSAID use.* Breast Cancer Res Treat, 2012. **132**(1): p. 259-66.

152. Terry, M.B., et al., *Nonsteroidal anti-inflammatory drugs and change in mammographic density: a cohort study using pharmacy records on over 29,000 postmenopausal women.* Cancer Epidemiol Biomarkers Prev, 2008. **17**(5): p. 1088-95.

153. Cushing, S.D., et al., *Minimally modified low density lipoprotein induces monocyte chemotactic protein 1 in human endothelial cells and smooth muscle cells.* Proc Natl Acad Sci U S A, 1990. **87**(13): p. 5134-8.

154. Standiford, T.J., et al., *Alveolar macrophage-derived cytokines induce monocyte chemoattractant protein-1 expression from human pulmonary type II-like epithelial cells.* J Biol Chem, 1991. **266**(15): p. 9912-8.

155. Carulli, M.T., et al., *Chemokine receptor CCR2 expression by systemic sclerosis fibroblasts: evidence for autocrine regulation of myofibroblast differentiation.* Arthritis Rheum, 2005. **52**(12): p. 3772-82.

156. Deshmane, S.L., et al., *Monocyte chemoattractant protein-1 (MCP-1): an overview.* J Interferon Cytokine Res, 2009. **29**(6): p. 313-26.

157. Sun, X., et al., *CCL2-driven inflammation increases mammary gland stromal density and cancer susceptibility in a transgenic mouse model.* Breast Cancer Res, 2017. **19**(1): p. 4.

158. Lu, X. and Y. Kang, *Chemokine (C-C motif) ligand 2 engages CCR2+ stromal cells of monocytic origin to promote breast cancer metastasis to lung and bone.* J Biol Chem, 2009. **284**(42): p. 29087-96.

159. Yoshimura, T., et al., *Monocyte chemoattractant protein-1/CCL2 produced by stromal cells promotes lung metastasis of 4T1 murine breast cancer cells.* PLoS One, 2013. **8**(3): p. e58791.

160. Dwyer, R.M., et al., *Monocyte chemotactic protein-1 secreted by primary breast tumors stimulates migration of mesenchymal stem cells.* Clin Cancer Res, 2007. **13**(17): p. 5020-7.

161. Valkovic, T., et al., *Expression of monocyte chemotactic protein-1 in human invasive ductal breast cancer.* Pathol Res Pract, 1998. **194**(5): p. 335-40.

162. Fujimoto, H., et al., *Stromal MCP-1 in mammary tumors induces tumor-associated macrophage infiltration and contributes to tumor progression.* Int J Cancer, 2009. **125**(6): p. 1276-84.

163. Ueno, T., et al., *Significance of macrophage chemoattractant protein-1 in macrophage recruitment, angiogenesis, and survival in human breast cancer.* Clin Cancer Res, 2000. **6**(8): p. 3282-9.

164. Goede, V., et al., *Induction of inflammatory angiogenesis by monocyte chemoattractant protein-1.* Int J Cancer, 1999. **82**(5): p. 765-70.

165. Lanca, T., et al., *Protective role of the inflammatory CCR2/CCL2 chemokine pathway through recruitment of type 1 cytotoxic gammadelta T lymphocytes to tumor beds.* J Immunol, 2013. **190**(12): p. 6673-80.

166. Li, M., et al., *A role for CCL2 in both tumor progression and immunosurveillance.* Oncoimmunology, 2013. **2**(7): p. e25474.

167. Moore, B.B., et al., *Protection from pulmonary fibrosis in the absence of CCR2 signaling.* J Immunol, 2001. **167**(8): p. 4368-77.

168. Smith, R.E., et al., *A role for C-C chemokines in fibrotic lung disease.* J Leukoc Biol, 1995. **57**(5): p. 782-7.

169. Inoshima, I., et al., *Anti-monocyte chemoattractant protein-1 gene therapy attenuates pulmonary fibrosis in mice.* Am J Physiol Lung Cell Mol Physiol, 2004. **286**(5): p. L1038-44.

170. Krenkel, O., et al., *Therapeutic inhibition of inflammatory monocyte recruitment reduces steatohepatitis and liver fibrosis.* Hepatology, 2018. **67**(4): p. 1270-1283.

171. Gharaee-Kermani, M., E.M. Denholm, and S.H. Phan, *Costimulation of fibroblast collagen and transforming growth factor beta1 gene expression by monocyte chemoattractant protein-1 via specific receptors.* J Biol Chem, 1996. **271**(30): p. 17779-84.

172. Khan, A.A., M.A. Alsahli, and A.H. Rahmani, *Myeloperoxidase as an Active Disease Biomarker: Recent Biochemical and Pathological Perspectives.* Med Sci (Basel), 2018. **6**(2).

173. Van Der Vliet, A., et al., *Myeloperoxidase and protein oxidation in cystic fibrosis.* Am J Physiol Lung Cell Mol Physiol, 2000. **279**(3): p. L537-46.

174. Pulli, B., et al., *Myeloperoxidase-Hepatocyte-Stellate Cell Cross Talk Promotes Hepatocyte Injury and Fibrosis in Experimental Nonalcoholic Steatohepatitis.* Antioxid Redox Signal, 2015. **23**(16): p. 1255-69.

175. Colon, S., et al., *Peroxidasin and eosinophil peroxidase, but not myeloperoxidase, contribute to renal fibrosis in the murine unilateral ureteral obstruction model.* Am J Physiol Renal Physiol, 2019. **316**(2): p. F360-F371.

176. Koller, D.Y., et al., *Serum eosinophil cationic protein, eosinophil protein X and eosinophil peroxidase in relation to pulmonary function in cystic fibrosis.* Clin Exp Allergy, 1998. **28**(2): p. 241-8.

177. DeNichilo, M.O., et al., *Peroxidase enzymes regulate collagen extracellular matrix biosynthesis.* Am J Pathol, 2015. **185**(5): p. 1372-84.

178. Samoszuk, M.K., et al., *Occult deposition of eosinophil peroxidase in a subset of human breast carcinomas.* Am J Pathol, 1996. **148**(3): p. 701-6.

179. Hennigan, K., et al., *Eosinophil peroxidase activates cells by HER2 receptor engagement and β1-integrin clustering with downstream MAPK cell signaling.* Clin Immunol, 2016. **171**: p. 1-11.

180. Walsh, M.T., et al., *Eosinophil peroxidase signals via epidermal growth factor-2 to induce cell proliferation.* Am J Respir Cell Mol Biol, 2011. **45**(5): p. 946-52.

181. Bradley, J.R., *TNF-mediated inflammatory disease.* J Pathol, 2008. **214**(2): p. 149-60.

182. Locksley, R.M., N. Killeen, and M.J. Lenardo, *The TNF and TNF receptor superfamilies: integrating mammalian biology.* Cell, 2001. **104**(4): p. 487-501.

183. Bozcuk, H., et al., *Tumour necrosis factor-alpha, interleukin-6, and fasting serum insulin correlate with clinical outcome in metastatic breast cancer patients treated with chemotherapy.* Cytokine, 2004. **27**(2-3): p. 58-65.

184. Tripsianis, G., et al., *Coexpression of IL-6 and TNF-alpha: prognostic significance on breast cancer outcome.* Neoplasma, 2014. **61**(2): p. 205-12.

185. Cai, X., et al., *Inflammatory factor TNF-α promotes the growth of breast cancer via the positive feedback loop of TNFR1/NF-κB (and/or p38)/p-STAT3/HBXIP/TNFR1.* Oncotarget, 2017. **8**(35): p. 58338-58352.

186. Wolczyk, D., et al., *TNF-alpha promotes breast cancer cell migration and enhances the concentration of membrane-associated proteases in lipid rafts.* Cell Oncol (Dordr), 2016. **39**(4): p. 353-63.

187. Kim, S., et al., *Berberine suppresses TNF-alpha-induced MMP-9 and cell invasion through inhibition of AP-1 activity in MDA-MB-231 human breast cancer cells.* Molecules, 2008. **13**(12): p. 2975-85.

188. Pirianov, G. and K.W. Colston, *Interactions of vitamin D analogue CB1093, TNFalpha and ceramide on breast cancer cell apoptosis.* Mol Cell Endocrinol, 2001. **172**(1-2): p. 69-78.

189. Zhang, Z., et al., *Transmembrane TNF-alpha promotes chemoresistance in breast cancer cells.* Oncogene, 2018. **37**(25): p. 3456-3470.

190. Wu, X., et al., *TNF-α sensitizes chemotherapy and radiotherapy against breast cancer cells.* Cancer Cell International, 2017. **17**(1): p. 13.

191. Reeves, K.W., et al., *Circulating levels of inflammatory markers and mammographic density among postmenopausal women.* Breast Cancer Res Treat, 2011. **127**(2): p. 555-63.

192. Toriola, A.T., et al., *Increased breast tissue receptor activator of nuclear factor-kappaB ligand (RANKL) gene expression is associated with higher mammographic density in premenopausal women.* Oncotarget, 2017. **8**(43): p. 73787-73792.

193. Distler, J.H., et al., *The controversial role of tumor necrosis factor alpha in fibrotic diseases.* Arthritis Rheum, 2008. **58**(8): p. 2228-35.

194. Vilcek, J., et al., *Fibroblast growth enhancing activity of tumor necrosis factor and its relationship to other polypeptide growth factors.* J Exp Med, 1986. **163**(3): p. 632-43.

195. Theiss, A.L., et al., *Tumor necrosis factor (TNF) alpha increases collagen accumulation and proliferation in intestinal myofibroblasts via TNF receptor 2.* J Biol Chem, 2005. **280**(43): p. 36099-109.

196. Greenwel, P., et al., *Tumor necrosis factor alpha inhibits type I collagen synthesis through repressive CCAAT/enhancer-binding proteins.* Mol Cell Biol, 2000. **20**(3): p. 912-8.

197. Huang da, W., B.T. Sherman, and R.A. Lempicki, *Bioinformatics enrichment tools: paths toward the comprehensive functional analysis of large gene lists.* Nucleic Acids Res, 2009. **37**(1): p. 1-13.

198. Huang da, W., B.T. Sherman, and R.A. Lempicki, *Systematic and integrative analysis of large gene lists using DAVID bioinformatics resources.* Nat Protoc, 2009. **4**(1): p. 44-57.

199. Boyd, N.F., et al., *Mammographic densities and breast cancer risk.* Cancer Epidemiol Biomarkers Prev, 1998. **7**(12): p. 1133-44.

200. Van Linthout, S., K. Miteva, and C. Tschöpe, *Crosstalk between fibroblasts and inflammatory cells.* Cardiovascular Research, 2014. **102**(2): p. 258-269.

201. LeBleu, V.S. and R. Kalluri, *A peek into cancer-associated fibroblasts: origins, functions and translational impact.* Dis Model Mech, 2018. **11**(4).

202. Sugimoto, H., et al., *Identification of fibroblast heterogeneity in the tumor microenvironment.* Cancer Biol Ther, 2006. **5**(12): p. 1640-6.

203. Clark, A.K., et al., *A bioengineered microenvironment to quantitatively measure the tumorigenic properties of cancer-associated fibroblasts in human prostate cancer.* Biomaterials, 2013. **34**(20): p. 4777-85.

204. Liao, D., et al., *Cancer associated fibroblasts promote tumor growth and metastasis by modulating the tumor immune microenvironment in a 4T1 murine breast cancer model.* PLoS One, 2009. **4**(11): p. e7965.

205. Unsworth, A., R. Anderson, and K. Britt, *Stromal fibroblasts and the immune microenvironment: partners in mammary gland biology and pathology?* J Mammary Gland Biol Neoplasia, 2014. **19**(2): p. 169-82.

206. Yang, N., et al., *Syndecan-1 in breast cancer stroma fibroblasts regulates extracellular matrix fiber organization and carcinoma cell motility.* Am J Pathol, 2011. **178**(1): p. 325-35.

207. Biernacka, A., M. Dobaczewski, and N.G. Frangogiannis, *TGF-β signaling in fibrosis.* Growth Factors, 2011. **29**(5): p. 196-202.

208. Kurumbail, R.G., J.R. Kiefer, and L.J. Marnett, *Cyclooxygenase enzymes: catalysis and inhibition.* Curr Opin Struct Biol, 2001. **11**(6): p. 752-60.

209. Soslow, R.A., et al., *COX-2 is expressed in human pulmonary, colonic, and mammary tumors.* Cancer, 2000. **89**(12): p. 2637-45.

210. Dannenberg, A.J., et al., *Cyclo-oxygenase 2: a pharmacological target for the prevention of cancer.* Lancet Oncol, 2001. **2**(9): p. 544-51.

211. Sonnylal, S., et al., *Selective expression of connective tissue growth factor in fibroblasts in vivo promotes systemic tissue fibrosis.* Arthritis Rheum, 2010. **62**(5): p. 1523-32.

212. Duncan, M.R., et al., *Connective tissue growth factor mediates transforming growth factor beta-induced collagen synthesis: down-regulation by cAMP.* FASEB J, 1999. **13**(13): p. 1774-86.

213. Lipson, K.E., et al., *CTGF is a central mediator of tissue remodeling and fibrosis and its inhibition can reverse the process of fibrosis.* Fibrogenesis & Tissue Repair, 2012. **5**(1): p. S24.

214. Li, G., et al., *Inhibition of connective tissue growth factor by siRNA prevents liver fibrosis in rats.* J Gene Med, 2006. **8**(7): p. 889-900.

215. Bonniaud, P., et al., *Connective tissue growth factor is crucial to inducing a profibrotic environment in "fibrosis-resistant" BALB/c mouse lungs.* Am J Respir Cell Mol Biol, 2004. **31**(5): p. 510-6.

216. Xie, D., et al., *Elevated Levels of Connective Tissue Growth Factor, WISP-1, and CYR61 in Primary Breast Cancers Associated with More Advanced Features.* Cancer Research, 2001. **61**(24): p. 8917-8923.

217. Kondo, S., et al., *Connective tissue growth factor increased by hypoxia may initiate angiogenesis in collaboration with matrix metalloproteinases.* Carcinogenesis, 2002. **23**(5): p. 769-76.

218. Kumari, S., T.K. Panda, and T. Pradhan, *Lysyl Oxidase: Its Diversity in Health and Diseases.* Indian J Clin Biochem, 2017. **32**(2): p. 134-141.

219. Aumiller, V., et al., *Comparative analysis of lysyl oxidase (like) family members in pulmonary fibrosis.* Sci Rep, 2017. **7**(1): p. 149.

220. Liu, S.B., et al., *Lysyl oxidase activity contributes to collagen stabilization during liver fibrosis progression and limits spontaneous fibrosis reversal in mice.* FASEB J, 2016. **30**(4): p. 1599-609.

221. Cox, T.R., et al., *LOX-mediated collagen crosslinking is responsible for fibrosis-enhanced metastasis.* Cancer Res, 2013. **73**(6): p. 1721-32.

222. Huang, M., et al., *Lysyl oxidase enzymes mediate TGF-β1-induced fibrotic phenotypes in human skin-like tissues.* Laboratory Investigation, 2019. **99**(4): p. 514-527.

223. López, B., et al., *Role of lysyl oxidase in myocardial fibrosis: from basic science to clinical aspects.* American Journal of Physiology-Heart and Circulatory Physiology, 2010. **299**(1): p. H1-H9.

224. Van Doren, S.R., *Matrix metalloproteinase interactions with collagen and elastin.* Matrix Biol, 2015. **44-46**: p. 224-31.

225. Giannandrea, M. and W.C. Parks, *Diverse functions of matrix metalloproteinases during fibrosis.* Dis Model Mech, 2014. **7**(2): p. 193-203.

226. Agren, M.S., et al., *Tumor necrosis factor-alpha-accelerated degradation of type I collagen in human skin is associated with elevated matrix metalloproteinase (MMP)-1 and MMP-3 ex vivo.* Eur J Cell Biol, 2015. **94**(1): p. 12-21.

227. Chou, D.H., W. Lee, and C.A. McCulloch, *TNF-alpha inactivation of collagen receptors: implications for fibroblast function and fibrosis.* J Immunol, 1996. **156**(11): p. 4354-62.

228. Landskron, G., et al., *Chronic inflammation and cytokines in the tumor microenvironment.* J Immunol Res, 2014. **2014**: p. 149185.

229. Chew, G.L., et al., *Increased COX-2 expression in epithelial and stromal cells of high mammographic density tissues and in a xenograft model of mammographic density.* Breast Cancer Res Treat, 2015. **153**(1): p. 89-99.

230. Pilling, D., et al., *TNF-α–stimulated fibroblasts secrete lumican to promote fibrocyte differentiation.* Proceedings of the National Academy of Sciences, 2015. **112**(38): p. 11929-11934.

231. Chen, X. and S.L. Thibeault, *Response of fibroblasts to transforming growth factor-β1 on two-dimensional and in three-dimensional hyaluronan hydrogels.* Tissue Eng Part A, 2012. **18**(23-24): p. 2528-38.

232. Tsutsui, S., et al., *Macrophage infiltration and its prognostic implications in breast cancer: the relationship with VEGF expression and microvessel density.* Oncol Rep, 2005. **14**(2): p. 425-31.

233. Lewis, C.E. and J.W. Pollard, *Distinct role of macrophages in different tumor microenvironments.* Cancer Res, 2006. **66**(2): p. 605-12.

234. Ploeger, D.T., et al., *Cell plasticity in wound healing: paracrine factors of M1/ M2 polarized macrophages influence the phenotypical state of dermal fibroblasts.* Cell Commun Signal, 2013. **11**(1): p. 29.

235. Song, E., et al., *Influence of alternatively and classically activated macrophages on fibrogenic activities of human fibroblasts.* Cell Immunol, 2000. **204**(1): p. 19-28.

236. Zhu, Z., et al., *Alternatively activated macrophages derived from THP-1 cells promote the fibrogenic activities of human dermal fibroblasts.* Wound Repair Regen, 2017. **25**(3): p. 377-388.

237. Gok Yavuz, B., et al., *Cancer associated fibroblasts sculpt tumour microenvironment by recruiting monocytes and inducing immunosuppressive PD-1(+) TAMs.* Sci Rep, 2019. **9**(1): p. 3172.

238. Ronca, R., J.A. Van Ginderachter, and A. Turtoi, *Paracrine interactions of cancer-associated fibroblasts, macrophages and endothelial cells: tumor allies and foes.* Curr Opin Oncol, 2018. **30**(1): p. 45-53.

239. Zhang, A., et al., *Cancer-associated fibroblasts promote M2 polarization of macrophages in pancreatic ductal adenocarcinoma.* Cancer Med, 2017. **6**(2): p. 463-470.

240. Ireland, L.V. and A. Mielgo, *Macrophages and Fibroblasts, Key Players in Cancer Chemoresistance.* Frontiers in Cell and Developmental Biology, 2018. **6**(131).

241. Liu, X., et al., *The CC chemokine ligand 2 (CCL2) mediates fibroblast survival through IL-6.* Am J Respir Cell Mol Biol, 2007. **37**(1): p. 121-8.

242. Deng, X., et al., *Transcriptional regulation of increased CCL2 expression in pulmonary fibrosis involves nuclear factor-kappaB and activator protein-1.* Int J Biochem Cell Biol, 2013. **45**(7): p. 1366-76.

243. Rose, C.E., Jr., S.S. Sung, and S.M. Fu, *Significant involvement of CCL2 (MCP-1) in inflammatory disorders of the lung.* Microcirculation, 2003. **10**(3-4): p. 273-88.

244. Steiner, J.L. and E.A. Murphy, *Importance of chemokine (CC-motif) ligand 2 in breast cancer.* Int J Biol Markers, 2012. **27**(3): p. e179-85.

245. Antoniades, C.G., et al., *Source and characterization of hepatic macrophages in acetaminophen-induced acute liver failure in humans.* Hepatology, 2012. **56**(2): p. 735-46.

246. Antoniades, H.N., et al., *Expression of monocyte chemoattractant protein 1 mRNA in human idiopathic pulmonary fibrosis.* Proc Natl Acad Sci U S A, 1992. **89**(12): p. 5371-5.

247. Kalderen, C., et al., *CCL2 mediates anti-fibrotic effects in human fibroblasts independently of CCR2.* Int Immunopharmacol, 2014. **20**(1): p. 66-73.

248. Mitchell, C., et al., *Dual role of CCR2 in the constitution and the resolution of liver fibrosis in mice.* Am J Pathol, 2009. **174**(5): p. 1766-75.

249. Distler, O., et al., *Overexpression of monocyte chemoattractant protein 1 in systemic sclerosis: role of platelet-derived growth factor and effects on monocyte chemotaxis and collagen synthesis.* Arthritis Rheum, 2001. **44**(11): p. 2665-78.

250. Ferrer, R.A., et al., *Dermal Fibroblasts Promote Alternative Macrophage Activation Improving Impaired Wound Healing.* J Invest Dermatol, 2017. **137**(4): p. 941-950.

251. Sica, A. and A. Mantovani, *Macrophage plasticity and polarization: in vivo veritas.* J Clin Invest, 2012. **122**(3): p. 787-95.

252. Murray, P.J., *Macrophage Polarization.* Annual Review of Physiology, 2017. **79**(1): p. 541-566.

253. Tang, X., *Tumor-associated macrophages as potential diagnostic and prognostic biomarkers in breast cancer.* Cancer Lett, 2013. **332**(1): p. 3-10.

254. Medrek, C., et al., *The presence of tumor associated macrophages in tumor stroma as a prognostic marker for breast cancer patients.* BMC Cancer, 2012. **12**: p. 306.

255. Cabrera, S., et al., *Overexpression of MMP9 in macrophages attenuates pulmonary fibrosis induced by bleomycin.* Int J Biochem Cell Biol, 2007. **39**(12): p. 2324-38.

256. Yoshiji, H., et al., *Tissue inhibitor of metalloproteinases-1 promotes liver fibrosis development in a transgenic mouse model.* Hepatology, 2000. **32**(6): p. 1248-54.

257. Thiele, N.D., et al., *TIMP-1 is upregulated, but not essential in hepatic fibrogenesis and carcinogenesis in mice.* Sci Rep, 2017. **7**(1): p. 714.

258. Beall, C.J., et al., *Site-directed mutagenesis of monocyte chemoattractant protein-1 identifies two regions of the polypeptide essential for biological activity.* Biochem J, 1996. **313 (Pt 2)**: p. 633-40.

259. Soria, G. and A. Ben-Baruch, *The inflammatory chemokines CCL2 and CCL5 in breast cancer.* Cancer Lett, 2008. **267**(2): p. 271-85.

260. Qian, B.Z., et al., *CCL2 recruits inflammatory monocytes to facilitate breast-tumour metastasis.* Nature, 2011. **475**(7355): p. 222-5.

261. Guy, C.T., R.D. Cardiff, and W.J. Muller, *Induction of mammary tumors by expression of polyomavirus middle T oncogene: a transgenic mouse model for metastatic disease.* Mol Cell Biol, 1992. **12**(3): p. 954-61.

262. Li, L., et al., *The Spleen Promotes the Secretion of CCL2 and Supports an M1 Dominant Phenotype in Hepatic Macrophages During Liver Fibrosis.* Cell Physiol Biochem, 2018. **51**(2): p. 557-574.

263. Tesch, G.H., *MCP-1/CCL2: a new diagnostic marker and therapeutic target for progressive renal injury in diabetic nephropathy.* Am J Physiol Renal Physiol, 2008. **294**(4): p. F697-701.

264. Nesbit, M., et al., *Low-level monocyte chemoattractant protein-1 stimulation of monocytes leads to tumor formation in nontumorigenic melanoma cells.* J Immunol, 2001. **166**(11): p. 6483-90.

265. Nakasone, Y., et al., *Host-derived MCP-1 and MIP-1alpha regulate protective anti-tumor immunity to localized and metastatic B16 melanoma.* Am J Pathol, 2012. **180**(1): p. 365-74.

266. Huang, B., et al., *CCL2/CCR2 pathway mediates recruitment of myeloid suppressor cells to cancers.* Cancer Lett, 2007. **252**(1): p. 86-92.

267. Cedile, O., A. Wlodarczyk, and T. Owens, *CCL2 recruits T cells into the brain in a CCR2-independent manner.* APMIS, 2017. **125**(11): p. 945-956.

268. Flaishon, L., et al., *Expression of the chemokine receptor CCR2 on immature B cells negatively regulates their cytoskeletal rearrangement and migration.* Blood, 2004. **104**(4): p. 933-41.

269. Penido, C., et al., *Involvement of CC chemokines in gammadelta T lymphocyte trafficking during allergic inflammation: the role of CCL2/CCR2 pathway.* Int Immunol, 2008. **20**(1): p. 129-39.

270. Zysk, A., et al., *Adoptive transfer of ex vivo expanded Vγ9Vδ2 T cells in combination with zoledronic acid inhibits cancer growth and limits osteolysis in a murine model of osteolytic breast cancer.* Cancer Lett, 2017. **386**: p. 141-150.

271. Chen, X., et al., *MAPK, NFκB, and VEGF signaling pathways regulate breast cancer liver metastasis.* Oncotarget, 2017. **8**(60): p. 101452-101460.

272. McMahon, G., *VEGF receptor signaling in tumor angiogenesis.* Oncologist, 2000. **5 Suppl 1**: p. 3-10.

273. Ahmad, R., et al., *The Synergy between Palmitate and TNF-α for CCL2 Production Is Dependent on the TRIF/IRF3 Pathway: Implications for Metabolic Inflammation.* J Immunol, 2018. **200**(10): p. 3599-3611.

274. Haukeland, J.W., et al., *Systemic inflammation in nonalcoholic fatty liver disease is characterized by elevated levels of CCL2.* J Hepatol, 2006. **44**(6): p. 1167-74.

275. Roh, Y.S. and E. Seki, *Chemokines and Chemokine Receptors in the Development of NAFLD.* Adv Exp Med Biol, 2018. **1061**: p. 45-53.

276. Currie, E., et al., *Cellular fatty acid metabolism and cancer.* Cell Metab, 2013. **18**(2): p. 153-61.

277. Kinlaw, W.B., et al., *Fatty Acids and Breast Cancer: Make Them on Site or Have Them Delivered.* J Cell Physiol, 2016. **231**(10): p. 2128-41.

278. Monaco, M.E., *Fatty acid metabolism in breast cancer subtypes.* Oncotarget, 2017. **8**(17): p. 29487-29500.

279. Hilvo, M. and A. Matej Orešiè, *Regulation of lipid metabolism in breast cancer provides diagnostic and therapeutic opportunities.* Clinical Lipidology, 2012. **7**(2): p. 177-188.

280. Milgraum, L.Z., et al., *Enzymes of the fatty acid synthesis pathway are highly expressed in in situ breast carcinoma.* Clin Cancer Res, 1997. **3**(11): p. 2115-20.

281. Alo, P.L., et al., *Expression of fatty acid synthase (FAS) as a predictor of recurrence in stage I breast carcinoma patients.* Cancer, 1996. **77**(3): p. 474-82.

282. Alo, P.L., et al., *Fatty acid synthase (FAS) predictive strength in poorly differentiated early breast carcinomas.* Tumori, 1999. **85**(1): p. 35-40.

283. Yang, Y., et al., *Regulation of fatty acid synthase expression in breast cancer by sterol regulatory element binding protein-1c.* Exp Cell Res, 2003. **282**(2): p. 132-7.

284. Suburu, J., et al., *Fatty acid synthase is required for mammary gland development and milk production during lactation.* Am J Physiol Endocrinol Metab, 2014. **306**(10): p. E1132-43.

285. Davie, S.A., et al., *Effects of FVB/NJ and C57Bl/6J strain backgrounds on mammary tumor phenotype in inducible nitric oxide synthase deficient mice.* Transgenic Research, 2007. **16**(2): p. 193-201.

286. Sharma, G.N., et al., *Various types and management of breast cancer: an overview.* J Adv Pharm Technol Res, 2010. **1**(2): p. 109-26.

287. Organisation, W.H. *Immunization, Vaccines and Biologicals*. 2018 10/12/2019]; Available from: https://www.who.int/immunization/en/.

288. Patel, C., et al., *The impact of 10 years of human papillomavirus (HPV) vaccination in Australia: what additional disease burden will a nonavalent vaccine prevent?* Euro Surveill, 2018. **23**(41).

289. Ironside, A.J. and J.L. Jones, *Stromal characteristics may hold the key to mammographic density: The evidence to date.* Oncotarget, 2016.

290. Huo, C.W., et al., *Mammographic density-a review on the current understanding of its association with breast cancer.* Breast Cancer Res Treat, 2014. **144**(3): p. 479-502.

291. Degnim, A.C., et al., *Alterations in the Immune Cell Composition in Premalignant Breast Tissue that Precede Breast Cancer Development.* Clin Cancer Res, 2017. **23**(14): p. 3945-3952.

292. Agnoli, C., et al., *Biomarkers of inflammation and breast cancer risk: a case-control study nested in the EPIC-Varese cohort.* Sci Rep, 2017. **7**(1): p. 12708.

293. Tobias, D.K., et al., *Markers of Inflammation and Incident Breast Cancer Risk in the Women's Health Study.* Am J Epidemiol, 2018. **187**(4): p. 705-716.

294. Ambrale, S.S., et al., *The influence of inflammation on mammographic breast density in women at increased risk of breast cancer.* Journal of Clinical Oncology, 2015. **33**(15_suppl): p. 1566-1566.

295. Hanna, M., et al., *Association between expression of inflammatory markers in normal breast tissue and mammographic density among premenopausal and postmenopausal women.* Menopause, 2017. **24**(5): p. 524-535.

296. Dethlefsen, C., G. Hojfeldt, and P. Hojman, *The role of intratumoral and systemic IL-6 in breast cancer.* Breast Cancer Res Treat, 2013. **138**(3): p. 657-64.

297. Harris, R.E., B.C. Casto, and Z.M. Harris, *Cyclooxygenase-2 and the inflammogenesis of breast cancer.* World J Clin Oncol, 2014. **5**(4): p. 677-92.

298. Sierra-Filardi, E., et al., *CCL2 shapes macrophage polarization by GM-CSF and M-CSF: identification of CCL2/CCR2-dependent gene expression profile.* J Immunol, 2014. **192**(8): p. 3858-67.

299. Mahdi, J.G., et al., *The historical analysis of aspirin discovery, its relation to the willow tree and antiproliferative and anticancer potential.* Cell Prolif, 2006. **39**(2): p. 147-55.

300. Wood, M.E., et al., *Aspirin use is associated with lower mammographic density in a large screening cohort.* Breast Cancer Res Treat, 2017. **162**(3): p. 419-425.

301. Qiao, Y., et al., *Associations between aspirin use and the risk of cancers: a meta-analysis of observational studies.* BMC Cancer, 2018. **18**(1): p. 288.

302. Algra, A.M. and P.M. Rothwell, *Effects of regular aspirin on long-term cancer incidence and metastasis: a systematic comparison of evidence from observational studies versus randomised trials.* Lancet Oncol, 2012. **13**(5): p. 518-27.

303. Luo, T., et al., *Aspirin use and breast cancer risk: a meta-analysis.* Breast Cancer Res Treat, 2012. **131**(2): p. 581-7.

304. Sneader, W., *The discovery of aspirin: a reappraisal.* BMJ, 2000. **321**(7276): p. 1591-4.

305. Derry, S. and Y.K. Loke, *Risk of gastrointestinal haemorrhage with long term use of aspirin: meta-analysis.* BMJ, 2000. **321**(7270): p. 1183-7.

306. Serebruany, V.L., et al., *Analysis of risk of bleeding complications after different doses of aspirin in 192,036 patients enrolled in 31 randomized controlled trials.* Am J Cardiol, 2005. **95**(10): p. 1218-22.

307. Li, X., et al., *"Three Hits" Hypothesis for Developmental Origins of Health and Diseases in View of Cardiovascular Abnormalities.* Birth Defects Res, 2017. **109**(10): p. 744-757.

308. Turashvili, G., et al., *Columnar cell lesions, mammographic density and breast cancer risk.* Breast Cancer Res Treat, 2009. **115**(3): p. 561-71.

309. Arendt, L.M., et al., *Obesity promotes breast cancer by CCL2-mediated macrophage recruitment and angiogenesis.* Cancer Res, 2013. **73**(19): p. 6080-93.

310. Ellulu, M.S., et al., *Obesity and inflammation: the linking mechanism and the complications.* Arch Med Sci, 2017. **13**(4): p. 851-863.

311. Baglietto, L., et al., *Associations of mammographic dense and nondense areas and body mass index with risk of breast cancer.* Am J Epidemiol, 2014. **179**(4): p. 475-83.